Graduate Theses, Dissertations, and Problem Reports

2007

Using gain of function genetics to explore the role of non-histone chromosomal protein D1 in Drosophila melanogaster

Marissa B. Smith
West Virginia University

Follow this and additional works at: https://researchrepository.wvu.edu/etd

Using gain of function genetics to explore the role of non-histone chromosomal protein D1 in *Drosophila melanogaster*

Marissa B. Smith

Thesis

Submitted to the Eberly College of Arts and Sciences
at West Virginia University
In Partial Fulfillment of the Requirements
For the Degree of

Master of Science
in
Cellular and Molecular Biology

Committee members:
Dr. Karen S. Weiler, Chair
Dr. Clifton Bishop
Dr. Ashok Bidwai

Department of Biology

Morgantown, WV
2007

ABSTRACT

Using gain of function genetics to explore the role of non-histone
chromosomal protein D1 in *Drosophila melanogaster*

Marissa B. Smith

The organization of eukaryotic genomes requires a harmony between efficient compaction and accessibility. This is achieved through the packaging of chromatin and the influence of chromosomal proteins, a topic not well understood. A chromosomal protein that remains a mystery at present is the D1 protein. Identified in 1974 by Alfageme *et al.*, *D1* has been highly characterized but its function remains unknown. The goal of this study was to elucidate the function of *D1* by overexpression analysis using the *GAL4*/UAS system in *Drosophila melanogaster*. Analysis of gain-of-function phenotypes due to *D1* overexpression in a variety of tissues determined that ectopic *D1* interfered in the genetic cascades of a number of unrelated processes and in unrelated tissues. In addition, ectopic expression of *D1* in the salivary glands led to ectopic associations of the polytene chromosomes resulting in chromosome entanglement. Mapping of the cytological intervals of these ectopic contacts resulted in a strong correlation to the localization of features of intercalary heterochromatin. An additional study indicated that D1 is activated by interaction with protein kinase CK2. I hypothesize overall, based on this study that the phosphoprotein D1, activated by protein kinase CK2, has a role in inducing and/or maintaining heterochromatic properties of the genome by binding to AT-rich satellite and satellite-related DNA in a variety of processes and tissues. The D1 protein, with ten copies of the AT hook binding motif, most likely functions in tandem with other transcription factors as a means of facilitating structural changes to chromatin resulting in the regulation of gene expression.

The D1 protein binds to the 1.688 g/cm^3 and 1.672 g/cm^3 satellite repeats of heterochromatin as well as several euchromatic loci. Analysis of D1 cDNA determined the presence of ten copies of the highly conserved AT hook binding motif, a motif hypothesized to participate in facilitating architectural changes in the DNA. D1 mRNA is maternally loaded and highly expressed at the beginning of embryonic development and later in adult gametogenesis. In addition, the D1 protein has been compared to proteins of the mammalian High Mobility Group A family (HMGA), proteins functioning as architectural elements that alter the structure of DNA to produce and enhance various DNA-dependent activities. Even though D1 has been highly studied, its function remains unknown. Elucidating the function of the D1 chromosomal protein may provide intriguing information of the relationship between chromatin structure, gene expression and gene regulation, an understanding that once fully elucidated would revolutionize many fields.

Acknowledgements

Table of Contents

List of Tables

List of Figures

Chapter One: Introduction

Introduction

In 2000, the *Drosophila melanogaster* genome sequence was completed which has greatly facilitated structural and functional studies in this model organism. The Drosophila genome is approximately 180 Mb in size, a third of which is centric heterochromatin [1]. Sequencing of the 120 Mb euchromatic part of the genome has been fully assembled and encodes approximately 13,600 genes [1]. The heterochromatic portion of the genome, approximately 60 Mb in size, is currently being sequenced and annotated. There have been several releases of annotated heterochromatic sequence from the Drosophila Heterochromatin Genome Project (DHGP) with estimations that Drosophila heterochromatin contains approximately 450 genes [47]. Drosophila heterochromatin consists mainly of repetitive sequences, both highly repetitive satellites and middle repetitive DNA. The transposable element families present in Drosophila heterochromatin tend to cluster in discrete, highly conserved heterochromatic regions [72].

In order for proper gene expression in both euchromatin and heterochromatin, chromosomal proteins are important in determining structural as well as functional properties of the genome. Several chromosomal proteins have been identified and characterized but many remain unknown. Determining the function and mode of interaction of these proteins is essential to understanding the distinction between chromatin states, gene expression and gene regulation, an understanding that once fully elucidated would revolutionize many fields.

A chromosomal protein that remains a mystery at present is the D1 protein. D1 is a non-histone chromosomal protein with double stranded DNA binding ability [4]. Studies have shown that D1 binds satellite repeats of Drosophila heterochromatin [56]. As well, D1 has been localized to four specific euchromatic loci of polytene chromosomes, 81F, 83C-E, 101 and 102, with a small concentration of D1 widely distributed throughout all of the polytene chromosomes [4]. Moreover, D1 has been shown to be associated with chromatin from the earliest stages of Drosophila development [74]. The fact that D1 binds euchromatin as well as heterochromatin and is present from the earliest stages of Drosophila development onward may be indicative of the importance of this chromosomal protein. Fully characterizing *D1* may provide

fascinating insight into the relationship between structural and functional states of the genome.

D1 is a non-histone chromosomal protein.

The D1 protein belongs to the broad group of Drosophila satellite binding proteins where it was one of the first satellite-specific DNA binding proteins identified [3]. In Drosophila, repetitive satellite sequences encompass much of the constitutive heterochromatin and are comprised of tandemly repetitive sequences originally identified as satellite bands in ultracentrifuge density gradients [68]. The primary satellite repeats in D. melanogaster are present in blocks of hundreds to thousands of tandem units [26] and are classified into four buoyant-density classes, 1.672, 1.686, 1.688 and 1.705 g/cm^3 in CsCl isolated with high purity as satellite peaks [31; 68]. The 1.672, 1.686 and 1.705 g/cm^3 satellites consist of a major simple repeating unit of five to ten base pairs while the 1.688 g/cm^3 satellite consists of a more complex 359 basepair repeating unit [22]. The 1.672 g/cm^3 satellite is primarily located on the Y chromosome and chromosome four as well as one site each on chromosome three and the X chromosome. The 1.686 g/cm^3 satellite is present on chromosome two and chromosome three while the 1.705 g/cm^3 satellite has been mapped to all Drosophila chromosomes. The 1.688 g/cm^3 satellite is located only on the X chromosome [61].

Two dimensional hybridization mapping of nucleosomes has revealed that D1 preferentially binds to the 1.672 g/cm^3 and 1.688 g/cm^3 satellite DNAs [56] but not the 1.705 g/cm^3 satellite [57]. AATAT repeats are the principal component of the 1.672 g/cm^3 satellite which comprises approximately 3% of the Drosophila genome [60; 61]. 359-basepair repeats are the major component of the 1.688g/cm^3 satellite which make up approximately 4% of the Drosophila genome [60; 61].

Biochemical properties of D1

Following the determination that D1 is a satellite DNA binding protein, studies of *D1* focused on its biochemical properties. Ashley *et al.,* [8] cloned and sequenced a *D1* cDNA. They identified ten copies of a repeating DNA binding motif that is highly conserved throughout evolution called the AT hook. The AT hook is a small DNA-

binding protein motif which has a sequence pattern centered around a highly conserved glycine-arginine-proline (GRP) tripeptide, a sequence pattern necessary to bind to the minor groove of DNA [73]. Its remarkable evolutionary conservation and presence in a large number of different proteins suggests that the AT hook domain fulfills an important role in targeting varied functional domains to AT-rich sequences of the genome [9]. It has been hypothesized to be an auxiliary protein motif cooperating with other DNA-binding activities and facilitating changes in the structure of the DNA [10].

The deduced amino acid sequence of D1 is very rich in charged residues, containing 18.3% acidic residues (Asp + Glu) and 17.7% basic residues (Arg + Lys), present in alternating blocks [8]. Because of the high proportion of positively charged residues (which have the potential to reduce electrophoretic mobility in SDS gels), the molecular weight of *D1* has been difficult to establish. According to Ashley *et al.*, [8] the predicted molecular weight of the 355-residue polypeptide D1, encoded by cDNA sequence is 37,005 daltons. This somewhat agrees with the 30,000 dalton apparent molecular weight of D1 relative to histones [5].

When D1 was initially identified, Alfageme *et al.,* [3; 4] noted that the D1 protein had properties resembling those of proteins of the mammalian High Mobility Group (HMG), notably, solubility in 5% perchloric acid, extractability from chromatin by 0.35M NaCl, and a high content of basic and acidic amino acids. D1 is considered to be most similar to proteins in a subset of the High Mobility Group family, the HMGA family. Like D1, HMGA proteins bind to AT-rich DNA with three AT-hook binding motifs [73]. The HMGA protein family is made up of nonhistone chromosomal proteins that function as architectural elements to facilitate and enhance various DNA-dependent activities. They do this by virtue of their ability to alter the structure of both DNA and chromatin substrates [2]. D1 is distinct from the HMGA proteins in its unusually high molecular weight and in having aspartic acid rather than glutamic acid as its most abundant amino acid [4].

D1 was identified as a phosphoprotein in a study by Glover *et al.*, [40] and determined to be a substrate of Drosophila CK2 [41]. Sequence analysis of *D1* revealed six serine residues followed by stretches of acidic residues, potential sites of phosphorylation by protein kinase CK2 [8]. Thus, the possibility that D1 is modulated by

phosphorylation is strong. Like D1, HMGA proteins are phosphorylated *in vivo* and contain potential CK2 recognition sites. Studies have shown that CK2 is responsible for the *in vivo* phosphorylation of HMGA proteins in the mammalian system, [87; 88] altering their conformation and modulating their DNA-binding properties [81]. As HMGA proteins are functionally regulated by phosphorylation as a result of protein kinase CK2 [12; 65; 71; 73; 80; 79; 93], and D1 and proteins of the HMGA family share many similarities in biochemical properties, perhaps D1 is functionally regulated by CK2 phosphorylation as well.

Expression of *D1*

Developmental expression profile assays of the *D1* gene indicate that *D1* mRNA is maternally loaded and is highly abundant at the beginning of embryonic development with decreasing levels as embryogenesis proceeds [9; 74]. *D1* expression levels remain low throughout larval development, in pupae and in adult males. Adult females exhibit higher mRNA levels, correlating with preferential expression in the ovaries [9]. Localization of D1 protein during early embryonic cell cycles indicates that D1 localizes exclusively to centromeric heterochromatin at cellularization [9]. A study by Blattes *et al.*, [16] determined that there were two foci of D1 immunosignal in cellular blastoderm embryos. They determined that these two foci correspond to the 1.688 g/cm^3 and the 1.672 g/cm^3 satellite repeats by exposing whole embryos to synthetic polyamides specific to each repetitive satellite. A dose-dependent decrease of the D1 immunosignal was seen in embryos exposed to the synthetic polyamides, indicating D1 binding specifically to the 1.688 g/cm^3 and the 1.672 g/cm^3 satellite repeats.

D1 localization was assayed in metaphase chromosomes from larval neuroblasts revealing that D1 associates with the centromeric region of chromosome three and of the X chromosome, large regions of the Y chromosome and almost all of chromosome four. Aulner *et al.*, [9] conclude from this that D1 is associated with 1.672g/cm^3 satellite repeats on the Y chromosome and on chromosomes three and four, and with 1.688g/cm^3 satellite repeats in the centromeric region of the X chromosome. The chromosomes of the eye imaginal discs displayed D1 immunosignal in an identical pattern [16].

5

Studies of D1 protein localization were done in the Drosophila adult gonads [9]. D1 localized to foci in the germarium of the female ovaries while the karyosome stained homogeneously. In follicle cells, D1 localized to bright foci while the nurse cells were largely negative for D1. Late-staged oocytes revealed two populations of D1 in the transcriptionally inactive cells: one was determined to be D1 localization to chromosomes while the other was hypothesized to represent a pool of stored protein [9]. The authors hypothesized from this that the distribution of D1 lends support to the idea that D1 is broadly redistributed onto bulk chromatin correlating with transcriptional repression. In transcriptionally active cells most of the D1 protein localizes to discrete foci. This may correspond to D1 storage sites in heterochromatin [9]. In the male testes, D1 was found to be present in all types of maturing spermatocytes and assumed a distinctive distribution at the apical pole of the testes. Assays of D1 protein in the germline and somatic stem cells revealed that D1 was distributed in dense foci in the top layer of the cells. In contrast, maturing spermatocytes past the mitotic stages of spermatogenesis showed a broad distribution of the D1 protein extending throughout the nucleoplasm [9].

D1 localization was assayed in the salivary gland chromosomes. These chromosomes are polytene; the replicated copies of DNA remain physically associated resulting in interphase chromosomes that are visible with bright field microscopy. Studies of heterochromatin are hindered in polytene chromosomes due to the fact that heterochromatic portions of the Drosophila genome are underreplicated. Immunofluorescence analysis of the polytene chromosomes with anti-D1 antibodies revealed D1 localization at a limited number of euchromatic loci: 81F, 83C-E, 101 and 102D [4]. Alfageme *et al*., [4] reported that there were also faintly fluorescing sites throughout all of the polytene chromosome arms and interpreted the marked difference in fluorescence intensity to be due to the difference in D1 content. They hypothesized that a large fraction of the D1 protein is localized in a few regions of the genome while the remainder is widely distributed over all of the Drosophila chromosomes.

Function of *D1*

Even though D1 protein localization has been extensively studied, questions

remain of a requirement for *D1* in development. A study by Aulner *et al*., [9] reported that *D1* was essential for viability. Utilizing the *P{EP}473* insertion in the 5'UTR of the *D1* gene, the authors reported this insertion as embryonic lethal as no homozygous larvae were ever recovered from a cross. In addition, Aulner *et al*., [9] noted that the mobilization of the *P{EP}473* element resulted in a clean excision greater than 90% of the time and in the subsequent restoration of a wild-type phenotype. In characterizing the mutant phenotype further, the authors noted that comparisons of wild-type nuclei to nuclei of forced-hatched *P{EP}473* homozygous larvae indicated differences in their morphologies with *P{EP}473* nuclei appearing smaller with different degrees of chromatin distribution. Interestingly, unpublished results from our lab indicate that *D1* is non-essential for fly viability and no null phenotype has yet been noted. Because of this, hypotheses of *D1* function based on data from the Aulner *et al.,* [9] study may not be valid.

Elucidating the function of *D1* remains important in the study of the structural and functional relationship of the genome. Therefore, I undertook an approach different from any done so far in elucidating *D1* function, that of gain-of-function genetics utilizing the *GAL4*/UAS system.

D1 overexpression analysis as a means of elucidating its function

The *GAL4*/UAS system of *Saccharamyces cerevisiae* was designed by Brand and Perrimon [19] for use in Drosophila in order to manipulate gene expression. It utilizes the yeast transcription factor *GAL4* and the *GAL4* binding sites, termed an upstream activating site (UAS), in order to manipulate gene expression. Specifically, the *GAL4*/UAS system is a bipartite approach in which the two components of the system, the target gene and the transcriptional activator, are maintained in two distinct transgenic lines. To generate transgenic lines expressing *GAL4* in a numerous cell and tissue specific patterns, the *GAL4* gene is present in the genome in which expression is driven from a certain tissue-specific enhancer. The *GAL4*-dependent target gene has the gene of interest subcloned behind its binding sites (the UAS sites). Thus, progeny from crossing the transgenic strain carrying the *GAL4* gene driven by a specific enhancer and the transgenic strain with the gene of interest fused with UAS sites will express the gene of

interest in an activator-specific manner [19; 29].

To facilitate the generation of transgenic responder and driver lines, Brand and Perrimon [19] constructed a number of vectors. pUAST is a P element based vector in which a gene of interest can be placed under *GAL4* control. It contains an upstream UAS element followed by the *heat shock protein70* (*hsp70*) basal promoter and multiple cloning sites. Variants of pUAST with altered configurations were constructed in order to increase the number of *GAL4*/UAS responder lines for all genes of the genome [77; 78]. One set of these variants, *EP* and *EP^S* constructs contain a UAS element and basal promoter adjacent to one of the P-element inverted repeats. In this configuration, when inserted into the Drosophila genome, these pUAST variants have the ability to direct the expression of neighboring genes in a *GAL4*-dependent manner. Three separate constructs, pGAWB, pGATB, and pGATN were generated to allow the expression of *GAL4* is distinct patterns. The pGAWB construct was designed as an enhancer-trap construct. In this construct, *GAL4* is inserted downstream of the P transposase promoter and upstream of the *hsp70* terminator. Enhancer trap elements act as mobile DNA elements that can become inserted into the Drosophila genome close to an endogenous enhancer of gene expression thus allowing visualization of the expression pattern via a reporter. The pGATB and pGATN constructs are both transformation vectors used to place specific regulatory elements upstream of *GAL4*. The presence of many constructs as sources for *GAL4* drivers has increased the number of approaches that the *GAL4*/UAS system can be utilized for in genetic assays.

Although the most common use for the *GAL4*/UAS system in flies is as a tool for misexpression studies with a specific gene, this is rapidly changing as the list of alternative uses is increasing. Some of its other uses include identification of genes involved in the process of interest via enhancer-trapping, analysis of cellular autonomy of a gene product through targeted mosaics, cellular marking to aid in screens for mutations affecting the process of interest and identification of loci that interact with the gene of interest through screens for modifiers of a specific misexpression phenotype. Even the inducibility of the *GAL4*/UAS system can be modified by utilizing such methods as a UAS-heat shock construct or the ability of FLP recombinase to promote recombination between two FRT sites involved with the *GAL*/UAS system [29]. As *GAL4* driver lines,

UAS responder lines and the elucidation of different approaches increases, the utility of the *GAL4*/UAS system in gain-of-function genetics is becoming extremely beneficial. Likely, the use of the *GAL4*/UAS system will be continually expanded overall, amplifying the enormous flexibility of this system as an experimental tool for genetic analysis.

       This study utilized the *GAL4*/UAS system in *Drosophila melanogaster* to induce ectopic expression of *D1* as a means to elucidate its function. Specifically, the *GAL4*/UAS system was employed with an additional element, the *EP* element of Rorth [77] described above, to drive ectopic *D1* expression. This *EP* element transposed into the 5'UTR of the *D1* gene and placed UAS sites upstream of the *D1* coding region. Thus *GAL4* protein driven by a specific enhancer bound to the UAS sites of the *EP* element and drove overexpression of the *D1* gene (Figure 1.1).
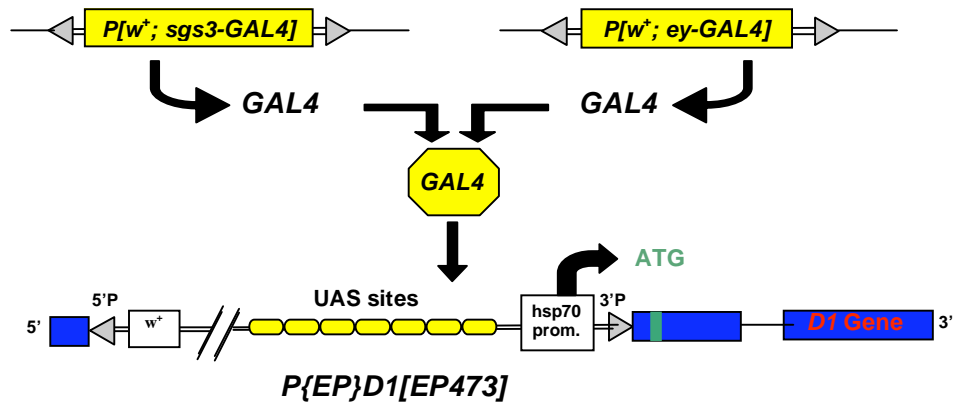
Figure 1.1: **The *GAL4*/UAS system was utilized as a means of directed overexpression of the D1 protein.** Transgenes were chosen that express *GAL4* via a tissue specific promoter in the temporal and spatial pattern of the promoter (in this example, the *salivary gland specific* (*sgs3*) promoter and the *eyeless* (*ey*) promoter). Upon *GAL4* expression, the protein binds the Upstream Activating Sequences (UAS) that are incorporated into the EP element. *EP473,* [77] is inserted into the 5' UTR of the *D1* sequence. Along with UAS sites, *EP473* carries a basal heat shock promoter oriented to direct expression of genomic sequences adjacent to the EP insertion site. Thereby, when *GAL4* protein binds to the UAS sites of *EP473*, *D1* expression will be directed in the tissue specific pattern of the transgenic *GAL4* promoter. (ATG, translation start site)

Chapter Two: The effect of ectopic *D1* expression on the differentiation and development of selected tissues

Introduction

This study focused on directing *D1* expression in specific tissues as an approach to elucidate *D1* function. Normal development requires a carefully orchestrated coordination of proliferation, cell fate specification, cell cycle control, apoptosis and gene regulation. Inducing *D1* expression in certain tissues that are involved in some of these processes may result in gain-of-function phenotypes. Analysis of these phenotypes could provide clues as to *D1*'s role.

The *GAL4*/UAS system of Brand and Perrimon [19] was utilized in these studies as a means of directing *D1* overexpression. The *GAL4*/UAS system is described in detail in chapter one of this thesis. Specifically, this approach employed an EP element, *P{EP}473* in order to facilitate *D1* overexpression (Figure 2.1).

GAL4 drivers were chosen to target *D1* gene expression in specific tissues. *D1* expression was directed in the eye and mechanosensory bristles with three separate *GAL4* drivers, *eyeless*, *scabrous* and *nina*. Bristle and eye morphogenesis are excellent systems in which to gain insights into gene regulation, cell fate specification, programmed cell death, cell cycle control and tissue patterning. The development of both organ systems has been extensively studied and utilized for centuries as models for developmental analysis. Although the eye and bristle differ in overall organization, they share a common requirement for neural versus epidermal cell determination during morphogenesis, a process involving many complex cell-cell interactions. If overexpression of *D1* results in the alteration of cell fate, perhaps further analysis can determine the specific cell-cell signaling pathways that *D1* may have perturbed. This knowledge would aid in the analysis of *D1* function by providing information regarding how *D1* may function in wild-type flies.

D1 expression was also directed in a mesodermal tissue specific pattern by the *twist* promoter. *twist* is a transcription factor which initiates Drosophila mesoderm development early during embryogenesis [82]. If a gain-of-function phenotype results due to *D1* overexpression, further analyses could identify proteins with which *D1* may be interacting, offering clues as to *D1*'s activities during normal development. Also, *twist* expression is initiated approximately three hours after embryo fertilization (stage 8 of embryogenesis). *D1* overexpression in a *twist* pattern could provide a temporal aspect to

the functional analysis of *D1*. *D1* has been demonstrated to be maternally contributed to the embryo [9]. This may be indicative of a role for *D1* early in fly development. By overexpressing *D1* with a promoter initiated early in embryogenesis, this hypothesis may be investigated.

The male germline was also chosen for *D1* overexpression to be directed by the *nanos GAL4* driver. *nanos* RNA is maternally contributed and encodes a protein that acts as a translational repressor establishing the posterior pattern of the Drosophila embryo [55]. In addition, nanos protein is essential for establishing germline/soma dichotomy in the embryo and is expressed in germline cells throughout the adult phase of D. melanogaster as it is required to maintain germline cell fate post-zygotically [35; 43]. One of three *D1* transcripts derives from a testis-specific promoter. By inducing *D1* expression in the male germline in a *nanos* pattern, further analysis of resulting phenotypes may provide hints as to a possible role for *D1* in spermatogenesis. Spermatogenesis is an excellent system for genetic analysis. The stages of spermatogenesis have been well characterized and the cells are large and easy to view cytologically [58]. The extreme cell shape changes that occur during spermatogenesis as well as the occurrence of mitosis, meiosis and spermatid differentiation provide a valuable program for identifying mutants involved in development. Also, chromosome analysis is possible in spermatogonia facilitating a powerful assay method. By viewing the chromosomes of a gain-of-function individual due to *D1* overexpression in the male germline, it may be possible to gain an understanding of how *D1* is behaving. Determining what aspects of a certain process or processes are specifically interrupted due to *D1* overexpression could provide valuable hints as to *D1*'s function.

The somatic cyst cells of the testes were additionally chosen for *D1* overexpression, directed by the *eyes absent* (*clift*) *GAL4* driver. In the adult testes, the somatic cyst cells support gametogenesis and are essential for continued spermatocyte development and viability. Each spermatagonium is encased within a cyst of two somatic cyst cells derived from an individual, somatic stem cell population. Following this, the cyst cell no longer divides but stays associated with the developing germ cell for the duration of spermatogenesis. This suggests that signaling between the two cell lineages regulates gametogenesis. In fact, regulators of stem cell germline lineages have been

identified which act within the soma [63]. If a gain-of-function phenotype occurs when *D1* is overexpressed in the somatic cyst cells, testis development, spermatocyte development or spermatocyte viability may be affected. Characterizing a phenotype due to this overexpression may provide a puzzle piece to the functional analysis of *D1*.

Along with *D1* overexpression specifically in the male, the female germline was also selected in which to ectopically express *D1*. Nanos protein is essential for the maintenance of germline cell fate in the female as well as the male germline [35]. Therefore, *D1* overexpression was directed by the *nanos GAL4* driver to the female germline. Drosophila oogenesis is a genetically valuable system suited for the investigation of key developmental biology questions. Oogenesis is a complex developmental process involving the coordinated differentiation of germ line and somatic cells. The correct execution and timing of cell fate specification and patterning events is achieved during this process, accomplished as a result of different cell-cell signaling pathways. As well, the overall developmental process of oogenesis has been well characterized (reviewed by Gigliotti *et al.*, [38]). All of this together lends to the idea that expressing *D1* during oogenesis could provide valuable information of *D1* function during development.

In the well characterized tissue systems of Drosophila described, *D1* functional analysis was carried out. This study is important in the analysis of *D1* function as it is a stepping stone for further investigation of *D1*. Thus information gained in this analysis is a means to an end in order to thoroughly elucidate *D1* function.
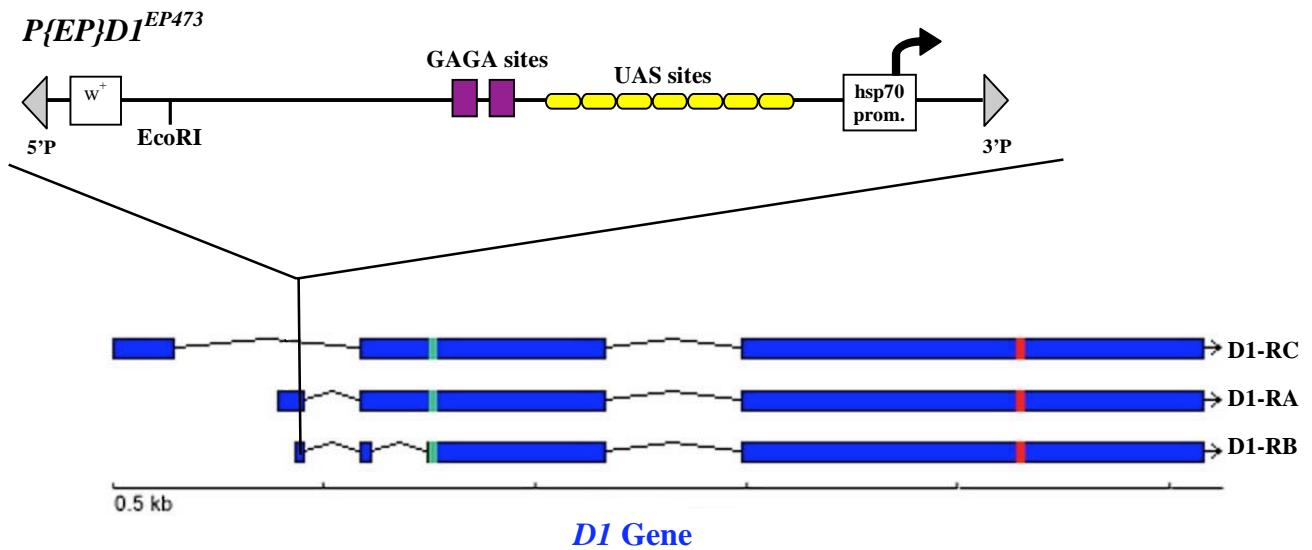
Figure 2.1: *D1* **has three annotated transcripts (blue) indicated as** *D1-RC* **(1814nt),** *D1-RA* **(1734nt) and** *D1-RB* **(1555nt).** *P{EP}473*, [77] is inserted into the 5' UTR of *D1* transcripts A and B. EP elements carry a basal heat shock promoter oriented to direct expression of genomic sequences adjacent to the EP insertion site. The UAS sites bind GAL4 protein to enhance expression in a tissue-specific manner. The translation start site is represented in green and the stop site in red.
(nt, nucleotides)

Materials and Methods

Stocks and culture conditions: Fly stocks and crosses were maintained in cotton-stoppered vials on a cornmeal and agar medium which was supplemented with yeast. Flies were maintained at 25°C unless otherwise noted. Table 2.1 lists the genotypes of strains used in this study. Strains obtained from the Bloomington Stock Center are denoted by B followed by the stock identification number. *eyeless-GAL4* (B8220) and *scaborous-GAL4* [64] flies were generous gifts from Dr. Ashok Bidwai. *eya-GAL4* was a generous gift from Dr. Steve DiNardo [18]. *D1^{Rev1B}* is a precise excision derivative of *P{EP}D1^{EP473}* generated by Dr. Karen S. Weiler (unpublished). All other strains utilized in this study were obtained from the Bloomington Stock Center.

Crosses to induce ectopic expression: Flies overexpressing *D1* were obtained as progeny of *w; P{EP}D1^{EP473}/TM3, Sb* females crossed to males of the *GAL4*-expressing strains listed in Table 2.1. As a control, females of *D1^{Rev1B}/TM3, Sb* were crossed to males of the *GAL4* expressing strains (Table 2.1) in side by side assays. For *GAL4* lines that were homozygous viable, Sb^{+} progeny were examined. For the *eya-GAL4*, *sca-GAL4* and *ey-Gal4* chromosome two lines, Sb^{+}, Cy^{+} progeny were selected. In the case of *twi-GFP* carried on *TM3*, the Dr^{+} progeny were examined. Crosses involving *eyeless-GAL4* were done at 25°C and 29°C utilizing the temperature dependence of *GAL4*. All other crosses to induce ectopic expression were done at 25°C.

Male fertility assay: The test of male fertility was modeled after that of Clark [23]. Males were aged for two days and individually crossed to three to four day old *w^{1118}* virgin females. After four days, each female was placed in an individual vial and the male was discarded. The female was cultured for four days and then discarded. The number of progeny per female was counted at fourteen days and eighteen days. Statistical analysis was performed using Student's t-test analysis with 95% confidence intervals.

The fertility of *eya-GAL/+; P{EP}D1^{EP473}/+* males and *eya-GAL4/+; D1^{Rev1B}/+* control males was also assayed with a less stringent male fertility assay. One two day old male was placed in a vial with three *w^{1118}* virgin and allowed to remain in the vial for nine days. The number of progeny per male was counted at fourteen days and eighteen days.

Female fertility assay: Four day old females were assayed for fertility reduction using a fertility assay in which one female was placed in a vial with two to three w^{1118} males aged for four days. Fertility was determined based on larval activity three days after the cross was set up. Fertility determinations were + (wild-type larval activity), +/- (reduced larval activity indicating reduced fertility) and – (no larval activity indicating sterility).

Crosses to verify *GAL4* expression patterns: w^{1118}; *Dr^{Mio}/TM3, P{GAL4-twi.G}2.3, P{UAS-2xEGFP}AH2.3, Sb^1 Ser^1* virgin females were crossed with *P{UAS-GFP-lacZ}* males and the testes of Dr^+ male progeny were dissected. Sibling Dr^- male testes were utilized as negative controls for beta-galactosidase staining. *D^1/TM6, UAS-lacZ* virgin females were crossed to *eya-GAL4/CyO* males and the testes of D^+, Cy^+ male progeny were dissected. Sibling D^+, Cy^- male testes were utilized as negative controls for beta-galactosidase staining.

Beta-galactosidase staining: Adult male testes were beta-galactosidase stained according to Wolff [92]. Briefly, a 15 to 20 minute fix in 1% formaldehyde in PBS was done followed by three subsequent 10 minute rinses in PBS at room temperature. Samples were incubated in staining solution with the addition of 0.2% X-Gal in DMSO for 45 minutes at 37°C followed by three 10 minute rinses in PBS at room temperature. Testes were mounted in 60% glycerol for viewing with brightfield microscopy.

Testis characterization: Testes were dissected in 0.7% NaCl and whole mounts were prepared. Testes were characterized by overall testis organ morphology, spermatogenic cell morphology and elongated spermatid presence in whole mounts by phase contrast microscopy.

Cytological characterization was carried out with a protocol by Bonaccorsi *et al.,* [17]. Each testis sample was dissected in Ringer's solution and fixed in 45% acetic acid for one minute. Samples were then stained in 3% orcein dissolved in 60% acetic acid for five minutes, rinsed in 60% acetic acid and transferred to 10 microliters of 60% acetic acid placed on a clean slide. Each testis was cut under the dissecting scope to release the contents and followed by the addition of a drop of Lacto-Aceto-Orcein (1:1 lactic acid to 3% orcein in 60% acetic acid). A coverslip was lowered over the specimen and excess liquid was removed from the edges with a piece of blotting paper. The coverslips were

sealed with clear nail polish. Testis preparations were viewed using oil immersion phase contrast microscopy at 1000X magnification.

Synthesis of *sca-GAL4* isogenized line: In order to isolate chromosome 2 bearing the enhancer trap element inserted upstream of the *sca* gene, and replace chromosome 3 and the X chromosome, the original *sca-GAL4* strain was initially outcrossed. Four males were selected as Kr^+, Sb^-, Tb^- progeny from *w; Kr^{If-1}/CyO; D^1/TM6C, Sb^1, Tb^1* females crossed with *w; sca-GAL4/CyO* males. Each *w; sca-GAL4/CyO; +/TM6C, Sb^1, Tb^1* individual male was then crossed to *y w sn^3; Sco/S^2 CyO cn^2 bw* females. S^-, Cy^-, Sb^- male and female progeny of the genotype *y w sn^3/w* & *y w sn^3; sca-GAL4/S^2 CyO cn^2 bw;+/TM6C, Sb^1,Tb^1* were selected for each line and separately mated in order to create stocks. *TM6C, Sb^1, Tb^1* was selected against in the next generation. Four independent *sca-GAL4* lines were established and the bristle phenotype assessed as described below. Two having a phenotype closest to wild-type were used in further experiments.

Bristle analysis: The bristles assayed for presence or absence were the anterior and posterior scutellars, anterior and posterior post-alars, anterior and posterior dorso-centrals and anterior and posterior supra-alars (a total of 16 bristles). Bristle morphology was described as wild-type or short/thin. A minimum of 30 flies were assayed for each strain. Statistical analysis was performed using Student's t-test analysis with 95% confidence intervals.

Table 2.1 Strains used in these experiments
y^1 w; P{w^+; GAL4-nos.NGT}40 (B4442)
w^{1118}; P{w^+; GAL4::VP16-nos.UTR}MVD1 (B4937)
w; P{w^+; GAL4-ninaE.GMR}12 (B1104)
w^{1118}; Dr^{Mio}/TM3, P{w^+; GAL4-twi.G}2.3, P{UAS-2xEGFP}AH2.3, Sb^1 Ser^1 (B6663)
y^1 w^{1118}; P{w^+; ey3.5-GAL4.Exel}2 (B8220)
y^1 w^{1118}; P{w^+; ey3.5-GAL4.Exel}/CyO
y^1 w^{1118}; P{w^+; ey3.5-GAL4.Exel}/TM3, Sb
y^1 w sn^3; GAL4-sca/S^2 CyO cn^2 bw
w ; P{w^+; eya-GAL4}/CyO

Results

Ectopic *D1* expression affects pattern formation and cellular differentiation in the eye.

In order to determine if *D1* may affect cell fate specification, *D1* ectopic expression was targeted to the eye with *eyeless-GAL4*. *eyeless* is expressed in the eye primordia in the embryo and before the morphogenetic furrow at the time of photoreceptor determination in the third instar larva. *D1* expressed in an *eyeless* pattern resulted in *P{EP}D1^{EP473}+; P{ey3.5-GAL4}/+* individuals displaying a rough eye phenotype at 25°C (Figure 2.2) which was exacerbated at 29°C (Figure 2.3). The eye field was reduced in these flies as well. This indicates that misexpressed *D1* may have had an effect on pattern formation resulting in a rough eye phenotype.

The *P{ninaE-GAL4.GMR}* transgene was used to target *D1* expression to all cells in the eye disc behind the morphogenetic furrow. Ommatidial assembly is initiated in the morphogenetic furrow of the late larval eye imaginal disc. Ahead of the furrow, cell division occurs and the nuclei of cells are distributed evenly through the epithelium. As the morphogenetic furrow sweeps anteriorly across the eye imaginal disc, cell division ceases and columns of ommatidia begin to assemble along the length of the furrow [85]. *D1* expression was thus targeted to cells in which pattern formation had been initiated. The resulting flies of *P{GAL4-ninaE.GMR}/+; P{EP}D1^{EP473}/+* genotype all had rough eyes as well as eyes in which a fraction of the ommatidia lacked pigment. (Figure 2.4).

Ectopic *D1* expression affects pattern formation and cellular differentiation in the mechanosensory bristles

In order to determine if *D1* overexpression perturbed cell fate specification elsewhere, *D1* was ectopically expressed in a *scabrous* (*sca*) expression pattern which is initiated early in the imaginal wing disc of the third instar larvae. Specifically, *sca* is expressed in the proneural domains in cells of the wing disc and at high levels in bristle precursors. Initially the *sca* enhancer trap strain utilized had variable ectopic bristles complicating an analysis of the effect of *D1* overexpression. In an attempt to reduce the bristle variability in the original *sca-GAL4* enhancer trap, the strain was outcrossed and

subsequently isogenized replacing the third and the X chromosome. Two *sca-GAL4* lines were chosen to drive ectopic *D1* expression (refer to Materials and Methods for details).

D1 ectopic expression in a *scabrous* pattern resulted in loss of bristles. This is seen for both *sca-GAL4* isogenic lines directing *D1* expression. Table 2.2 illustrates the significant loss of bristles in both the scutellum and the notum due to *D1* overexpression. For experiment one and two with *sca-GAL4* line A, 19 (20.0%) and 4 (6.5%) of *D1* overexpressing flies assayed had at least one bristle missing whereas 1 (1.9%) and 3 (2.8%) of control *sca-GAL4* line A flies exhibited loss of bristles. Experiment one and two with *sca-GAL4* line B resulted in 4 (6.7%) and 21(17.0%) of *sca-GAL4/+; P{EP}D1^{EP473}/+* flies exhibiting bristle loss. In comparison, 3 (4.5%) and 5 (6.3%) control flies displayed a loss of at least one bristle with *sca-GAL4* line B (Table 2.2).

Along with bristle loss, *D1* overexpressing flies had slightly irregular bristles. For *sca-GAL4* line A targeting *D1* expression, approximately 1/8 of the total flies assayed had at least one bristle with abnormal morphology (short/thin) while approximately 1/6 of the total flies in which *D1* was overexpressed with *sca-GAL4* line B had at least one bristle with abnormal morphology. No abnormal bristle morphology was seen in control flies for both *sca-GAL4* lines assayed.

Ectopic *D1* expression early in embryogenesis does not affect fertility.

D1 expression was targeted to the male and female germline by *nanos-GAL4* in order to determine if excess D1 protein would perturb the extensive cell to cell signaling that is required during germline development. A strain carrying a more potent transcription activator, *nanos-GAL4.VP16,* was also utilized in order to drive ectopic *D1* expression at a higher rate.

nanos (*nos*) functions as a posterior determinant in the early embryo as well as in establishing germline/soma dichotomy [35]. *nos* is also expressed later in development during oogenesis and spermatogenesis in adult germline cells [15]. According to Bhat (1999), *nos* is required for the functioning of germline stem cells in both the female and the male adult fly. In *nos* mutants, while the stem cells are specified, these cells divide only a few times at the most and then degenerate. The loss of germline stem cells in *nos*

mutants appears to be due to a progressive degeneration of the plasma membrane ultimately leading to male and female sterility [15].

P{nos-GAL4.NGT}/+; P{EP}D1^{EP473}/+ males showed no significant difference in fertility in comparison to P{nos-GAL4.NGT}/+; P{EP}D1^{Rev1B}/+ assayed with a test for male fertility modeled after that of Clark [23]. Table 2.3 illustrates these results.

P{nos-GAL4.NGT}/+; P{EP}D1^{EP473}/+ females and P{nos-GAL4.VP16}/+; P{EP}D1^{EP473}/+ females showed no difference in fertility in comparison to identical assays with D1^{Rev1B}. These data must be interpreted in the context of the low sensitivity of the fertility assay itself (see Materials and Methods).

Ectopic *D1* expression in somatic cyst cells of the testis causes sterility.

D1 expression was driven in the somatic cyst cells of the male testes by *eyes absent-GAL4* to assay if ectopic *D1* in the germline support cells would disrupt germ cell development. Male testes that express *eyes absent-GAL4* and the reporter *TM6, UAS-lacZ* exhibit a beta-galactosidase staining pattern consistent with somatic cyst cell expression (Figure 2.5) [32].

The fertility of males in which *D1* was overexpressed in an *eyes absent* pattern was assayed using two different methods (see Materials and Methods). Table 2.4 indicates that *D1* overexpression in the somatic cyst cells results in male sterility.

Testes from *eya-GAL4/+; P{EP}D1^{EP473}/+* males were identical to testes from *eya-GAL4/+; P{EP}D1^{Rev1B}/+* males in organ morphology. Unlike testes of *eya-GAL4/+; P{EP}D1^{Rev1B}/+* males though, motile sperm were not present in *eya-GAL4/+; P{EP}D1^{EP473}/+* testes. In fact, elongated spermatid were present in *D1*-overexpressing individual testis but were non-motile and thus nonfunctional. *eya-GAL4/+; P{EP}D1^{Rev1B}/+* testes exhibited motile sperm in the seminal vesicles and in the surrounding fluid.

Further testis characterization focused on the stages of spermatogenesis. In testis of wild-type flies, primary spermatocytes are present in high numbers and are relatively large in volume as these cells undergo four mitotic divisions followed by growth in which they experience an approximate 25-fold increase in volume (reviewed by Fuller [36]). Following this, primary spermatocyte cells undergo meiosis I and meiosis II in

metasynchrony resulting in a cyst of 64 interconnected haploid spermatids. All stages of spermatogenesis were represented in the testes of *eya-GAL4/+; P{EP}D1^{EP473}/+* males but with an excess of early and late primary spermatocytes. Primary spermatocytes were present in high numbers noted by 16 cell cysts and cells of relatively large volume as the primary spermatocyte cells undergo four mitotic divisions followed by growth in which they increase by approximately 25 times in volume. Following the primary spermatocyte stage, 16 cell cysts undergo meiosis I and meiosis II in metasynchrony resulting in a cyst of 64 interconnected haploid spermatids. At this point, spermatid tails lengthen resulting in bundles of elongated spermatid (reviewed by Fuller [36]).

In *eya-GAL4/+; P{EP}D1^{EP473}/+* male testes, there was an accumulation of primary spermatocytes and all meiotic stages were underrepresented (Figure 2.7B). As in Figure 2.7A, wild-type flies and flies of *eya-GAL4/+; P{EP}D1^{Rev1B}/+*, elongated sperm tails fill the majority of the testis tube with 64 cell cysts in differing stages of spermatid elongation interspersed amongst the tails. *eya-GAL4/+; P{EP}D1^{EP473}/+* male testes exhibit a reduction in elongated spermatids and 64 cell cysts.

In examining the meiotic stages closer, it can be seen that the 64 cell cysts, often termed to be onion-stage spermatid cysts, are aberrant. In wild-type testes, after the late primary spermatocytes enter meiosis giving rise to 64 haploid spermatids, the nucleus in each spermatid reforms and the mitochrondria fuse to form the mitochrondrial derivative, termed the nebenkern. Both of these structures in wild-type testes are highly uniform in size and shape and are in a 1:1 ratio [37]. In testes of *eya-GAL4/+; P{EP}D1^{EP473}/+* individuals, the nebenkern and nuclei of the 64 cell cysts are not in a 1:1 ratio (Figure 2.8).

Ectopic *D1* overexpression in mesodermal tissue also affects male fertility.

D1 expression was driven in the mesoderm in a *twist* (*twi*) expression pattern. Males that overexpress *D1* via the *twist* promoter show a significant fertility reduction. *P{EP}D1^{EP473}/ TM3, P{GAL4-twi}, P{UAS-2xEGFP}* males sired significantly less progeny than control males, *D1^{Rev1B}/ TM3, P{GAL4-twi}, P{UAS-2xEGFP}* (Table 2.5). In order to investigate this fertility reduction further, male testis of adults in which *D1* was ectopically expressed in a *twist* pattern were dissected and assayed for abnormal

morphology by whole mount analysis and phase contrast microscopy. Morphological comparisons between control testes and *D1* overexpression testes showed no difference in size, sperm mobility, or the morphology of cells involved in each stage of spermatogenesis.

Because *twist* is a transcription factor which initiates Drosophila mesoderm development it was difficult to know exactly where *D1* was being expressed ectopically that resulted in the male fertility reduction. In order to determine where in the testis *twi* is expressed, a strain with a *UAS-lacZ* reporter construct was introduced. *TM3, P{GAL4-twi}, P{UAS-2xEGFP}/P{UAS-GFP-lacZ}* adults testes were dissected and stained for beta-galactosidase activity. This revealed that *twi* is expressed in the ejaculatory duct of the male testis (n=32) (Figure 2.6). The male ejaculatory duct in Drosophila functions in propelling sperm out of the testes in the transfer to the female during mating. Several genes are expressed in the ejaculatory duct as well whose products elicit specific responses in the female such as increase in egg laying rates and reduction in sexual receptivity [75].

Figure 2.2: *D1* **overexpression in an** *eyeless* **pattern at 25°C results in a rough eye phenotype.** Adult eyes of (A) *P{EP}D1^{EP473}/TM3, Sb* compared to (B) *P{EP}D1^{EP473}/+;Ey-GAL4/+* individuals incubated at 25°C.

Figure 2.3: *D1* **overexpression in an** *eyeless* **pattern at 29°C results in a rough, reduced eye phenotype.** Adult eyes of (A) *P{EP}D1^{EP473}/TM3, Sb* compared to (B) *P{EP}D1^{EP473}/+;Ey-GAL4/+* individuals incubated at 29°C.
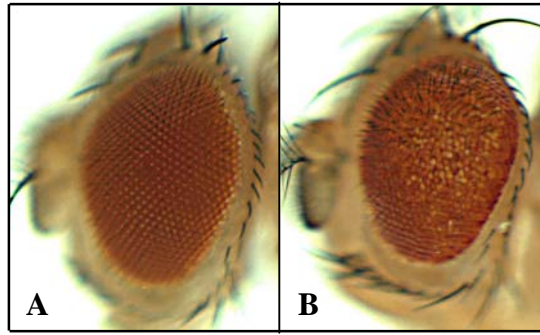
Figure 2.4: *D1* **overexpression in a** *ninaE* **pattern at 25°C results in a rough eye phenotype with a fraction of the ommatidia lacking pigment.** Adult eyes of (A) *P{GAL4-ninaE.GMR}/+; +/TM3, Sb* compared to (B) *P{GAL4-ninaE.GMR}/+; P{EP}D1^{EP473}/+* individuals incubated at 25°C.

Table 2.2: The effect of *D1* overexpression in a *scabrous* pattern on bristle number and morphology

Genotype		# flies assayed	Average bristle # on notum	Average bristle # on scutellum	Bristle phenotype				Abnormal bristles
					wild-type (%)	ectopic bristles only (%)	loss of bristles only (%)	ectopic and loss of bristles (%)	# flies with short/thin bristles
sca-GAL4/+; P{EP}D1[EP473]/+ Line A	Experiment 1	95	15.8[a]	3.9[b]	65 (68%)	11 (12%)	19 (20%)	0 (0%)	16[e]
	Experiment 2	61	15.9[a]	3.9[b]	45 (74%)	9 (15%)	4 (6%)	3 (5%)	7[e]
sca-GAL4/+; D1[Rev1B]/+ Line A	Experiment 1	51	16.4	4.3	33 (65%)	16 (31%)	1 (2%)	1 (2%)	0
	Experiment 2	104	16.4	4.3	76 (73%)	25 (24%)	3 (3%)	0 (0%)	0
sca-GAL4/+; P{EP}D1[EP473]/+ Line B	Experiment 1	48	16.1[c]	4.1[d]	35 (73%)	6 (13%)	4 (8%)	3 (6%)	10[f]
	Experiment 2	123	16.1[c]	4.1[d]	68 (55%)	32 (26%)	21 (17%)	2 (2%)	22[f]
sca-GAL4/+; D1[Rev1B]/+ Line B	Experiment 1	48	16.3	4.3	30 (63%)	13 (27%)	3 (6%)	2 (4%)	0
	Experiment 2	112	16.3	4.3	76 (68%)	29 (26%)	5 (4%)	2 (2%)	0

[a]Two sample paired t-test analysis with 95% confidence intervals indicate a significant difference in the number of notal bristles t(154)=5.1855, p<0.0001 compared with the control
[b]Two sample paired t-test analysis with 95% confidence intervals indicate a significant difference in the number of scutellar bristles t(154)=4.5611, p<0.0001 compared with the control
[c]Two sample paired t-test analysis with 95% confidence intervals indicate a significant difference in the number of notal bristles t(171)=2.4559, p<0.0152 compared with the control
[d]Two sample paired t-test analysis with 95% confidence intervals indicate a significant difference in the number of scutellar bristles t(171)=2.4264, p<0.0165 compared with the control
[e]Two sample sample paired t-test analysis with 95% confidence intervals indicate a significant difference in the number of abnormal bristles t(154)=5.1773, p<0.0001 compared with the control
[f]Two sample sample paired t-test analysis with 95% confidence intervals indicate a significant difference in the number of abnormal bristles t(171)=6.2559, p<0.0001 compared with the control

Table 2.3: The effect of *D1* overexpression in a *nanos* pattern on male fertility

Genotype		# males assayed	Average progeny per fertile male	Average % females giving progeny	Average # progeny per fertile female (SD)[a]	# fertile males
P{nosGAL4.NGT}/+; P{EP}D1^{EP473}/+	Experiment 1	24	82.9	80.2%	11 (13.2)[b]	23
	Experiment 2	24	85.0	83.0%	10.5 (7.1)[b]	24
P{nos-GAL4.NGT}/+; D1^{Rev1B}/+	Experiment 1	24	65.6	83.0%	9 (7.8)	23
	Experiment 2	24	81.9	82.0%	10.3 (6.9)	24

[a]standard deviation (SD)
[b]A two sample paired Student's t-test analysis with 95% confidence intervals indicates no significant difference t(47)=1.6785, p=0.0999

Table 2.4: The effect of *D1* overexpression in the somatic cyst cells of the testis on male fertility

Genotype		# males assayed	Average progeny per fertile male	Average % females giving progeny	Average # progeny per fertile female (SD)[a]	# fertile males
P{eya-GAL4}/+;P{EP}D1^EP473/+	Experiment 1[b]	20	0	0.0%	0 (0)	0
	Experiment 2[b]	20	0	0.0%	0 (0)	0
	Experiment 3[c]	10	0	0.0%	0 (0)	0
P{eya-GAL4}/+;D1^Rev1B/+	Experiment 1[b]	20	45	30.3%	14.7 (6.5)	18
	Experiment 2[b]	20	25	12.3%	19.8 (3.7)	15
	Experiment 3[c]	10	28	66.4%	14.9 (5.9)	9

[a]standard deviation (SD)
[b]test of male fertility modeled after that of Clark (1990)
[c]less stringent test of male fertility
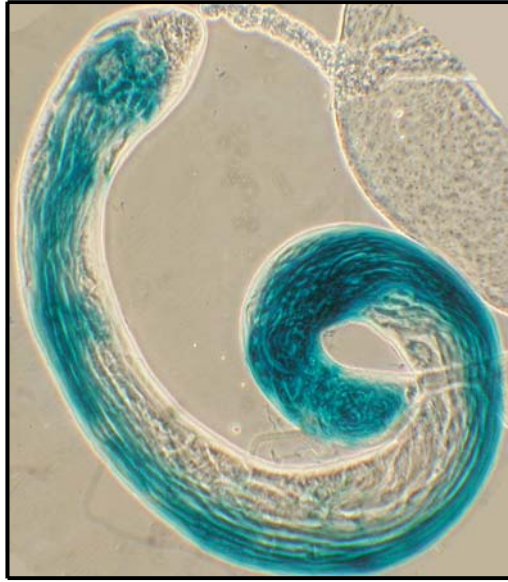
Figure 2.5: *eyes absent* **is expressed in the somatic cyst cells of the male testis.** Beta-galactosidase stained *eya-GAL4/+; TM6, UAS-lacZ/+* testis viewed by phase contrast microscopy.

Figure 2.6: *twist* **is expressed in the ejaculatory duct of the adult male testis.** Beta-galactosidase stained *TM3, P{GAL4-twi.G}, P{UAS-2xEGFP}, Sb[1] Ser /P{UAS-GFP-lacZ}* testis viewed by bright field microscopy.
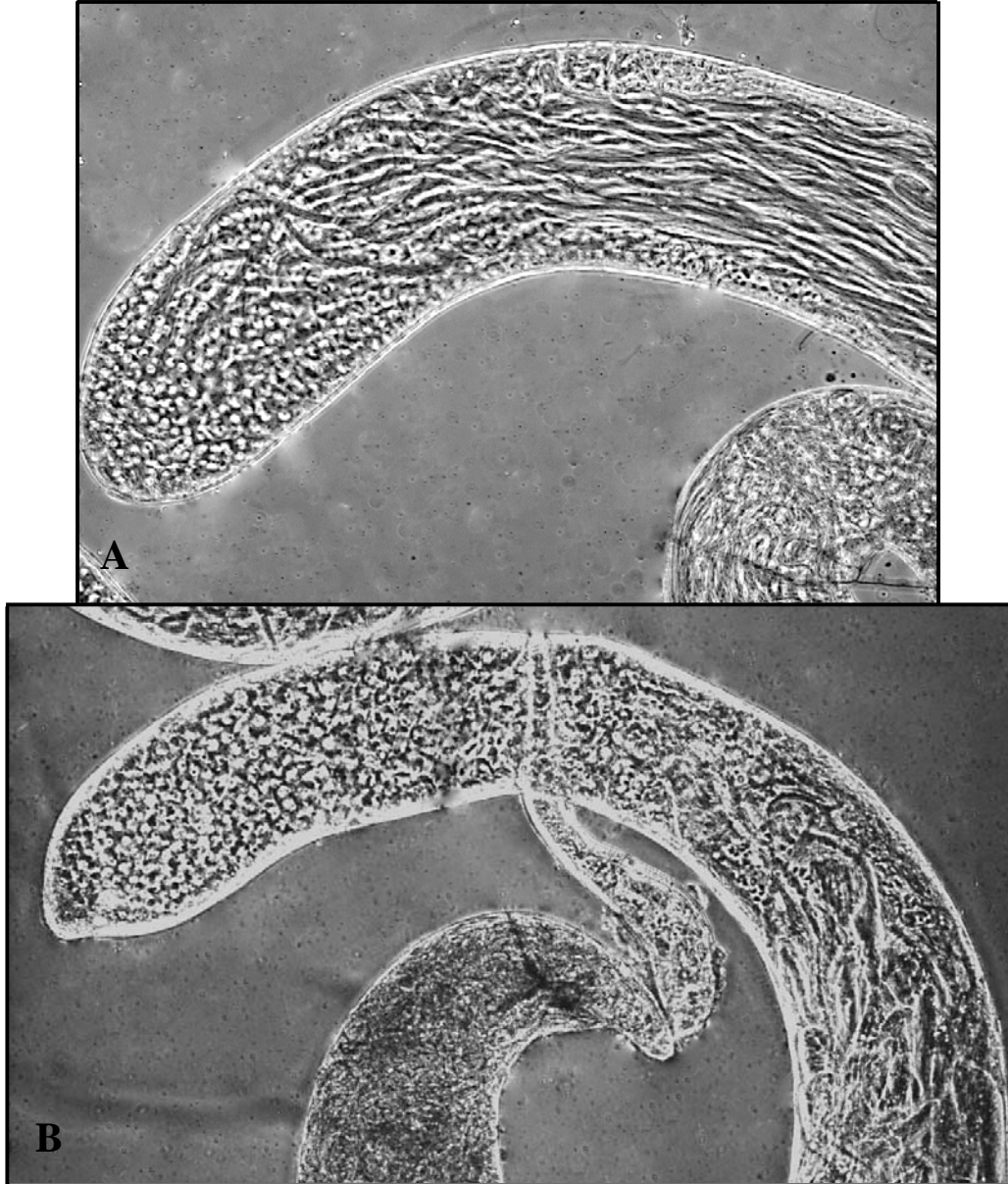
Figure 2.7: Testes of males in which *D1* is expressed in an *eyes absent* pattern exhibit arrest of spermatogenesis. Adult testis of (A) *P{eya-GAL4}/+; D1^{Rev1B}/+* exhibit wild-type spermatogenesis while (B) *P{eya-GAL4}/+; P{EP}D1^{EP473}/+* display an accumulation of mature primary spermatocytes and an underrepresentation of post meiotic cells as visualized by phase contrast microscopy.
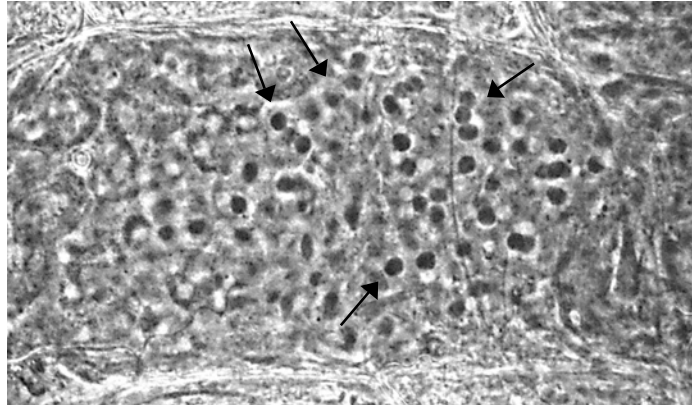
Figure 2.8: Testes of males in which *D1* is expressed in an *eyes absent* pattern have abnormal 64 cell cysts. Wild-type spermatids contain one nebenkern (dark circle) and one nucleus (pale circle). Nebenkern and nuclei of *P{eya-GAL4}/+; P{EP}D1^{EP473}/+* testes are not in a 1:1 ratio. Arrows indicate excess nebenkern; visualized by phase contrast microscopy.

Table 2.5: The effect of *D1* overexpression in a *twist* pattern on male fertility

Genotype		# males assayed	Average progeny per fertile male	Average % females giving progeny	Average # progeny per fertile female (SD)[a]	# fertile males
P{EP}D1^{EP473}/TM3, P{GAL4-twi), P{UAS-2xEGFP}	Experiment 1	25	84	35%	29 (21.5)[b]	14
	Experiment 2	25	108	58%	19 (14.3)[b]	19
D1^{Rev1B}/ TM3, P{GAL4-twi), P{UAS-2xEGFP}	Experiment 1	25	217	95%	23 (10.2)	25
	Experiment 2	25	154	97%	16 (11.3)	25

[a]standard deviation (SD)
[b]A two sample paired Student's t-test analysis with 95% confidence intervals indicates that the fertility reduction of D1 overexpressing males is significant t(49)=5.1679, p<0.0001

Discussion

Ectopic *D1* expression in the eye and the mechanosensory bristles results in abnormal morphology as well as bristle loss.

Overexpression analysis indicates that *D1* could have a role in the process of pattern formation and cell differentiation during Drosophila eye and bristle formation. The compound eye of Drosophila consists of several hundred ommatidia each containing a stereotyped arrangement of photoreceptor, pigment and cone cells. These ommatidia develop during late larval and pupal life in the eye imaginal disc in a process that involves the recruitment of undifferentiated epithelial cells into gradually growing ommatidial clusters (reviewed by Tomlinson [86]). Ommatidial assembly is initiated in the morphogenetic furrow which sweeps anteriorly across the eye imaginal disc with time. Ahead of the furrow, cell division occurs and the nuclei of cells are distributed evenly through the apical/basal axis of the epithelium.

A rough eye phenotype is a result of disruption of an early stage of ommatidial assembly in the developing Drosophila eye imaginal disc [28; 44; 85]. *D1* overexpression driven by *eyeless-GAL4* and *GAL4-ninaE.GMR* both result in flies with rough eyes. One interpretation of this result is that ectopic *D1* could be perturbing a stage of ommatidial assembly in the developing eye imaginal disc resulting in cells that do not attain the correct cell fate. *eyeless* targeted *D1* expression in the Drosophila eye disc before the morphogenetic furrow at the time of photoreceptor determination. *ninaE* drove *D1* expression to cells in the eye disc behind the morphogenetic furrow thus targeting *D1* expression to cells in which the cell specification pathway had been activated. I hypothesize that because individual cells had began the process of pattern formation, *D1* expression did not alter their fate as drastically as cells in which *D1* was expressed prior to cell fate specification.

Ectopic *D1* expression driven by *scabrous* results in a significant loss of bristles as well as bristles with an altered morphology. This indicates that prior to neuronal bristle cell fate specification, ectopic *D1* may have perturbed cell specification such that these cells adopted an epidermal fate. Thus, bristle development for that cluster of cells would be halted because no cells would be present possessing neuronal fate resulting in the adult as a loss of bristle. A fraction of flies in which *D1* was overexpressed exhibited

bristles that were short and thin. Perhaps ectopic *D1* in a *scabrous* pattern did not disturb bristle cell fate specification sufficiently in these cells to result in loss of bristle but altered pattern formation of the neuronal cell enough to result in abnormal bristle cell development.

Further studies are necessary in order to determine the mechanism of this perturbation. One hypothesis is that ectopic D1 protein is directly disturbing the eye as well as the bristle specification signal transduction pathway by binding to a required transcription factor and interfering with its ability to bind downstream. This is likely if one or more of the proteins involved in each pathway have satellite-related sequences or are AT-rich in general.

Another hypothesis is that excess *D1* protein is indirectly disturbing cell specification by binding to AT-rich DNA sequences and negatively regulating transcription. Thus, the signal transduction pathway would be disrupted resulting in abnormal neuronal cell specification. If the D1 protein is directly or indirectly altering the neuronal cell specification pathway of the eye and bristle cell lineage, it would be beneficial to determine the mechanism of D1 interference.

An alternative hypothesis to the disruption of cell fate specification by D1 is that overexpression of *D1* disrupted gene expression in a generalized manner resulting in abnormal morphology and bristle loss in these flies. Ectopic D1 protein could have directly or indirectly disturbed normal gene expression in a widespread manner by binding to areas of the DNA or transcription factors necessary for normal development. Such a generalized disruption could be exhibited as abnormal development and/or lethality.

Both of the above hypotheses explaining the abnormal bristle and eye morphology and bristle loss of flies in which *D1* was overexpressed are equally likely. Further studies are necessary to investigate these hypotheses, perhaps providing clues of *D1* function in wild-type flies.

Ectopic *D1* expression early in embryogenesis does not affect male or female fertility.

Male and female fertility was investigated in flies in which *D1* was overexpressed

in the germline using *nanos-GAL4*. Assays of *D1* overexpression driven by *nanos-GAL4* indicate that *D1* overexpression in a *nanos* pattern did not have an affect on female or male fertility. This was surprising in that oogenesis and spermatogenesis are highly regulated systems and overexpression of a chromosomal DNA binding protein would likely have some effect on gamete formation and thus fertility. An effect on female fertility may have been missed, though, due to the assay itself, which did not allow for noting slight fertility reductions. Another possibility for the lack of effect on female or male fertility due to *D1* overexpression is that UAS transgenes are poorly expressed in both the male and female germline [66]. To overcome this, investigators have tried numerous combinations of drivers and targets in the male and female germline to assess for high levels of expression and found that the expression level of a UAS transgene in the germline is dependent on the number of drivers utilized [66]. Therefore, *D1* overexpression in the germline most likely was very slight with the use of only one *GAL4* driver. If ectopic *D1* had been targeted by multiple transgenes, perhaps an affect on fertility would have been present. If ectopic *D1* targeted to the germline resulted in a fertility reduction or sterility, it would be interesting to assay what protein or sequences ectopic *D1* protein was interfering with to aid in determining *D1* function. This would be especially interesting in the male in light of the presence of a testis specific promoter on one of the three *D1* transcripts.

Ectopic *D1* expression in somatic cyst cells of the testis causes sterility.

D1 overexpression was targeted to the somatic cyst cells of the male testes with *eyes absent-GAL4*. During spermatogenesis, the somatic cyst cells support gametogenesis and are essential for wild-type spermatid development. *D1* overexpression targeted to these cells resulted in male sterility. I observed abnormal events during the meiotic divisions of spermatogenesis, as the meiotic stages were underrepresented and the onion-stage spermatid 64 cell cysts were aberrant. According to Fuller [36], for most male-sterile mutants, spermatogenesis proceeds despite defects in one or even several morphogenetic events leading to production of aberrant spermatids. This has been investigated and validated for many spermatogenic mutants determined to be necessary for meiotic cell cycle progression and cell

differentiation (reviewed by Fuller [36]). This is the case in individuals overexpressing *D1* with *eyes absent-GAL4* in that elongated spermatids are present in low amounts compared to wild-type but are non-motile. In addition, males in which *D1* is overexpressed by *eyes absent*, accumulate primary spermatocytes but lack the appropriate amount of the following spermatogenic cell types.

I hypothesize that ectopic *D1* in the somatic cyst cells is interfering directly or indirectly with genes required for the meiosis and spermatid morphogenesis of spermatogenesis resulting in a meiotic-arrest phenotype and sterility. In wild-type Drosophila, germline stem cells divide to produce spermatogonia. After four mitotic amplification divisions, spermatogonia cells become primary spermatocytes, committed to differentiation. This developmental transition results in transcriptional activation in primary spermatocytes of a large suite of genes required for meiosis and spermiogenesis. In Drosophila, transcription stops before the meiotic divisions, so transcripts for late-acting proteins are made pre-meiotically.

The genetic pathways involved in the meiotic-arrest phenotype of spermatogenesis are in the process of being elucidated. Ten "spermatocyte arrest" genes have been found to be required for both meiosis and differentiation and are sorted into two classes according to their molecular targets and specific role in promoting transcription [11; 39; 46; 49; 59; 70]. The *always early* (*aly*) class affects transcription of meiotic genes such as *boule, twine* and *cyclin B* [89] and are thought to alter chromatin structure to permit the high levels of transcription necessary in spermatocytes [11; 49; 70; 90]. Less is known about the second class of genes, the *cannonball* (*can*) class which functions mainly in cell differentiation post transcriptionally [89]. Both classes of genes work independently and but converge in the later stages of spermatogenesis to regulate the twine protein, which is required for both male and female meiotic divisions [25; 91]. This regulatory circuit is a "fail-safe mechanism" to ensure that transcripts required for post-meiotic differentiation are expressed before allowing entry into the first meiotic division [89; 90]. A mutation in a gene of the *always early* or *cannonball* class of genes results in a meiotic-arrest phenotype indicated by an accumulation of primary spermatocytes with decreasing amounts of ensuing spermatogenic cells as well as sterility. It is difficult to determine which class of spermatocyte arrest genes *D1* may be

interfering with without further analysis. Ectopic D1 with its ten AT-hook binding domains could be disrupting normal chromatin alterations made by the *always early* class of genes or in the regulation of the *cannonball* class of genes. Establishing this would be beneficial in determining the function of *D1* in wild-type flies.

Another hypothesis to explain the meiotic-arrest phenotype of spermatogenesis in flies in which *D1* is overexpressed by *eyes absent* is that ectopic *D1* may be interfering in a generalized manner and disrupting widespread gene expression. This hypothesis is less likely due to that fact that flies in which *D1* was overexpressed by *eyes absent* were not morphology abnormal as *eyes absent* is expressed elsewhere in the fly as well. If ectopic *D1* expression disturbed gene expression in a generalized manner, I would expect an abnormal morphology of these flies.

Ectopic *D1* overexpression in mesodermal tissue affects male fertility.

D1 overexpression driven by *twist-GAL4* resulted in male fertility reduction. Assays of the *twist* expression pattern in the testes determined it to be in the ejaculatory duct. The ejaculatory duct of the Drosophila male testes functions in propelling sperm out of the testes in the transfer to the female during mating. Perhaps ectopic *D1* interfered with the pathway leading to proper muscle development in the ejaculatory duct rendering it unable to properly propel sperm out of the testes. The fact that testes of *D1*-overexpressing individuals appeared wild-type in organ morphology, spermatocyte morphology and had motile sperm present supports the idea that functional sperm are formed but do not get transferred to the female. The male fertility reduction present indicates that perhaps the ejaculatory duct is able to transfer a small amount of sperm but not as in wild-type.

Another possibility to explain the reduction in fertility of males overexpressing *D1* in a *twist* pattern is that these males cannot physically mate. *twist* is expressed in the developing mesoderm early in development, which results in tissue throughout much of the adult fly. Therefore, *D1* was ectopically expressed in areas other than the ejaculatory duct. Assays were only done to determine the location of *twist* expression and thereby *D1* ectopic expression in the testes. Perhaps ectopic *D1* interfered with mesoderm development elsewhere in the fly leading to problems in a tissue involved in the act of

mating, like muscles. The fact that *D1*-overexpressing individuals appear wild-type in activity and health makes this hypothesis less attractive. Even though this is the case, it is important to note that males have an additional muscle not present in females that is required for mating. Despite the fact that flies in which *D1* was expressed appeared active and healthy, ectopic *D1* could have had an effect on this muscle solely.

An additional possibility to explain the fertility reduction is that males in which *D1* was overexpressed in a *twist* pattern produce only a fraction of viable sperm when compared to wild-type. This is unlikely, though, as all of the stages of spermatogenesis were represented and appeared wild-type in cell quantity and morphology.

Chapter Three: Analysis of ubiquitous *D1* expression

Introduction

Ubiquitous overexpression of the *D1* gene was utilized in this study as a means of determining *D1* function with three drivers of *GAL4* expression, *hsp70-GAL4*, *tubulin-GAL4* and *actin-GAL4*. Analyzing the result of ubiquitous *D1* overexpression is a potential means of gaining insight into *D1* function in wild-type flies. By assaying gain-of-function phenotypes at specific stages of the Drosophila life cycle, clues of *D1* function may be obtained.

Materials and Methods

Stocks and culture conditions: Fly stocks and crosses were maintained in cotton-stoppered vials on a cornmeal and agar medium which was supplemented with yeast. Flies were maintained at 25°C unless otherwise noted. Table 3.1 lists the full genotypes of strains used in this study. All stocks were obtained from the Bloomington Stock Center (denoted by B followed by stock identification number).

Crosses to induce ectopic expression: Flies overexpressing *D1* in a *tubulin* or *actin* expression pattern were obtained as Sb$^+$ progeny of *w; P{EP}D1^{EP473}/TM3, Sb* females crossed to *y w; P{w$^+$; tubP-GAL4}/TM3, Sb* males and Sb$^+$, Tb$^+$ progeny of *w; P{EP}D1^{EP473}/TM3, Sb* females crossed to *y w; P{w$^+$; Act5C-GAL4}/TM6B, Tb* males. *P{w$^+$; hsp70-GAL4}/+; P{EP}D1^{EP473}/+* flies were obtained as Sb$^+$, Cy$^+$ progeny of *w; P{EP}D1^{EP473}/TM3, Sb* females crossed to *P{w$^+$; hsp70-GAL4}/CyO* males at 25°C. *w; P{EP}D1^{EP473}/ TM3, Ser, P{w$^+$; hs-GAL4}, P{w$^+$; UAS-GFP}* flies were obtained as Sb$^+$, Tb$^+$, Ser progeny of *w; P{EP}D1^{EP473}/TM3, Sb* females crossed to *w; TM6B, Tb/TM3, Ser, P{w$^+$; hsp70-GAL4}, P{w$^+$; UAS-GFP}* males at 25°C. As a control, *w; P{EP}D1^{Rev1B}/TM3, Sb* virgin females were used in the above crosses instead of *w; P{EP}D1^{EP473}/TM3, Sb* females. Progeny from each cross were scored and counted according to the presence of dominant markers indicating genotype. These numbers were compared to genotype expected progeny values in order to assay for reduced viability or lethality of progeny classes.

Lethal phase analysis: *P{w$^+$; tubP-GAL4}LL7/TM3, P{GAL4-twi.G}2.3, P{UAS-2xEGFP}* and *P{w$^+$; Act5C-GAL4}/ TM3, P{GAL4-twi.G}2.3, P{UAS-2xEGFP}* females were derived from crossing *y w; P{tubP-GAL4}LL7/TM3, Sb* females and *y w; P{Act5C-*

GAL4}17bFOI/TM6B, Tb females with *w^{1118}; Dr^{Mio}/TM3, P{GAL4-twi.G}2.3, P{UAS-2xEGFP} Sb, Ser* males, respectively and selecting Dr⁺, Tb⁺ progeny. They were mated to *P{EP}D1^{EP473}/P{w⁺; UAS-GFP-lacZ}* males obtained by selecting Sb⁺ progeny from a cross of *P{EP}D1^{EP473}/TM3, Sb* virgin females with *P{UAS-GFP-lacZ}* males.

Figure 3.1 displays the experimental setup of lethal phase analysis of *D1* overexpressing flies in an *actin* pattern. The same setup was utilized for ectopic *D1* expression in a *tubulin* pattern. Approximately 300 virgin females were mated with 100 males in the presence of fresh yeast paste at 25°C a minimum of two days prior to embryo collections. Embryo collections were on grape-apple juice egg laying plates supplemented with yeast paste. Embryos were scored for fluorescence approximately three hours after egg laying.

Approximately 30 hours after egg laying, first instar *w; P{EP}D1^{EP473}/P{w⁺; Act5C-GAL4}* larvae and control first instar *P{w⁺; Act5C-GAL4}/P{w⁺; UAS-GFP-lacZ}* larvae differentiated via fluorescence microscopy, were collected. The *w; P{EP}D1^{EP473}/P{w⁺; Act5C-GAL4}* larvae did not exhibit green fluorescence. Control *P{w⁺; Act5C-GAL4}/P{w⁺; UAS-GFP-lacZ}* first instar larvae could be distinguished from other green-fluorescing progeny via the presence of GFP versus EGFP. Larvae of each genotype were placed in individual culture vials in groups of 10 to 15 and their survival and developmental progression were monitored daily. Upon lethality, larval mouthhooks were dissected and viewed with brightfield microscopy to determine the lethal stage. Unhatched embryos that did not fluoresce were viewed under mineral oil by bright field microscopy to determine if they were fertilized and if so, the embryonic stage of lethality. Unfertilized eggs were subtracted from the data. Unhatched embryos that fluoresced green were beta-galactosidase stained to determine the genotype.

20-Hydroxyecdysone feeding: Figure 3.2 illustrates the setup for 20-hydroxyecdysone (20-HE) feeding. *P{EP}D1^{EP473}/P{w⁺; tubP-GAL4}* and *P{w⁺; tubP-GAL4}/P{w⁺; UAS-GFP-lacZ}* first instar larvae were obtained as described in lethal phase analysis, above. Larvae of each genotype were placed in separate culture vials supplemented with 15 ul of a 0.5 ug/ul 20-hydroxyecdysone in 10% ethanol yeast paste solution in groups of 10 to 15. 10-15 *P{EP}D1^{EP473}/P{w⁺; tubP-GAL4}* larvae were placed in a vial containing 15 ul of a 10% ethanol yeast paste solution as the negative control (Figure 3.2). Fresh

supplements were added daily. Variations of this feeding assay included increasing the 20-HE concentration to 1.0 ug/ul, and either exposing the larvae to the supplement from the start (as above) or delaying addition until 40 hours post larval eclosion.

Vials of all assays were maintained at 25°C and monitored daily for survival. Upon lethality, larval mouthhooks were dissected and viewed under brightfield microscopy to determine the lethal stage. 20-HE was purchased from Alexis Biochemicals.

Enhancer trap analysis: Approximately 300 *P{lacW}br, w/FM7B y w^a; P{w$^+$; tubP-GAL4}/ TM3, P{w$^+$; twi-GAL4}, P{w$^+$; UAS-EGFP}* or *FM7B y w^a/y w ; cn^1 P{ry$^+$; PZ}Kr-h1/ CyO, Ts, Kr, y$^+$; P{w$^+$; tubP-GAL4}/ TM3, y$^+$, Ser* virgin females were crossed to 100 *y w; P{EP}D1^{EP473}/ P{w$^+$; UAS-mCD8-GFP}* males in the presence of fresh yeast paste at 25°C. Embryos were collected on grape-apple juice egg laying plates supplemented with yeast paste a minimum of two days after the cross was set up. Upon hatching, first instar larvae were scored for fluorescence and y versus y$^+$ to differentiate progeny classes (Figure 3.3 and 3.4). Larvae of the genotypes *P{lacW}br, w/y w; P{w$^+$; tubP-GAL4}/ P{EP}D1^{EP473}* (experimental) and *P{lacW}br, w/ y w; P{w$^+$; tubP-GAL4}/ P{w$^+$; UAS-mCD8-GFP}* (control) for the *broad* enhancer trap analysis and *cn^1 P{ry$^+$; PZ} Kr-h1/+; P{w$^+$; tubP-GAL4}/ P{EP}D1^{EP473}* (experimental) and *cn^1 P{ry$^+$; PZ}Kr-h1/+ ; P{w$^+$; tubP-GAL4}/P{w$^+$;UAS-mCD8-GFP}* (control) for the *Kruppel-homolog* analysis were placed in separate culture vials in groups of 10 to 15. All individuals were aged to the late second larval instar stage (65 to 68 hours after egg laying) and beta-galactosidase stained.

Beta-galactosidase staining: Unhatched, fluorescing embryos from lethal stage analyses and late second larval instars from enhancer trap analyses were beta-galactosidase stained according to Wolff [92]. A 15 to 20 minute fix in 1% formaldehyde in PBS was done followed by three subsequent 10 minute rinses in PBS at room temperature. Samples were incubated in staining solution with the addition of 0.2% X-Gal in DMSO for 45 minutes at 37°C followed by three 10 minute rinses in PBS at room temperature. Embryos and larvae were mounted in 60% glycerol for viewing with brightfield microscopy.

Table 3.1 Strains used in these experiments
y^1 w; P{w$^+$; Act5C-GAL4}17bFOI/TM6B, Tb^1 (B3954)
y^1 w; P{w$^+$; Act5C-GAL4}/25FOI/Cyo, y$^+$ (B4414)
y^1 w; P{w$^+$; tubP-GAL4}LL7/TM3, Sb^1 (B5138)
w^1; TM6B/TM3, P{w$^+$; GAL4-Hsp70.PB}TR2, P{w$^+$; UAS-GFP.Y}TR2, y$^+$, Ser (B5704)
w; P{w$^+$; GAL4-Hsp70.PB}2/CyO (B2077)
w^{1118}; Dr^{Mio}/TM3, P{w$^+$; GAL4-twi.G}2.3, P{UAS-2xEGFP}AH2.3, Sb^1 Ser^1 (B6663)
y^1 w; P^{in}{Yt}/CyO; P{w$^+$; UAS-mCD8-GFP.L}LL6 (B5130)
cn^1, P{ry$^+$; PZ}Kr-h1^{10642}/CyO; ry^{506} (B12380)
P{w$^+$; lacW}br^{G0318} w^{67c23}/FM7c (B10832)
y^1 w; TM3, y$^+$, Ser^1/Sb^1 (B1614)
y^1 w; Chi$^{e5.5}$/CyO, Ts(Y;2Lt) B80 Kr, y$^+$ (B4541)
y^1 w; P{UAS-GFP-lacZ.nls}15.3 (B6451)

$$\frac{P\{w^+;\ Act5C\text{-}GAL4\}}{TM3,\ P\{w^+;\ twi\text{-}GAL4\},\ P\{w^+;\ UAS\text{-}EGFP\}} \quad X \quad \frac{P\{EP\}D1^{EP473}}{P\{w^+;\ UAS\text{-}GFP\text{-}lacZ\}}$$

Expected Progeny:	Expected Fluorescence:	B-galactosidase stain:	Viability:
$\dfrac{P\{EP\}\ D1^{EP473}}{P\{w^+;\ Act5C\text{-}GAL4\}}$	Yellow (yolk)	----	?
$\dfrac{P\{EP\}D1^{EP473}}{TM3,\ P\{w^+;\ twi\text{-}GAL4\},\ P\{w^+;\ UAS\text{-}EGFP\}}$	Green	----	Viable
$\dfrac{P\{w^+;\ Act5C\text{-}GAL4\}}{P\{w^+;\ UAS\text{-}GFP\text{-}lacZ\}}$	Green	Blue	Viable
$\dfrac{P\{w^+;\ UAS\text{-}GFP\text{-}lacZ\}}{TM3,\ P\{w^+;\ twi\text{-}GAL4\},\ P\{w^+;UAS\text{-}EGFP\}}$	Green	Blue	Viable

Figure 3.1: The experimental setup for lethal phase analysis is illustrated for the *P{Act5C-GAL4}* cross but is identical for the *P{tubP-GAL4}* experiment (not shown). *P{w+; Act5C-GAL4}/ TM3, P{w+; twi-GAL4}, P{w+;UAS-EGFP}* females were mated with *P{EP}D1^EP473/ P{w+; UAS-GFP-lacZ}* males. The four expected progeny classes are at the left-most column. Expected embryonic fluorescence indicates how progeny classes were distinguished via fluorescence microscopy. The expected beta-galactosidase stain of unhatched embryos was utilized as a means of differentiating unhatched, fertilized embryo progeny classes. No color (---) indicates a lack of beta-galactosidase stain. The left most column indicates the expected viability of the progeny classes, with the question mark indicating that *P{EP}D1^EP473/ P{w+; Act5C-GAL4}* viability is unknown as the stage of lethality is what is being investigated.
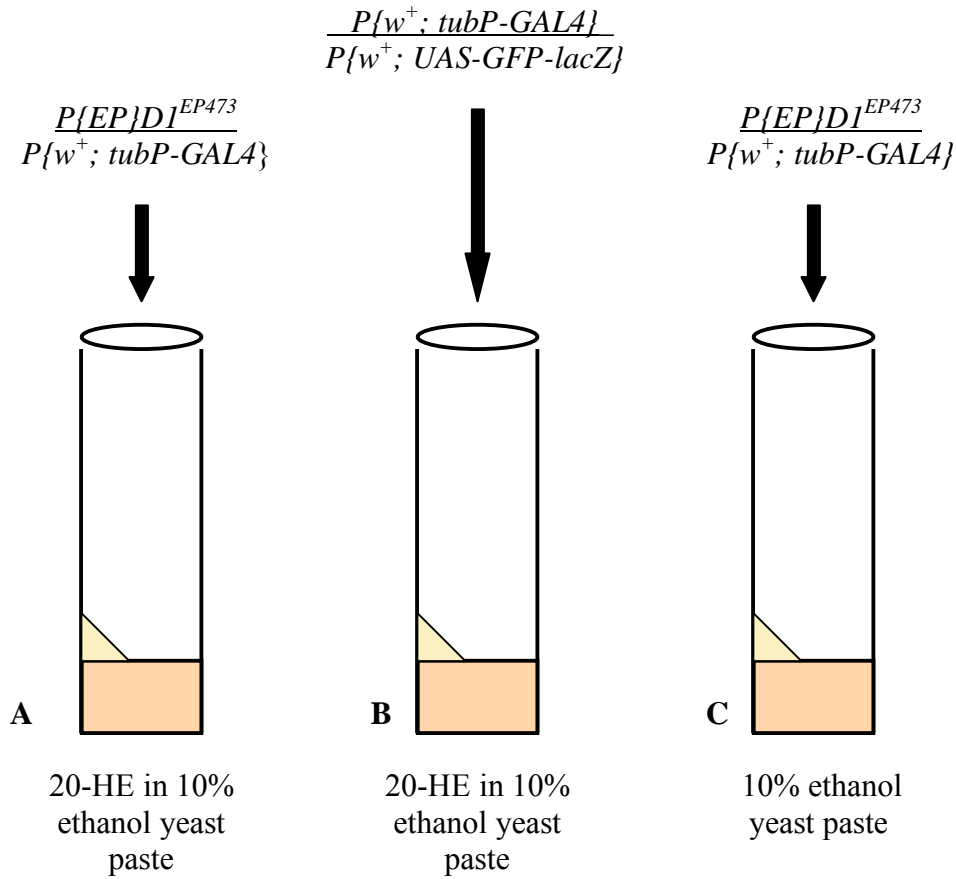
Figure 3.2: The setup for 20-hydroxyecdysone (20-HE) feeding involves *D1*-overexpressing larvae and several controls. (A) The assay to determine if 20-HE rescues the lethality due to ectopic, ubiquitous *D1* expression includes *P{EP}D1^{EP473}/P{w^+; tubP-GAL4}* first instar larvae in a vial containing 20-HE in yeast paste. (B) *P{w^+; tubP-GAL4}/P{w^+; UAS-GFP-lacZ}* first instar larvae placed in a vial containing 20-HE in yeast paste are a control in order to verify that the 20-HE in 10% ethanol yeast paste solution is not harmful to flies. (C) *P{EP}D1^{EP473}/P{w^+; tubP-GAL4}* first instar larvae placed in a vial containing only a 10% ethanol yeast paste solution are an additional control to ensure that in this assay, *D1* overexpression driven by *tubulin-GAL4* results in lethality in the absence of added 20HE. Three assays were carried out, one using 20-HE at a concentration of 0.5 ug/ul and two using 1.0 ug/ul 20-HE.

$$\frac{FM7B\ y\ w^a}{y\ w}\ ;\ \frac{cn^1,\ P\{PZ\}Kr\text{-}h1}{CyO,\ Ts,\ Kr,\ y^+}\ ;\ \frac{P\{w^+;\ tubP\text{-}GAL4\}}{TM3,\ y^+,\ Ser}\qquad \text{X}\qquad \frac{y\ w}{\neg}\ ;\ \frac{P\{EP\}D1^{EP473}}{P\{w^+;\ UAS\text{-}mCD8\text{-}GFP\}}$$

Expected Progeny: **Larval phenotype:**

$\dfrac{FM7B\ y\ w^a}{\neg}$ or $y\ w$; $\dfrac{cn^1,\ P\{PZ\}Kr\text{-}h1}{+}$; $\dfrac{P\{w^+;\ tubP\text{-}GAL4\}}{P\{EP\}D1^{EP473}}$ y, No GFP

$\dfrac{FM7B\ y\ w^a}{\neg}$ or $y\ w$; $\dfrac{cn^1,\ P\{PZ\}Kr\text{-}h1}{+}$; $\dfrac{P\{w^+;\ tubP\text{-}GAL4\}}{P\{w^+;\ UAS\text{-}mCD8\text{-}GFP\}}$ y, GFP

$\dfrac{FM7B\ y\ w^a}{\neg}$ or $y\ w$; $\dfrac{+}{CyO,\ Ts,\ Kr,\ y^+}$; $\dfrac{P\{w^+;\ tubP\text{-}GAL4\}}{P\{EP\}D1^{EP473}}$ y^+, No GFP

$\dfrac{FM7B\ y\ w^a}{\neg}$ or $y\ w$; $\dfrac{+}{CyO,\ Ts,\ Kr,\ y^+}$; $\dfrac{P\{w^+;\ tubP\text{-}GAL4\}}{P\{w^+;\ UAS\text{-}mCD8\text{-}GFP\}}$ y^+, GFP

$\dfrac{FM7B\ y\ w^a}{\neg}$ or $y\ w$; $\dfrac{cn^1,\ P\{PZ\}Kr\text{-}h1}{+}$; $\dfrac{P\{EP\}D1^{EP473}}{TM3,\ y^+,\ Ser}$ y^+, No GFP

$\dfrac{FM7B\ y\ w^a}{\neg}$ or $y\ w$; $\dfrac{cn^1,\ P\{PZ\}Kr\text{-}h1}{+}$; $\dfrac{P\{w^+;\ UAS\text{-}mCD8\text{-}GFP\}}{TM3,\ y^+,\ Ser}$ y^+, GFP

$\dfrac{FM7B\ y\ w^a}{\neg}$ or $y\ w$; $\dfrac{+}{CyO,\ Ts,\ Kr,\ y^+}$; $\dfrac{P\{EP\}D1^{EP473}}{TM3,\ y^+,\ Ser}$ y^+, No GFP

$\dfrac{FM7B\ y\ w^a}{\neg}$ or $y\ w$; $\dfrac{+}{CyO,\ Ts,\ Kr,\ y^+}$; $\dfrac{P\{w^+;\ UAS\text{-}mCD8\text{-}GFP\}}{TM3,\ y^+,\ Ser}$ y^+, GFP

Figure 3.3: The experimental setup for *Kruppel-homolog* enhancer trap analysis is illustrated above. *FM7B y w^a/y w ; cn^1 P{ry$^+$; PZ}Kr-h1/ CyO, Ts, Kr, y$^+$; P{tubP-GAL4}/ TM3, y$^+$, Ser* virgin females were mated with *y w; P{EP}D1^{EP473}/ P{UAS-mCD8-GFP}* males. The expected progeny classes, distinguishable by the presence of y and GFP as larvae, are at the left column.

$\underline{P\{w^+; lacW\}br, w}$; $\underline{\qquad\qquad P\{w^+; tubP\text{-}GAL4\}\qquad\qquad}$ X $\underline{yw}$; $\underline{\qquad P\{EP\}D1^{EP473}\qquad}$

$FM7B, y, w^a$ $TM3, P\{w^+; twi\text{-}GAL4\}, P\{w^+;UAS\text{-}EGFP\}$ $\neg$ $P\{w^+;UAS\text{-}mCD8\text{-}GFP\}$

Expected Progeny: **Larval phenotype:**

$\underline{P\{w^+; lacW\}br, w}$ or $\underline{P\{w^+; lacW\}br, w}$; $\underline{P\{w^+; tubP\text{-}GAL4\}}$ y^+, No GFP

$y\,w$ $\neg$ $P\{EP\}D1^{EP473}$

$\underline{P\{w^+; lacW\}br, w}$ or $\underline{P\{w^+; lacW\}br, w}$; $\underline{P\{w^+; tubP\text{-}GAL4\}}$ y^+, GFP

$y\,w$ $\neg$ $P\{UAS\text{-}mCD8\text{-}GFP\}$

$\underline{P\{w^+; lacW\}br, w}$ or $\underline{P\{w^+; lacW\}br, w}$; $\underline{TM3, P\{w^+; twi\text{-}GAL4\}, P\{w^+;UAS\text{-}EGFP\}}$ y^+, GFP

$y\,w$ $\neg$ $P\{EP\}D1^{EP473}$

$\underline{P\{w^+; lacW\}br, w}$ or $\underline{P\{w^+; lacW\}br, w}$; $\underline{TM3, P\{w^+; twi\text{-}GAL4\}, P\{w^+;UAS\text{-}EGFP\}}$ y^+, GFP

$y\,w$ $\neg$ $P\{UAS\text{-}mCD8\text{-}GFP\}$

$\underline{FM7B, y, w^a}$ or $\underline{FM7B, y, w^a}$; $\underline{P\{w^+; tubP\text{-}GAL4\}}$ y, No GFP

$y\,w$ $\neg$ $P\{EP\}D1^{EP473}$

$\underline{FM7B, y, w^a}$ or $\underline{FM7B, y, w^a}$; $\underline{P\{w^+; tubP\text{-}GAL4\}}$ y, GFP

$y\,w$ $\neg$ $P\{UAS\text{-}mCD8\text{-}GFP\}$

$\underline{FM7B, y, w^a}$ or $\underline{FM7B, y, w^a}$; $\underline{TM3, P\{w^+; twi\text{-}GAL4\}, P\{w^+;UAS\text{-}EGFP\}}$ y, GFP

$y\,w$ $\neg$ $P\{EP\}D1^{EP473}$

$\underline{FM7B, y, w^a}$ or $\underline{FM7B, y, w^a}$; $\underline{TM3, P\{w^+; twi\text{-}GAL4\}, P\{w^+;UAS\text{-}EGFP\}}$ y, GFP

$y\,w$ $\neg$ $P\{UAS\text{-}mCD8\text{-}GFP\}$

Figure 3.4: The experimental setup for *broad* enhancer trap analysis is illustrated above. *P{lacW}br, w/FM7B y w^a; P{tubP-GAL4}/ TM3, P{twi-GAL4, P{UAS-EGFP}* virgin females were mated with *y w; P{EP}D1^{EP473}/ P{UAS-mCD8-GFP}* males. The expected progeny classes, distinguishable by the presence of y and GFP as larvae, are at the left column.

Results

GAL4 protein is present in the early embryo due to maternal expression of *actin-GAL4*.

An experiment was conducted to determine if *GAL4* synthesized under the control of the *actin* or *alphatubulin84B* regulatory regions was maternally contributed to the embryo. Embryos collected separately from the crosses of $P\{w^+; Act5C\text{-}GAL4\}/CyO, y^+$ and $P\{w^+; tubP\text{-}GAL4\}/TM3, Sb$ females to $P\{w^+; UAS\text{-}GFP\text{-}lacZ\}$ males were beta-galactosidase stained and subsequently counted in order to determine the percentage of stained embryos, as illustrated in Figure 3.5. If *GAL4* was synthesized prior to zygotic transcription under the control of the *actin* or *alphatubulin84B* regulatory regions in the maternal ovaries and subsequently contributed to the egg (maternal loading), all resulting progeny of the cross should have *GAL4* protein present in the embryo regardless of genotype. Thus if *GAL4* was maternally contributed, all progeny embryos should stain positive for beta-galactosidase. If *GAL4* is not synthesized under the control of the *actin* or *alphatubulin84B* regulatory regions in the maternal ovaries and contributed to the egg, 50% of the progeny embryos should stain positive for beta-galactosidiase as a result of zygotic expression of *GAL4*. Therefore, if GAL4 is maternally contributed, 100% of embryo progeny should stain positive for beta-galactosidase while only 50% of the embryo progeny should stain positive for beta-galactosidase if *GAL4* is not maternally contributed. As a control to ensure that the beta-galactosidase staining procedure was able to detect all *GAL4* expressing embryos, a cross was performed that would yield 100% beta-galactosidase expressing embryos. $P\{w^+; UAS\text{-}GFP\text{-}lacZ\}$ females were crossed to $P\{w^+; Act5C\text{-}GAL4\}/TM3, P\{w^+; twi\text{-}GAL4\}, P\{w^+; UAS\text{-}EGFP\}$ or $P\{w^+; tubP\text{-}GAL4\}/TM3, P\{w^+; twi\text{-}GAL4\}, P\{w^+; UAS\text{-}EGFP\}$ males to produce $P\{w^+; Act5C\text{-}GAL4\}/ P\{w^+; UAS\text{-}GFP\text{-}lacZ\}$ and $P\{w^+; UAS\text{-}GFP\text{-}lacZ\}/ TM3, P\{w^+; twi\text{-}GAL4\}, P\{w^+; UAS\text{-}EGFP\}$ or $P\{w^+; tubP\text{-}GAL4\}/ P\{w^+; UAS\text{-}GFP\text{-}lacZ\}$ and $P\{w^+; UAS\text{-}GFP\text{-}lacZ\}/ TM3, P\{w^+; twi\text{-}GAL4\}, P\{w^+; UAS\text{-}EGFP\}$ embryos appropriately. 221/221 embryos from the $P\{w^+; Act\text{-}GAL4\}$ control cross and 159/159 embryos from the $P\{w^+; tubP\text{-}GAL4\}$ control cross were positive for beta-galactosidase. This result confirmed

that the staining procedure was 100% efficient at detecting beta-galactosidase expressing embryos.

195/195 (100%) embryos from the cross of $P\{w^+; Act5C\text{-}GAL4\}/CyO, y^+$ females to $P\{w^+; UAS\text{-}GFP\text{-}lacZ\}$ males were positive for beta-galactosidase staining. This indicated that *GAL4* was synthesized under the control of the *actin* regulatory region in the maternal ovaries and subsequently contributed to all eggs (maternally contributed). In contrast, 82/173 (47.4%) of the embryos from the cross of $P\{w^+; tubP\text{-}GAL4\}/TM3, Sb$ females to $P\{w^+; UAS\text{-}GFP\text{-}lacZ\}$ males were positive for beta-galactosidase stain while 91/173 (52.6%) showed no stain. This indicated that *GAL4* was not transcribed in the maternal ovaries as a result of the *alphatubulin84B* regulatory region and maternally contributed to the embryo (and thereby not maternally contributed).

D1 ubiquitous overexpression results in lethality prior to the adult stage

D1 overexpression was assayed utilizing three ubiquitous *GAL4* drivers: $P\{w^+; Act5C\text{-}GAL4\}$, $P\{w^+; tubP\text{-}GAL4\}$, and two different insertions of $P\{w^+; hsp70\text{-}GAL4\}$. The $P\{w^+; hsp70\text{-}GAL4\}$ experiments were performed under non-inducing conditions (25°C). Progeny was counted from the crosses of $w; P\{EP\}D1^{EP473}/TM3, Sb$ females with $P\{w^+; Act5C\text{-}GAL4\}/CyO, y^+$, $P\{w^+; tubP\text{-}GAL4\}/TM3, Sb$, $P\{w^+; hsp70\text{-}GAL4\}/CyO, y^+$ and $TM6B/TM3, P\{w^+; hsp70\text{-}GAL4\}, P\{w^+; UAS\text{-}GFP\}$ males, respectively (see Materials and Methods). Table 3.2 shows the possible progeny classes and counts of progeny per class from each of the above crosses. $+/P\{w^+; Act5C\text{-}GAL4\}; P\{EP\}D1^{EP473}/+$, $P\{EP\}D1^{EP473}/P\{w^+; tubP\text{-}GAL4\}$, and $P\{EP\}D1^{EP473}/TM3, P\{w^+; hsp70\text{-}GAL4\}, P\{w^+; UAS\text{-}GFP\}$ individuals died prior to the adult stage. $P\{hsp70\text{-}GAL4\}/+; P\{EP\}D1^{EP473}/+$ individuals were viable as adults.

The lethality of $P\{w^+; Act5C\text{-}GAL4\}/P\{EP\}D1^{EP473}$ individuals occurs predominantly at the third larval instar stage.

Utilizing the setup illustrated in Figure 3.1, embryos of the genotype $P\{EP\}D1^{EP473}/P\{w^+; Act5C\text{-}GAL4\}$ were identified and their development monitored in order to determine the phase of Drosophila development that lethality resulted. Two lethal phase analysis experiments indicated that lethality was predominantly at the third

larval instar stage (Table 3.3). An average of 66% of *P{EP}D1^{EP473}/P{w$^+$; Act5C-GAL4}* individuals died at the third instar stage, and were smaller than *P{w$^+$; Act5C-GAL4}/P{w$^+$; UAS-GFP-lacZ}* control third instar larvae (Figure 3.6). An average of 13% of *P{EP}D1^{EP473}/P{w$^+$; Act5C-GAL4}* individuals died as small, crescent-shaped pupae. An average of 9% of *P{EP}D1^{EP473}/P{w$^+$; Act5C-GAL4}* individuals exhibited lethality as embryos, which was determined to occur at stage 16 of embryogenesis, the stage prior to hatching.

The somewhat low hatching rate for the control classes of embryos (92%) prompted me to try to distinguish the genotypes of the unhatched embryos using beta-galactosidase staining (see Figure 3.1). Out of all unhatched embryos, an average of 64% were positive for beta-galactosidase (Table 3.4). This indicates that approximately two-thirds of the unhatched, green fluorescent embryos were of the genotypes *P{w$^+$; Act5C-GAL4}/ P{w$^+$; UAS-GFP-lacZ}* and *P{w$^+$; UAS-GFP-lacZ}/ TM3, P{w$^+$; twi-GAL4}, P{w$^+$; UAS-EGFP}*, as would be expected (Figure 3.1).

The lethality of *P{w$^+$; tubP-GAL4}/P{EP}D1^{EP473}* individuals occurs predominantly during the second to third larval instar molt.

Utilizing the setup illustrated in Figure 3.1, *D1* was misexpressed in an *alphatubulin84B* expression pattern. Embryos of the genotype *P{EP}D1^{EP473}/P{w$^+$; tubP-GAL4}* were identified and their development monitored in order to assess subsequent stage(s) of lethality. Lethality occurred predominantly during the second to third instar larval molt (Table 3.3). An average of 63% of *P{EP}D1^{EP473}/P{w$^+$; tubP-GAL4}* individuals exhibited lethality during the second to third larval molt with two sets of mouthhooks and two sets of larval spiracles. The phenotype is illustrated in Figure 3.7. These larvae underwent the morphological changes cited to occur approximately one hour prior to ecdysis [67] such as developing new mouthhooks over the old mouthhooks and new vertical plates. These individuals also began pre-ecdysis behaviors [67] but died somewhere between this time point and the completion of ecdysis, approximately a fifteen minute interval. Those larvae progressing to the third instar stage were smaller than the control siblings (data not shown). Larvae overexpressing *D1* in an *alphatubulin84B* expression pattern were not able to pupate. An average of 17 % of *D1-*

51

overexpressing individuals exhibited embryonic lethality at stage 16 of embryogenesis (Table 3.3).

The low hatching rate for the control classes of embryos (82%) prompted me to try to distinguish the genotypes of the unhatched embryos using beta-galactosidase staining (see Figure 3.1). Out of all unhatched embryos, an average of 34% stained positively for beta-galactosidase (Table 3.4). This proportion is half of that expected and indicates that the majority of unhatched, green fluorescent embryos were of the genotypes *P{w+; Act5C-GAL4}/ P{w+; UAS-GFP-lacZ}* and *P{EP}D1^{EP473}/TM3, P{w+; twi-GAL4}, P{w+; UAS-EGFP}*.

$D1$ overexpression in an *alphatubulin84B* expression pattern does not interfere with 20-Hydroxyecdysone biosynthesis

The majority of larvae in which *D1* was overexpressed in a *tubulin* pattern died unable to complete the second to third larval molt. Because of this, I initially hypothesized that ectopic *D1* expression interfered with 20-hyroxyecdysone (20-HE) biosynthesis. 20-hydroxyecdysone is a steroid hormone that initiates metamorphosis in *Drosophila melanogaster* [6; 21; 84]. The complex synthesis of Drosophila ecdysteroids occurs primarily in the prothoracic gland, part of the ring gland, which also includes the corpus cardiacum and corpus allatum [27]. Ecdysteroidogenesis involves initiation by prothoracicotropic hormone (PTTH), synthesis of 20-HE as a result of a transductory cascade in cells of the prothoracic gland as well as upregulation and downregulation of 20-HE as a result of a regulatory feedback loop to control the rate of ecdysteroid biosynthesis (reviewed by Gilbert *et al.*, [40]). Following ecdysteroidgenesis, 20-HE binds to the Ecdysone receptor (EcR) complex that along with Ultraspiracle (USP) regulates the release of the hormone from the prothoracic gland [56]. Once 20-HE is released, a complex cascade of gene activity and secondary response structural genes are activated resulting in larval molting, pupariation and metamorphosis [76].

To determine if *D1*-overexpressing individuals exhibited defects in larval molting due to a 20-HE deficiency, exogenous 20-HE was fed to *P{EP}D1^{EP473}/P{w+; tubP-GAL4}* larvae utilizing the setup illustrated in Figure 3.2 (and see Materials and Methods). This method has been shown to delay lethality for specific mutants [39].

P{EP}D1^{EP473}/P{w^+; tubP-GAL4} larvae, regardless of 20-HE feeding method or 20-HE
concentration, died predominantly during the second to third instar molt (Table 3.5).
P{EP}D1^{EP473}/P{w^+; tubP-GAL4} larvae were fed ethanol yeast paste without the
addition of 20-HE simultaneously as a positive control to ensure that the 20-HE was not
harmful. These individuals died predominantly during the second to third larval instar
molt (Table 3.5).

**Kruppel-homolog and broad expression were not altered in individuals ectopically
expressing *D1*.**

      Because ectopic *D1* expression was not rescued by exogenous 20-HE feeding, I
hypothesized that the lethality of ubiquitous *D1* overexpression may be a result of ectopic
D1 interfering with ecdysis downstream of 20-HE biosynthesis. As described above, the
onset of larval molting, puparium formation and metamorphosis are driven by widespread
changes in gene expression triggered by 20-HE via its association with the EcR/Usp
receptor heterodimer [94; 83]. A number of early response genes have been identified
that respond directly to the hormone, some of which encode families of transcription
factors. These early ecdysone-inducible genes are expressed in complicated spatial and
temporal patterns at the onset of larval molting and metamorphosis and have been
proposed to play roles in transducing the systemic hormonal signal into tissue-restricted
patterns of gene expression that direct each tissue down its appropriate developmental
pathway [84; 30; 34]. Two early response genes were chosen, preliminarily, to assess for
expression level in *D1*-overexpressing larvae: *Kruppel-homolog* (*Kr-h1*) and *broad* (*br*).
Whole larval transcript analyses showed that *Kr-h1* mRNA is present from mid instar
stage onwards [69] and ubiquitous for all larval instars [13]. Cytological location 2B5 is
known as the *Broad-Complex* (BR-C), composed of the *broad* (*br*), *reduced bristles on
palpus* (*rbp*), *l(l)2Bc* and *l(l)2Bd* genes, all essential for ecdysis [16]. Western blot
analyses demonstrate that BR-C isoforms are induced at the onset of both larval molts
and metamorphosis, each with unique kinetics of induction and repression [16].
Enhancer trap lines exist for both genes, which allows gene expression to be monitored
by beta-galactosidase assay.

Utilizing the setups illustrated in Figures 3.3 and 3.4, first instar larvae of the genotypes *P{lacW}br, w/y w; P{w⁺; tubP-GAL4}/ P{EP}D1^{EP473}* (experimental) and *P{lacW}br, w/ y w; P{w⁺; tubP-GAL4}/ P{w⁺; UAS-mCD8-GFP}* (control) for the *broad* enhancer trap analysis and *cn¹ P{ry⁺; PZ} Kr-h1/+; P{w⁺; tubP-GAL4}/ P{EP}D1^{EP473}* (experimental) and *cn¹ P{ry⁺; PZ}Kr-h1/+ ; P{w⁺; tubP-GAL4}/P{w⁺;UAS-mCD8-GFP}* (control) for the *Kruppel-homolog* analysis were placed in separate culture vials in groups of 10 to 15. All individuals were aged to the late second larval instar stage (65 to 68 hours after egg laying) and beta-galactosidase stained. Second instar larvae of the genotypes *cn¹ P{ry⁺; PZ} Kr-h1/+; P{tubP-GAL4}/ P{EP}D1^{EP473}* (n = 63) and *cn¹ P{ry⁺; PZ} Kr-h1/+; P{tubP-GAL4}/ P{w⁺; UAS-GFP-lacZ}* (n = 71) stained for beta-galactosidase activity showed identical *Kr-h1* expression. This expression pattern included a dense midline stain, darkly staining salivary glands, brain and imaginal discs with all other larval structures lightly staining. These results are similar to those utilizing the *broad* enhancer trap. *P{lacW}br, w/y w ; P{tubP-GAL4}/ P{EP}D1^{EP473}* (n = 47) and *P{lacW}br, w/y w ; P{tubP-GAL4}/ P{w⁺;UAS-GFP-lacZ}* (n = 34) second instar larvae stained for beta-galactosidase showed identical *br* expression. This expression pattern showed beta-galactosidase stain ubiquitously in all larval tissues. These results indicated that ectopic *D1* driven by *tubulin-GAL4* does not interfere with the expression of the ecydsone-induced genes *Kr-h1* and *br*. The lethality of *cn¹ P{ry⁺; PZ} Kr-h1/+; P{tubP-GAL4}/ P{EP}D1^{EP473}* (n = 38) and *P{lacW}br, w/y w ; P{tubP-GAL4}/ P{EP}D1^{EP473}* (n = 49) larvae was confirmed by allowing some of the larvae to develop. None of these individuals survived to the adult stage.

Experimental cross:

$\underline{GAL4 \text{ driver}}$ X   *y w; P{w⁺; UAS-GFP-lacZ}*
Balancer

Beta-galactosidase staining

Expected progeny:	maternal & zygotic <u>*GAL4* expression</u>	zygotic *GAL4* <u>expression only</u>
$\dfrac{GAL4 \text{ driver}}{P\{w^+; UAS\text{-}GFP\text{-}lacZ\}}$	+	+
$\dfrac{\text{Balancer}}{P\{w^+; UAS\text{-}GFP\text{-} lacZ\}}$	+	-

Figure 3.5: The experimental setup illustrated above was utilized in order to determine if *GAL4* was synthesized prior to zygotic transcription under the control of the *actin* or *alphatubulin84B* regulatory regions in the maternal ovaries and subsequently contributed to the egg (maternal loading). *P{w⁺; Act5C-GAL4}/CyO, y⁺* or *P{w⁺; tubP-GAL4}/TM3, Sb* females were mated with *P{w⁺; UAS-GFP-lacZ}* males and the embryos were collected and stained for beta-galactosidase activity. If *GAL4* maternal loading occurred, 100% of the resulting progeny of the cross would have *GAL4* protein present in the embryo and stain positive for beta-galactosidase. If *GAL4* was not maternally loaded, only 50% of the progeny embryos would stain positive for beta-galactosidase activity as a result of zygotic expression of *GAL4*. The simplified expected embryonic genotypes are at the left while the expected *GAL4* maternal or zygotic expression is indicated by present (+) or absent (-) on the right. This will be determined by beta-galactosidase staining. As a control to ensure that the beta-galactosidase staining procedure was able to detect all *GAL4* expressing embryos, a cross was performed that would yield 100% *GAL4* expressing embryos. *P{w⁺; UAS-GFP-lacZ}* females were crossed to *P{w⁺; Act5C-GAL4}/TM3, P{w⁺; twi-GAL4}, P{w⁺; UAS-EGFP}* or *P{w⁺; tubP-GAL4}/TM3, P{w⁺; twi-GAL4}, P{w⁺; UAS-EGFP}* males to produce *P{w⁺; Act5C-GAL4}/ P{w⁺; UAS-GFP-lacZ}* and *P{w⁺; UAS-GFP-lacZ}/ TM3, P{w⁺; twi-GAL4}, P{w⁺; UAS-EGFP}* or *P{w⁺; tubP-GAL4}/ P{w⁺; UAS-GFP-lacZ}* and *P{w⁺; UAS-GFP-lacZ}/ TM3, P{w⁺; twi-GAL4}, P{w⁺; UAS-EGFP}* embryos appropriately (not shown). These embryos were beta-galactosidase stained to verify the beta-galactosidase staining procedure.

Table 3.2: Viability analysis of ubiquitous *D1* overexpression

Genotype	Progeny (%)	
	Experiment 1	**Experiment 2**
+/P{w$^+$; Act5C-GAL4}; P{EP}D1^{EP473}/+	0 (0%)	0 (0%)
+/CyO; P{EP}D1^{EP473}/+	84 (46%)	58 (49%)
+/P{w$^+$; Act5C-GAL4}; TM3, Sb/+	58 (32%)	36 (30%)
+/ CyO; TM3, Sb/+	39 (22%)	25 (21%)
P{EP}D1^{EP473}/P{w$^+$; tubP-GAL4}	0 (0%)	0 (0%)
P{EP}D1^{EP473}/TM3, Sb P{w$^+$; tubP-GAL4}/TM3, Sb	159 (100%)	102 (100%)
+/P{w$^+$; hsp70-GAL4}; P{EP}D1^{EP473}/+	27 (31%)	29 (28%)
+/CyO; D1^{EP473}/+	13 (15%)	18 (18%)
+/P{w$^+$; hsp70-GAL4}; TM3, Sb/+	30 (34%)	30 (29%)
+/CyO; TM3, Sb/+	18 (20%)	25 (25%)
P{EP}D1^{EP473}/ TM3, P{w$^+$; hsp70-GAL4},P{w$^+$; UAS-GFP}	0 (0%)	0 (0%)
P{EP}D1^{EP473}/TM6B	67 (54%)	54 (55%)
TM6B/TM3, Sb	57 (46%)	45 (45%)

Table 3.3: Lethal Phase analysis of *D1* ubiquitous overexpression

Genotype	Exper -iment	n	Embryonic lethality (%)	1st Instar (%)	2nd Instar (%)	2nd/3rd DMH[a] (%)	3rd Instar (%)	Pupae (%)	Missing larvae (%)
						Stage of lethality			
P{EP}D1^{EP473}/ P{Act5C-GAL4}	1	133	15 (11.3%)	2 (1.5%)	15 (11.3%)	0 (0%)	75 (56.4%)	25 (18.8%)	1 (0.8%)
	2	187	14 (7.5%)	1 (0.5%)	15 (8.0%)	0 (0%)	136 (72.7%)	17 (9.1%)	4 (2.2%)
Fluorescing larvae (control)	1	535	42 (7.9%)	N/A	N/A	N/A	N/A	N/A	N/A
	2	544	43 (7.9%)	N/A	N/A	N/A	N/A	N/A	N/A
P{EP}D1^{EP473}/ P{tubP-GAL4}	1	184	27 (14.7%)	4 (2.2%)	7 (3.8%)	101 (54.9%)	30 (16.3%)	0 (0%)	15 (8.1%)
	2	189	38 (20.1%)	7 (3.7%)	16 (8.5%)	75 (39.7%)	39 (20.6%)	0 (0%)	14 (7.4%)
Fluorescing larvae (control)	1	696	130 (18.7%)	N/A	N/A	N/A	N/A	N/A	N/A
	2	641	108 (16.8%)	N/A	N/A	N/A	N/A	N/A	N/A
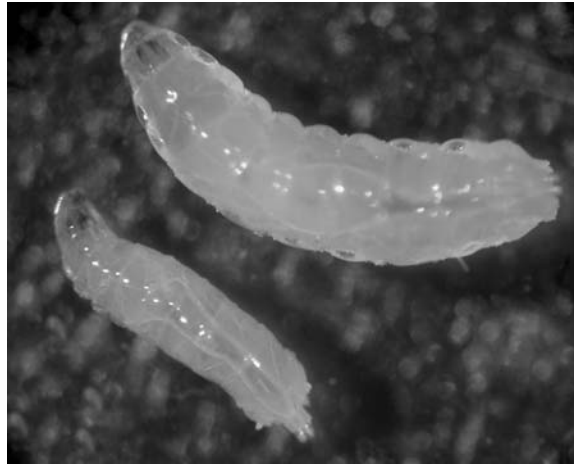
Figure 3.6: *P{EP}D1^EP473/P{Act5C-GAL}* **(left) third instar larvae are smaller than their** *P{Act5C-GAL}/P{UAS-GFP-lacZ}* **siblings (right).** Both larvae featured above are the same age.

Table 3.4 Analysis of unhatched, GFP[+] embryos from lethal phase assays

Genotype		Observed results	
		Experiment 1	Experiment 2
P{EP}D1^{EP473}/ TM3,P{w$^+$; twi-GAL4}, P{w$^+$; UAS-EGFP}	B-gal[a] negative	16 (38.1%)	15 (34.9%)
P{w$^+$; Act5C-GAL4}/ P{w$^+$; UAS-GFP-lacZ} or P{w$^+$; UAS-GFP-lacZ}/ TM3,P{w$^+$; twi-GAL4}, P{w$^+$; UAS-EGFP}	B-gal[a] positive	26 (61.9%)	28 (65.1%)
P{EP}D1^{EP473}/ TM3,P{w$^+$; twi-GAL4}, P{w$^+$; UAS-EGFP}	B-gal[a] negative	92 (70.8%)	66 (61.1%)
P{w$^+$; tubP-GAL4}/ P{w$^+$; UAS-GFP-lacZ} or P{w$^+$; UAS-GFP-lacZ}/ TM3,P{w$^+$; twi-GAL4}, P{w$^+$; UAS-EGFP}	B-gal[a] positive	38 (29.2%)	42 (38.9%)

[a]Beta-galactosidase

2nd larval instar spiracle

3rd larval instar spiracle

2nd and 3rd larval instar mouthparts
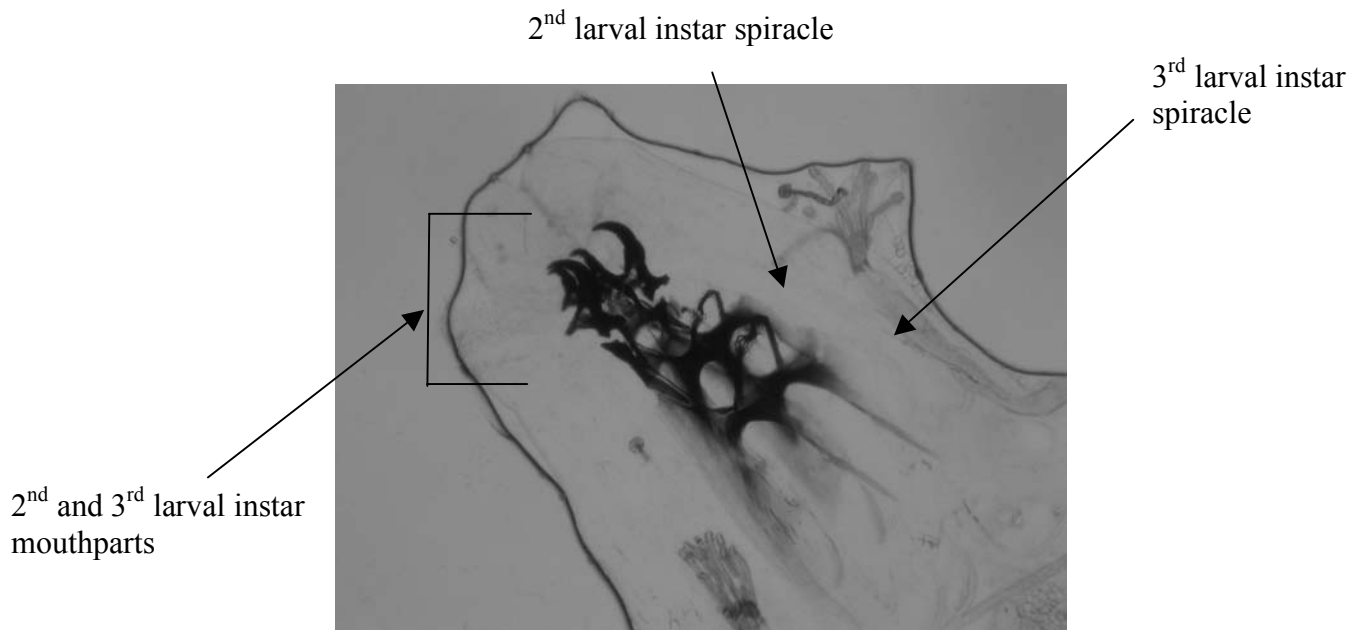
Figure 3.7: **The predominant stage of lethality for *P{EP}D1^{EP473}*/*P{tubP-GAL4}* larvae is at the second to third instar molt.** These larvae have two sets of mouthhooks and both sets of larval spiracles but do not complete ecdysis from the second to the third molt.

Table 3.5 20-HE feeding to *P{EP}D1^{EP473}/P{w^+; tubP-GAL4}* larvae

Treatment	n	1st Instar (%)	2nd Instar (%)	2nd/3rd DMH[a] (%)	3rd Instar (%)	Adult (%)
+ ecdysone (0.5 ug/ul)	183	1 (0.5%)	9 (4.5%)	146 (80%)	27 (15%)	0 (0%)
- ecdysone (0.5 ug/ul)	97	1 (1%)	6 (6%)	78 (80%)	12 (13%)	0 (0%)
+ ecdysone (1.0 ug/ul)	435	1 (0.5%)	14 (2.5%)	348 (80%)	72 (17%)	0 (0%)
- ecdysone (1.0 ug/ul)	99	1 (1%)	4 (4%)	76 (77%)	18 (18%)	0 (0%)
+ ecdysone (1.0 ug/ul) pulse	105	0 (0%)	8 (8%)	80 (76%)	17 (16%)	0 (0%)
- ecdysone (1.0 ug/ul) pulse	65	0 (0%)	2 (3%)	50 (77%)	13 (20%)	0 (0%)

[a]DMH double mouth hook

Discussion

D1 ubiquitous expression results in lethality

Ubiquitous *GAL4* drivers utilized to target *D1* overexpression were *Act5C-GAL4*, *tubP-GAL4*, *hsp70-GAL4* (chromosome 2) and *hsp70-GAL4* (chromosome 3). *D1* overexpression driven by *Act5C-GAL4*, *tubP-GAL4* and *hsp70-GAL4* on chromosome three resulted in lethality. Lethal phase analyses were done to investigate the predominant lethal phase due to ectopic *D1* driven by *Act5C-GAL4* and *tubP-GAL4*. These analyses revealed the predominant lethal phase of *P{EP}D1^{EP473}/P{Act5C-GAL4}* individuals to be the third larval instar stage. Some *P{EP}D1^{EP473}/P{Act5C-GAL4}* individuals were able to pupate although the resulting pupal cases had an abnormal morphology. Maternal loading experiments determined that *actin* is maternally contributed to the developing embryo. Thus, when driven with *P{Act5C-GAL4}*, *D1* was maternally contributed to the embryo and thereby expressed very early in development onward. The predominant stage of lethality for *P{EP}D1^{EP473}/P{tubP-GAL4}* individuals was during the second to third larval molt. Some *P{EP}D1^{EP473}/P{tubP-GAL4}* individuals were able to get past the second to third instar molt but died as third instars prior to the wandering stage. Maternal loading experiments determined that *alphatubuling84B* is not maternally contributed to the developing embryo. Therefore, when driven with *P[tubP-GAL4]*, *D1* was expressed zygotically during early embryogenesis at stage 10 onward.

Together these data suggest that the *GAL4 l*evel of *D1* overexpression makes a difference in stage of lethality. Individuals in which *D1* was overexpressed in non-inducing conditions with the chromosome 2 *P{hsp70-GAL4}* driver were viable while individuals in which *D1* was overexpressed with the chromosome 3 *P{hsp70-GAL4}* driver died prior to the adult stage. I hypothesize that the dose of *D1* was reduced when driven with the chromosome 2 *P{hsp70-GAL4}* driver in comparison to the chromosome 3 *P{hsp70-GAL4}* driver. This reduced expression level may be the result of position effects or *GAL4* transgene construction. The *GAL4* level of *D1* overexpression makes a difference in the stage of lethality for *D1* expression driven by *actin* and *tubulin* as well. Maternally loaded *D1*, driven by *P{Act5C-GAL4}*, leads to lethality predominantly at the third larval instar stage. Non-maternally loaded D1, driven by *P{tubP-GAL4}*, leads to

lethality principally during the second to third larval instar molt. These results are counter-intuitive. When driven by *P{Act5C-GAL4}*, *D1* is expressed very early in development in comparison to when driven by *P{tubP-GAL4}* and expression is a little later in embryo development. Individuals of the former die at a later stage of life than the latter. This may be because of the subtle differences in the expression patterns between *tubulin* and *actin* and therefore, where *D1* is being expressed. Position effects modifying expression levels could also explain these atypical results.

The D. melanogaster steriod hormone 20-hydroxyecdysone (20-HE) guides the transition from one developmental stage to the next [6; 21; 84]. The well-studied 20-HE hormone titer starts a gene cascade in which expression of target genes including primary response (early) genes are directly and rapidly induced by 20-HE and secondary response genes are regulated by the primary response gene products. This complicated 20-HE signaling cascade elicits not only molting but most of the morphogenetic processes that comprise insect growth and metamorphosis [21]. The predominant stage of lethality of individuals in which *D1* was overexpressed by *P{tubP-GAL4}* during the second to third molt was indicative that *D1* may be interfering with either 20-HE biosynthesis or downstream in the ecdysone cascade. Larvae mutant for genes involved in ecdysteroidogenesis exhibit lethality prior to the adult stage, rescuable with exogenous 20-HE feeding. Four of these genes, *phantom, disembodied, shadow* and *shade* (Halloween genes) encode cytochrome P450 enzymes that are responsible for the final four hydroxylations of steroid precursors into 20-hydroxyecdysone [39]. To determine if ectopic *D1* disturbed ecdysteroidogenesis by interfering with the Halloween genes or other genes involved in 20-HE biosynthesis, exogenous 20-HE was fed to developing *D1*-overexpressing larvae. I assayed for rescue of the lethality at the second to third instar molt. Rescue did not occur, suggesting that lethality was not a consequence of interference with ecdysteroidogenesis. In hindsight, the experimental setup for the 20-hydroxyecdysone experiment was not strong enough to definitively conclude that lack of rescue by exogenous 20-HE indicates that ectopic *D1* did not interfere with 20-HE biosynthesis. For the assay itself, a negative control was present ensuring that the lethality due to ectopic *D1* expression in a *alphatubulin84B* pattern occurred when larvae were fed 10% ethanol yeast paste. A positive control of *P{tubP-GAL4}/P{UAS-GFP-*

lacZ} larvae fed 20-HE in 10% ethanol yeast paste ensured that 20-HE in 10% ethanol yeast paste itself did not harm larvae that should develop into adults (refer to Figure 3.2 and Materials and Methods). A control for the experiment that was lacking involved feeding 20-HE in 10% ethanol yeast paste to a mutant previously described as required for 20-HE biosynthesis and therefore rescuable with exogenous 20-HE. Larvae mutant for one of the Halloween genes for example are developmentally arrested at a known stage but with exogenous 20-HE are able to be rescued from this lethality. This would ensure that the 20-HE in 10% ethanol yeast paste is the correct concentration, makeup, etc. to replace the lack of endogenous 20-HE. Because of this, the possibility that ectopic *D1* expression in a *tubulin* pattern interferes with 20-hydroxyecdysone biosynthesis remains.

To examine the possibility that *D1* overexpression affected the ecdysone pathway downstream of ecdysone biosynthesis, two early response genes were chosen to assess for transcriptional effects. As there are a large number of genes participating in the ecdysone cascade, assaying two early response genes was a preliminary assay in hopes of obtaining data to address this question. Enhancer trap insertions into the *broad* (*br*) and *Kruppel-homolog* (*Kr-h1*) genes were utilized in separate assays to determine if ectopic *D1* perturbed wild-type expression of these early response genes. Beta-galactosidase staining of second instar larvae overexpressing *D1* indicated that *Kruppel-homolog* expression of a dense midline stain, darkly staining salivary glands, brain and imaginal discs with all other larval structures lightly staining was identical to *Kr-h1* expression in control second instar larvae. Beta-galactosidase staining of second instar larvae overexpressing *D1* additionally indicated that the ubiquitous staining in all larval tissues of *broad* expression was identical to *br* expression in control second instar larvae. However, these results are considered preliminary. Two assays of *Kr-h1* expression in individuals in which *D1* was overexpressed were done with n values of 27 and 36 for *cn¹ P{ry⁺; PZ} Kr-h1/+; P{tubP-GAL4}/ P{EP}D1^{EP473}* individuals and 32 and 39 for the control *cn¹ P{ry⁺; PZ} Kr-h1/+; P{tubP-GAL4}/ P{w+; UAS-GFP-lacZ}* second instar larvae. Conversely, only one assay was done of *br* expression in second instar larvae in which *D1* was overexpressed with n values of 47 for *P{lacW}br, w/y w ; P{tubP-GAL4}/ P{EP}D1^{EP473}* individuals and 42 for control *P{lacW}br, w/y w ; P{tubP-GAL4}/*

P{w⁺;UAS-GFP-lacZ} second instar larvae. The fact that the experimental n values are relatively low and the assays themselves were carried out twice at best does not promote high confidence in the results. Also, comparisons between beta-galactosidase staining of *br* and *Kr-h1* expression in *D1*-overexpressing individuals versus individuals in which *D1* was not overexpressed were strictly qualitative in nature, introducing a highly subjective component to the assay. All of these issues taken together indicate a need to repeat and quantify these assays in order to confidently conclude whether *D1* overexpression in individuals affects the transcription of *broad* or *Kruppel-homolog*.

A possible hypothesis to explain the lethality due to dose-dependent ubiquitous D1 overexpression is that ectopic *D1* is disrupting gene expression in a generalized manner. Ectopic D1 protein could have directly or indirectly disturbed normal gene expression in a widespread manner by binding to areas of the DNA or transcription factors necessary for normal development. Such a generalized disruption could be exhibited as lethality if the magnitude of disruption was large enough. This hypothesis is supported by the above data indicating that the *GAL4* level of *D1* overexpression affects the stage of lethality.

Another possible hypothesis is that ectopic *D1* could be binding to AT-rich DNA or satellite-like sequences of the euchromatin specifically and interfering with wild-type transcription. If this were the case, certain specific signal transduction pathways could be disrupted either directly or indirectly. The possibility of disrupting the 20-HE signal transduction cascade by *D1* overexpression driven by *P{tubP-GAL4}*could be explained by either hypothesis. Further studies are necessary to investigate these hypotheses, perhaps providing clues of *D1* function in wild-type flies.

Chapter Four: The effect of *D1* overexpression on salivary gland polytene chromosome morphology

Introduction

The purpose of this study was to analyze *D1* function utilizing the polytene chromosomes of the Drosophila larval salivary glands. *Drosophila melanogaster* polytene chromosomes are an excellent model for cytological analysis as they have been extensively studied and well characterized. With the unique chromosome morphology of the polytene chromosomes and the ability to view temporal gene expression through salivary chromosome puffing, overexpressing *D1* in the polytene chromosomes may result in phenotypes associated with specific cytological regions or with a certain chromosomal morphology. Analysis of these phenotypes may provide clues of *D1* function.

In *Drosophila melanogaster*, the salivary gland chromosomes are polyteny in nature [7]. Polyteny is a form of polyploidy in which the replicated copies of DNA remain physically associated. The polytene phenomenon involves at least two events. First the centromeres belonging to the four pairs of fruit fly chromosomes fuse in a heterochromatic structure, the chromocenter. Almost simultaneously, a somatic pairing of homologues takes place, followed by the phenomenon of polytenization, the occurrence of many rounds of replication without subsequent separation of chromatids. In the mature third instar larval salivary gland of Drosophila, the overall process of polytenization results in giant chromosomes that are visible with light microscopy and have a unique banded pattern [7] (Figure 4.1A). The banded pattern results from alternating regions of more compact and less compact chromatin along the length of the chromatid. When the compact regions are brought into close proximity by sister chromatic synapsis, chromosomal bands result. The decondensed regions of chromatids between these bands are termed interbands. In 1935, Bridges [20] documented the banding pattern through hand drawings. He divided each of the five long arms into twenty segments of equal length. The fourth chromosome was divided into only two segments due to its small size. Each numbered division of Bridges map (1 through 102) was further subdivided into six lettered regions (A through F) that each begin with a prominent band. The bands within each lettered interval were consecutively numbered. Bridges maps provide a reference system for describing the location of genetic loci and

other cytogenetic features. The *D1* gene is cytologically located at 85D1-2 on the right arm of the third chromosome (Figure 4.1B).

Not all chromosomal regions appear banded. During the DNA replication of polytenization, satellite sequences of heterochromatin often fail to replicate because of a shortened S phase [53]. Due to this underreplication, heterochromatic portions of the Drosophila genome are drastically reduced in polytene chromosomes, a phenomenon making studies of heterochromatin in these chromosomes difficult. Although it comprises a third of the diploid genome, the heterochromatin of each chromosome in polytene cells coalesces into a single chromocenter, a small, grainy area from which the X chromosome and autosomes extend.

Within the banded euchromatin are sites that have properties typically associated with heterochromatin, and which have therefore been referred to as regions of intercalary heterochromatin [50]. These properties include late DNA replication, DNA underreplication, ectopic pairing (*i.e.* the physical association of nonhomologous regions) and the binding of Heterochromatin Protein 1 (HP1). Although numerous studies have been performed to better define intercalary heterochromatin, a clear set of characteristics has not emerged (reviewed by Zhimulev *et al.,* [98]). Zhimulev *et al.* [96] proposed that a chromosomal region be considered as intercalary heterochromatin if it exhibits two or more properties of heterochromatin. The molecular basis for these properties is uncertain. Sequence analyses show that euchromatin displaying heterochromatic properties is not primarily gene rich or gene poor.   The presence of certain middle repetitive DNA repeats has been verified by several studies [42; 97; 99] but this presence is not detected in all euchromatic regions exhibiting properties of heterochromatin.

The role of the D1 protein in the functions or morphology of either the euchromatin or heterochromatin of the salivary gland polytene chromosomes is unclear. Immunolocalization of D1 along the chromosomes revealed that it associates with the chromocenter and several sites within the euchromatin [4; 5]. Less intense immunostaining was observed for numerous additional euchromatic sites which have not yet been mapped [4]. The chromocenter localization is expected, as D1 binds to the AT-rich satellite DNAs referred to as the 1.688 g/cm^3 and 1.672 g/cm^3 satellites [56]. By analogy, the euchromatic binding sites might reflect AT-rich regions within the

euchromatin. Alfageme *et al.* [5] noted the coincidence of sites of D1 localization and sites that stained brightly with the DNA stain quinacrine, which preferentially binds to AT-rich sequences. The association of D1 with other proteins could influence its distribution as well. Unfortunately, none of these studies has been revealing as to the function or activity of heterochromatin or euchromatin-associated D1 protein.

   As a means to investigate *D1* function, I have been examining the consequences of overexpression of the *D1* gene in the salivary glands. Ectopic *D1* expression was directed using the *salivary gland specific3 GAL4* driver *P{sgs3-GAL4}* and the *P{EP}D1^{EP473}* insertion as described in chapter one of this thesis. Preliminary studies had revealed that *D1* overexpression caused an increase in ectopic associations between chromosomes such that the euchromatic chromosome arms were entangled (K.S. Weiler, unpublished). This result indicated that *D1* could mediate associations between chromosomes. Importantly, the phenotype provided a means to map sites where *D1* was active. This chapter describes my results from mapping the sites of ectopic association between chromosomes due to *D1* overexpression.
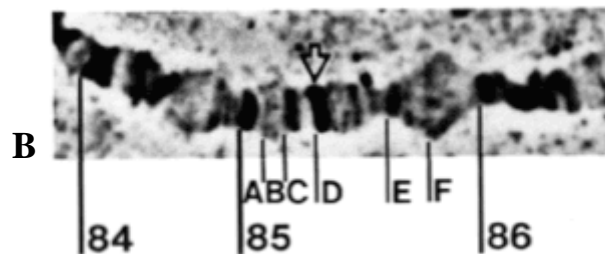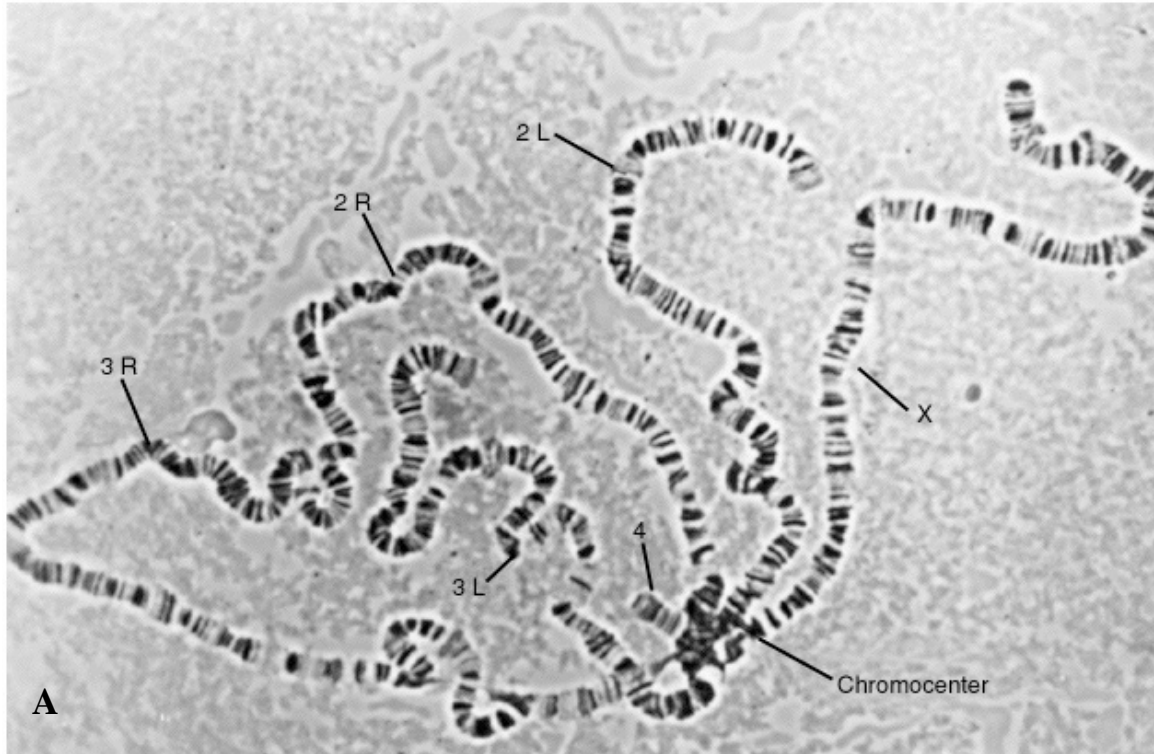
Figure 4.1: Polytene chromosomes exhibit a unique banding pattern in which genes can be localized. (A) wild-type Drosophila polytene chromosomes with chromocenter and chromosome arms identified; (B) the cytological location of the *D1* gene localized by Ashley *et al.*, [8] on the right arm of chromosome 3 at 85D1-2 (arrow).

Materials and Methods

Stocks and Culture conditions: Fly stocks and crosses were maintained in cotton-stoppered vials on a cornmeal and agar medium that was supplemented with yeast. Flies were maintained at 25°C unless otherwise noted. Table 4.1 lists the genotypes of strains used in this study. Strains obtained from the Bloomington Stock Center are denoted by B followed by the stock identification number. $D1^{Rev1B}$, a precise excision derivative of $P\{EP\}D1^{EP473}$, and the $P\{w^+; sgs3\text{-}GAL4\}$ transpositions were both generated by Dr. Karen S. Weiler (unpublished).

Crosses to analyze ectopic *D1* expression in salivary polytene chromosomes: Males homozygous for one of eleven independent $P\{w^+; sgs3\text{-}GAL4\}$ insertions lines were each crossed with $w^1; P\{EP\}D1^{EP473}/ TM6B, Tb^1$ and $P\{EP\}D1^{Rev1B}/ TM6B, Tb^1$ virgin females. $P\{w^+; sgs3\text{-}GAL4\}\#34$, homozygous lethal was balanced with $T(2;3)TSTL, CyO, TM6B, Tb^1$. $P\{w^+; sgs3\text{-}GAL4\}\#34/ T(2;3)TSTL, CyO, TM6B, Tb^1$ males were crossed to $w^1; P\{EP\}D1^{EP473}/ TM6B, Tb^1$ and $P\{EP\}D1^{Rev1B}/ TM6B, Tb^1$ virgin females. Tb^+ wandering third instar larvae were selected for polytene chromosome analysis.

Salivary polytene chromosome squashes: Third instar larvae raised at 25°C in non-crowded conditions, were used for all assays. Polytene chromosome squashes were done according to the protocol of Kennison [51]. Briefly, salivary glands were dissected in 0.7% NaCl and transferred to 10 ul of 45% acetic acid for 30 seconds. 15 ul of staining solution (2% orcein in a 50% acetic acid, 30% lactic acid solution) was deposited on a siliconized coverslip. Salivary glands were placed in staining solution for two minutes and then squashed. Excess staining solution was removed and coverslip sealed with nail polish. Slides were stored at 4°C prior to scoring. A rating scale was used ranging from one to ten to score the degree of spreading of the polytene chromosomes. A rating of one represented extreme tangling and a rating of ten represented the spreading typical of wild-type polytene chromosome squashes.

Cytological mapping of ectopic contacts: Ectopic contacts were mapped utilizing the photographic maps of polytene chromosomes of Lefevre [54] tied to Bridges' [20] drawings. All mapping was carried out under brightfield microscopy at 400X magnification. Nuclei to be mapped were chosen based on the required presence of each chromosome arm with the exception of chromosome 4. Chromosome 4 could only be

visualized in four out of 65 chromosome squashes. In the 61 nuclei in which chromosome four could not be visualized, it was most likely too close to the chromocenter to be distinguished. Because of this, there may have been a bias of contacts between chromosome four and the chromocenter. The nuclei to be mapped were also chosen based on the ability to accurately map each and every ectopic association. Nuclei that were too tightly tangled to discern chromosome arms were disregarded.

BLAST analysis: Ten tandem copies of the AATAT satellite repeat were applied as a query for BLAST analysis of the fly genome (http://flybase.bio.indiana.edu/blast/). A bit score of 30.2 was used as the minimum cutoff for homology on the X chromosome, which reflects a minimum of 15 out of 50 identical, consecutive letter to letter positions in the alignment. Localization of the 359 bp satellite repeat was performed utilizing one copy of the 359bp sequence query for BLAST analysis of the fly genome. A bit score of 69.9 was used as the minimum homology cutoff on the X chromosome, which reflects a minimum of 35 out of 359 identical, consecutive letter to letter positions in the alignment.

Table 4.1: Strains used in these experiments
y w sn³; P{w⁺; sgs3-GAL4} insertion line 1/*S² CyO cn² bw*
y w ; P{w⁺; sgs3-GAL4} insertion line 3/*S² CyO cn² bw*
y w ; P{w⁺; sgs3-GAL4} insertion line 9/*S² CyO cn² bw*
y w ; P{w⁺; sgs3-GAL4} insertion line 19/*S² CyO cn² bw*
y w ; P{w⁺; sgs3-GAL4} insertion line 27/*S² CyO cn² bw*
y w ; P{w⁺; sgs3-GAL4} insertion line 32/*S² CyO cn² bw*
y w sn³; P{w⁺; sgs3-GAL4} insertion line 37/*S² CyO cn² bw*
y w ; P{w⁺; sgs3-GAL4} insertion line 39/*S² CyO cn² bw*
P{w⁺; sgs3-GAL4}/FM7c B insertion line 40/*S² CyO cn² bw*
y w ; P{w⁺; sgs3-GAL4} insertion line 42/*S² CyO cn² bw*
y w ; P{w⁺; sgs3-GAL4} insertion line 43/*S² CyO cn² bw*
y w sn³; P{w⁺; sgs3-GAL4} insertion line 34/*T(2;3)TSTL, CyO, TM6B, Tb¹*
w¹¹¹⁸; P{w⁺; sgs3-GAL4} (B6870)

Results

An analysis of independent insertions of the *P{w⁺; sgs3-GAL4}* transgene for expression level.

Previous analyses of *D1* overexpression in the salivary glands mediated by *P{sgs3-GAL4}* revealed that the polytene chromosomes would not spread but rather were entangled as shown in Figure 4.2B. The points of contact between chromosome arms could not be identified due to the extremity of the tangling. As a potential means to decrease the *GAL4* expression level, and thereby lessen the degree of tangling, the *P{sgs3-GAL4}* transgene was mobilized and new insertions recovered. The transposed *P{sgs3-GAL4}* insertions lines might exhibit decreased expression due to euchromatic position effects. Twelve insertions lines were tested. Polytene chromosomes of $D1^{Rev1B}$ were tested simultaneously as the positive control.

When *D1* was overexpressed in the salivary glands using *P{sgs3-GAL4}* insertion lines 1, 3, 27, 34, 37 and 43, the polytene chromosomes showed extreme entanglement (Figure 4.2B).   *P{sgs3-GAL4}* insertion lines 39 and 40 directing *D1* expression exhibited wild-type polytene chromosome spreading while *D1* overexpression with *P{sgs3-GAL4}* insertion lines 9, 19, 32 and 42 resulted in polytene chromosomes that were intermediately entangled. When assayed with $D1^{Rev1B}$, all *P{sgs3-GAL4}* insertion lines demonstrated wild-type polytene chromosome spreading (Table 4.2, Figure 4.2A). *P{sgs3-GAL4}* line 9 was chosen to target *D1* expression to the salivary glands for cytological mapping of the *D1*-induced ectopic contacts (Figure 4.2C).

Cytological mapping of polytene chromosome ectopic contacts

To precisely map the ectopic contacts due to *D1* overexpression, the salivary glands of eleven larvae each of *P{sgs3-GAL4}/+; P{EP}D1^{EP473}/+* and *P{sgs3-GAL4}/+; D1^{Rev1B}/+* were dissected. The ectopic contacts of sixty-five nuclei were cytologically mapped at the level of the lettered division for each genotype. 514 (83.9%) out of 612 total cytological intervals were involved in *D1*-induced ectopic contacts.   Data analysis revealed that chromosomes of cells in which *D1* was overexpressed exhibited over three-fold more contacts than cells in which there was no *D1* overexpression (Table 4.3). Chromosome arm 3R exhibited the greatest number of ectopic associations (480 in 65

nuclei). When the length of the arms are taken into account, 3R shows a greater frequency of contacts per kb of arm length. The degree to which the involvement of each arm in ectopic contacts was affected by *D1* overexpression, as measured by fold-increase, was 3L (4.5) > 3R (4.2) > 2R = X (3.6) > 2L (2.8).

Intervals in which multiple *D1*-induced ectopic contacts occurred were also taken into account. Cytological intervals in which five or more ectopic contacts due to *D1* overexpression occurred were considered high frequency contacts indicated in bold in Table 4.4. These intervals totaled 153 (29.8%) out of the total 514 cytological intervals involved in *D1*-induced ectopic contacts.

A comparison of *D1*-induced ectopic contacts and sites of intercalary heterochromatin (IH)

In Drosophila polytene chromosomes, specific regions are scattered throughout the euchromatic chromosome arms that demonstrate features similar to pericentric heterochromatin. These features include late replication, underreplication, ectopic pairing and HP1 binding. Each characteristic has been localized to specific cytological locations throughout the euchromatin.

The ectopic contact sites induced by *D1* overexpression were compared to sites of underreplication [99], regions of late replication [99], sites of HP1 binding [33] and sites of "natural" ectopic contacts [96] in polytene chromosomes. These data are presented in Table 4.4 and Figure 4.3 and are discussed individually below. When examined as a whole, 128 (95.5%) out of 134 sites defined as intercalary heterochromatin by exhibiting at least two of these properties, also participate in the ectopic contacts induced by *D1* overexpression. Moreover, out of the 514 cytological intervals in which ectopic contacts induced by *D1* expression were present, 330 (64.2%) of these possess at least one property associated with intercalary heterochromatin. Additionally, the high frequency sites involved in *D1*-induced ectopic contacts were compared to the cytological loci in which features of intercalary heterochromatin have been localized. These data are presented in Table 4.5 and Figure 4.4.

The sites of *D1*-induced ectopic associations were compared to the sites of underreplication in the polytene chromosomes. These regions have a different

morphological appearance and appear as weak points or breaks in the chromosomes [99]. Out of 58 total weak points localized in the polytene chromosomes [130], 55 (94.8%) are represented in the ectopic contact sites mediated by *D1* (Table 4.4, Figure 4.3) and 25 (43.1%) are represented specifically at high frequency (Table 4.5, Figure 4.4). Weak points present on 2R, 3L and the X chromosome are represented 100% in the ectopic contact sites due to *D1* overexpression. The three cytological intervals of weak point localization that are not represented do not share a common chromosome or general location.

The ectopic contact sites mediated by *D1* were also compared to sites of late DNA replication. 239 sites of late DNA replication have been localized in the polytene chromosomes [99]. Out of those, 218 (91.2%) are represented as ectopic sites mediated by *D1* (Table 4.4, Figure 4.3) and 71 (29.7%) are represented as high frequency ectopic sites mediated by *D1* (Table 4.5, Figure 4.4). 3R exhibits a strong correlation between ectopic contact sites due to *D1* and sites of DNA replication with 52 out of 53 (98.1%). Sites corresponding to both late DNA replication and ectopic contact regions due to *D1* are present on all Drosophila chromosomes.

The ectopic contact sites mediated by *D1* were also compared to another feature of intercalary heterochromatin, HP1 binding. Heterochromatin protein 1, HP1 normally associated with pericentric heterochromatin has been localized to 185 sites in the euchromatin of polytene chromosomes [33]. 173 (93.5%) of these sites are represented as sites of ectopic contacts due to *D1* (Table 4.4, Figure 4.3) while 50 (27.0%) are present as high frequency *D1*-induced ectopic contacts (Table 4.5, Figure 4.4).

Zhimulev *et al.* [96] consider the natural ectopic contacts of euchromatin to be the most important feature of intercalary heterochromatin-"a guide for its identification." A comparison of the *D1*-mediated ectopic contacts with natural ectopic contacts show that 45 (91.8%) of 49 natural ectopic contacts correspond with ectopic associations due to *D1* overexpression (Table 4.4, Figure 4.3). When solely looking at the high frequency *D1*-mediated ectopic contacts, 24 (48.9%) correlate with the sites of natural ectopic contacts (Table 4.5, Figure 4.4).

A comparison of *D1*-induced ectopic contacts and euchromatin satellite-like sequences of the X chromosome

D1 has been localized at a limited number of euchromatic loci in polytene chromosomes by immunofluorescence analysis: 81F, 83C-E, 101 and 102D [4]. Alfageme *et al*. [4] also noted that there were faintly fluorescing sites throughout all polytene chromosome arms and hypothesized that a large fraction of D1 is localized in a few regions of the genome while the remainder is widely distributed over all of the Drosophila chromosomes.

D1 binding in the euchromatin may be to satellite-like sequences. To examine this, the occurrence of ectopic contacts due to *D1* overexpression was compared with the presence of sequences homologous to the 1.688 g/cm^3 satellite and the AATAT satellite in the euchromatin of the X chromosome. Figures 4.5 and 4.7 illustrate the overlap between the cytological intervals containing repeat homology to the 1.688 g/cm^3 and the AATAT satellites on the X chromosome and the cytological intervals participating in the *D1*-mediated ectopic contacts. Of the 97 intervals involved in ectopic associations, 55 (56.7%) include sequence with homology to one or both satellite repeats. Conversely, only five intervals with homology to one or both repeats out of 89 do not participate in ectopic associations.

The high frequency intervals of *D1*-mediated ectopic contacts were also compared to the presence of sequences homologous to the 1.688g/cm^3 satellite and the AATAT satellite in the euchromatin of the X chromosome. Figures 4.6 and 4.7 show the overlap between the intervals involved in ≥ 5 ectopic contacts due to *D1* with cytological intervals associated with sequences homologous to the 1.688g/cm^3 satellite and the AATAT euchromatic satellites of the X chromosome. Of the 55 (56.7%) intervals involved in *D1*-induced ectopic associations that include sequence homology to one or both satellite repeats stated above, 32 (58.1%) occur at high frequency.
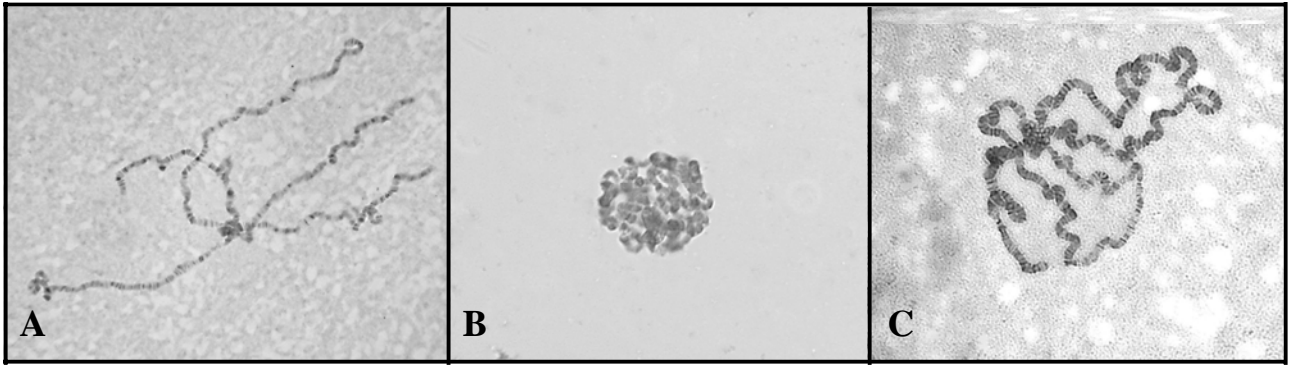
Figure 4.2: *D1* overexpression in the salivary gland leads to polytene chromosome entanglement.
(A) Orcein stained wild-type polytene chromosome squash. (B) Orcein stained polytene chromosomes from an individual with the *P{w⁺; sgs3-GAL4}* insertion on chromosome 3 directing *D1* expression and (C) the *P{w⁺; sgs3-GAL4}* insertion line 9 on chromosome 2 directing *D1* expression.

Table 4.2: Analysis of *P{w⁺; sgs3-GAL4}* insertion lines for expression level

P{sgs3-GAL4} insertion lines	Chromosome spreading[a]	
	P{EP}D1^{EP473}	*D1^{Rev1B}*
Line 1	3	10
Line 3	2	10
Line 9	7	10
Line 19	7	10
Line 27	5	10
Line 32	7.5	10
Line 34	3	10
Line 37	2	10
Line 39	10	10
Line 40	10	10
Line 42	6.5	10
Line 43	6	10

[a]A rating scale was used ranging from one to ten to evaluate the degree of spreading of the polytene chromosomes. One represents extreme tangling and 10 represents tangling typical of wild-type polytene chromosome squashes.

Table 4.3: Analysis of ectopic contacts due to *D1* overexpression in the polytene chromosomes

	X 22,232kb[b]	2L 21,329kb[b]	2R 20,785kb[b]	3L 24,132kb[b]	3R 27,878kb[b]	4 1271kb[b]	ALL
P{sgs3-GAL4}/+; P{EP}D1^{EP473}							
Total ectopic contacts	361	380	300	394	480	4	1919
Average ectopic contacts per nucleus	5.55	5.85	4.62	6.06	7.38	0.06	29.52
# of lettered subdivisions associated with ectopic contacts (high frequency intervals)[a]	102 (32)	93 (31)	101 (16)	105 (28)	110 (46)	3 (0)	514 (153)
P{sgs3-GAL4}/+; D1^{Rev1B}							
Total ectopic contacts	95	82	83	87	120	0	467
Average ectopic contacts per nucleus	1.46	1.26	1.28	1.34	1.85	0	7.18
# of lettered subdivisions associated with ectopic contacts (high frequency intervals)[a]	57 (1)	56 (0)	56 (1)	51(2)	67 (0)	0 (0)	287 (4)

[a]High frequency intervals refer to any lettered subdivision involved in greater than or equal to five associations
[b]Length of chromosome arms from flybase (http://flybase.net/cgi-bin/gbrowse/dmel)

Table 4.4: *D1*-mediated ectopic contact sites compared to localization of weak points, sites of late replication, HP1 binding sites and the sites of natural ectopic contacts

All cytological intervals	Frequency of *D1*-mediated ectopic contacts	Localization of weak points	Sites of late replication	HP1 binding sites	Natural ectopic pairing sites
1A	**21**		1AB	1A 1,2	1A
1B	**5**			1B11	
1C	0				
1D	1		1D	1D1,2	
1E	0		1E		
1F	1		1F		
2A	0				
2B	**5**			2B	
2C	3				
2D	0			2D1,2	
2E	0				
2F	1				
3A	4		3A1-4		
3B	1				
3C	2	3C3-5	3C		3C
3D	3			3 D 1,2	
3E	3			3 E 3,4	
3F	1				
4A	1		4A		
4B	**5**		4B		
4C	3		4C		4C
4D	1	4D1-2	4D	4 D 3-7	
4E	1		4E	4 E 3	
4F	1		4F	4 F 9,10	
5A	2		5A	5 A 7	
5B	2				
5C	1		5C		
5D	3	5D1-6	5D		
5E	1				
5F	1				
6A	**6**		6A	6 A 3,4	
6B	2				
6C	0				
6D	0			6 D 7,8	
6E	0			6 E 9-11	
6F	0				
7A	3			7A 3-5	7ABC
7B	3	7B1-2	7B	7 B 3,4	
7C	**9**		7C		
7D	**6**			7 D	
7E	4		7E		
7F	4				
8A	**7**		8AB		
8B	1				8B
8C	2		8C	8 C 7,8	
8D	**5**				
8E	3		8E	8 E 5-12	
8F	1				
9A	**5**		9A	9 A 4	9AB
9B	2				
9C	**8**				
9D	1			9 D 1,2	
9E	4			9 E 1,2	
9F	1				
10A	3		10A1-2	10A3-11	
10B	**7**	10B1–2	10B1-2		
10C	1			10 C 1,2	
10D	1				
10E	2				
10F	1			10 F 10,11	
11A	**7**	11A6–9	11A		11A
11B	**14**			11 B 17,18	
11C	0		11C		
11D	1		11D	11 D 3-11	
11E	1				

Table 4.4 continued

All cytological intervals	Frequency of *D1*-mediated ectopic contacts	Localization of weak points	Sites of late replication	HP1 binding sites	Natural ectopic pairing sites
11F	1			11 F 7-9	
12A	**6**		12A	12 A 1,2	
12B	**8**				
12C	3				
12D	3		12D		
12E	2	12E7-8	12EF		12EF
12F	3				
13A	**6**		13A		
13B	1		13B		
13C	**5**				
13D	0				
13E	**6**	13E1-2			
13F	2				
14A	**7**			14 A 1,2	
14B	4		14B		
14C	**5**			14 C 6,7	
14D	**5**				
14E	2				
14F	1			14 F 4	
15A	3				
15B	4		15B		
15C	2			15 C 1,2	
15D	**6**		15D		
15E	1				
15F	0				
16A	**9**		16A	16 A 3,4	
16B	2			16 B 12	
16C	1			16 C 9,10	
16D	**5**				16D
16E	1			16 E 1,2	
16F	**5**	16F1-4	16F		
17A	4		17A		
17B	4		17B		
17C	0		17C		
17D	0		17D		
17E	3		17E		
17F	0		17F	17 F 1,2	
18A	**5**		18A		
18B	**7**				
18C	4				
18D	**5**		18D		
18E	1				
18F	3			18 F 4,5	18F/19A
19A	1		19AD		
19B	3				
19C	2				
19D	0				
19E	**6**	19E1-4	19E		19E
19F	**6**				
20A	**7**		20AF	20 A	
20B	1	20B			
20C	1				
20D	1				
20E	0				
20F	0				
101A	1				
101B	0				
101C	0				
101D	0		101DF		
101E	0				
101F	0				101F
102A	0				
102B	0				
102C	0				
102D	1		102D		
102E	0				
102F	2		102F		102F

Table 4.4 continued

All cytological intervals	Frequency of *D1*-mediated ectopic contacts	Localization of weak points	Sites of late replication	HP1 binding sites	Natural ectopic pairing sites
21A	4		21A	21 A 1,2	21A
21B	1			21 B 4,5	
21C	0		21C		
21D	0		21D		
21E	1				
21F	0				
22A	2	22A1-3	22A	22 A 6	22AB
22B	**7**		22B		
22C	1		22C		
22D	1			22 D 1-5	
22E	0				
22F	0		22F-23A		
23A	3				
23B	0				
23C	0			23 C 1,2	
23D	0				
23E	**5**		23E	23 E	
23F	4				
24A	0			24 A 3-5	
24B	0				
24C	1	24D1-2			
24D	2		24DE	24 D 2,3	
24E	2				
24F	1			24 F 3-8	
25A	0	25A1-4	25A		25A
25B	2			25 B	
25C	3				
25D	**5**			25 D 1-5	
25E	**7**		25EF		25E
25F	1				
26A	4	26A	25F-26A	26 A 2,3	
26B	0			26 B 10,11	
26C	1	26C1-2	26C		
26D	1				
26E	0			27 E 1,2	
26F	0				
27A	**7**				
27B	1				
27C	0				
27D	1				
27E	3				
27F	0				
28A	1	28A	28A	28 A 3-6	
28B	0		28B	28 B 1,2	
28C	0		28C		
28D	4		28D		
28E	0				
28F	1			28 F 5	
29A	1				
29B	1				
29C	1				
29D	0				
29E	**9**				
29F	1		29F	29 F 1,2	
30A	3	30A	30A	30 A 3-6	
30B	**6**			30 B 3-12	
30C	3				
30D	2				
30E	0				
30F	0			30 F	
31A	4		31A		
31B	3			31B	
31C	1			31C	
31D	0				

Table 4.4 continued

All cytological intervals	Frequency of *D1*-mediated ectopic contacts	Localization of weak points	Sites of late replication	HP1 binding sites	Natural ectopic pairing sites
31E	1			31E	
31F	3				
32A	3	32A1-2	32A		
32B	3				
32C	4			32 C 3-5	
32D	0				
32E	**5**				
32F	2		32F-33A		
33A	**9**	33A1–2			33A
33B	4			33 B 1,2	
33C	1		33CD	33 C	
33D	**5**	33D1-4			
33E	**5**			33 E 3-10	
33F	4		33F-34A		
34A	**10**	34A1–4		34 A 5,6	
34B	**10**			34 B 6,7	
34C	**8**				
34D	**6**				
34E	**7**		34EF		
34F	**6**				
35A	3				35A
35B	**12**		35B	35 B	
35C	3	35C	35C		
35D	**7**	35D1-4	35D		
35E	3		35E		
35F	**6**		35F		35F
36A	3			36 A 6,7	
36B	3				
36C	3	36C1-2	36C		
36D	**6**	36D	36D		36D
36E	**15**		36E		
36F	2			36 F	
37A	**8**		37A		
37B	**13**				
37C	**7**				
37D	3		37D		
37E	**6**				
37F	**5**				
38A	1		38A		
38B	**16**		38B	38 B 3-6	
38C	**7**	38C1–2	38C	38 C 1,2	
38D	3				
38E	4		38E		
38F	4				
39A	3			39 A 1,2	39A
39B	**5**				
39C	1			39 C 1,2	
39D	2	39DE	39DE		
39E	**10**				39E
39F	4				
40A	2		40AB	40 A 1-4	
40B	0				
40C	0	40C	40C		
40D	0		40DF		
40E	1				
40F	1				
41A	0		41AC	41	
41B	0			41	
41C	2			41	
41D	2		41DE	41	
41E	4			41	
41F	4		41F	41	

Table 4.4 continued

All cytological intervals	Frequency of *D1* - mediated ectopic contacts	Localization of weak points	Sites of late replication	HP1 binding sites	Natural ectopic pairing sites
42A	4		42A	42 A 3-12	
42B	4	42B1-3	42B	42 B	42B
42C	3				
42D	0				
42E	1			42 E	
42F	1				
43A	1		43A		
43B	2				
43C	4			43 C	
43D	0				
43E	2			43 E	
43F	1				
44A	**5**				
44B	0				
44C	1		44CD		
44D	0				
44E	1				
44F	1		44F		
45A	1		45A		
45B	**5**			45 B 1,2	
45C	4		45C		
45D	1		45D		
45E	0		45E		
45F	1			45 F	
46A	0		46A		
46B	2				
46C	3			46 C	
46D	1				
46E	1				
46F	0			46 F	
47A	2		47A	47 A 14-16	
47B	2				
47C	2		47C		
47D	4		47D	47 D 5-8	
47E	2				
47F	3				
48A	**5**		48AB		
48B	**5**			48 B 1-5	
48C	4		48C	48 C	
48D	2		48DE		
48E	2				
48F	1				
49A	1				
49B	4				
49C	4		49C		
49D	**5**				
49E	2				
49F	2			49 F 1-8	
50A	4		50A		
50B	3				
50C	4	50C1-4	50C	50 C 6-10	
50D	2			50 D 4,5	
50E	1			50 E 1,2	
50F	2				
51A	1		51A		
51B	0		51B		
51C	1		51C		
51D	3		51D		
51E	2		51E		
51F	3			51 F	
52A	2			52 A	
52B	**8**				

Table 4.4 continued

All cytological intervals	Frequency of *D1* - mediated ectopic contacts	Localization of weak points	Sites of late replication	HP1 binding sites	Natural ectopic pairing sites
52C	3			52 C 3,4	
52D	4			53 D 3-9	
52E	2				
52F	4				
53A	4		53A	54 A 1,2	
53B	0		53BC		
53C	1				
53D	1				
53E	1				
53F	0				
54A	1		54AB		
54B	2				
54C	1				
54D	3				
54E	3				
54F	4				
55A	2		55AB	55 A	
55B	1				
55C	**5**		55C		
55D	0		55D		
55E	1			55 E 1,2	
55F	**5**				
56A	3		56AB		
56B	2				
56C	**5**				
56D	3			56 D	
56E	2			56 E	
56F	**7**		56F		56F
57A	3	57A1-4	57A		57AB
57B	**5**		57B	57 B 3	
57C	4			57 C 5-9	
57D	0				
57E	**10**				
57F	**5**			57 F 3-11	
58A	4		58A		
58B	2				
58C	0				
58D	**5**				
58E	**5**			58 E	
58F	0				
59A	3				
59B	0				
59C	2				
59D	1		59D	59 D 5-11	59D
59E	1				
59F	0				
60A	2				
60B	4			60 B 12,13	
60C	0		60CD		
60D	1				
60E	2				
60F	**21**		60F	60 F	60F

Table 4.4 continued

All cytological intervals	Frequency of *D1* - mediated ectopic contacts	Localization of weak points	Sites of late replication	HP1 binding sites	Natural ectopic pairing sites
61A	**10**		61A	61 A 1–3	61A
61B	**6**				
61C	0		61C	61 C 1-4	
61D	1			61 D 3,4	
61E	2		61E	61 E 3	
61F	1		61F		
62A	3				
62B	2				
62C	2		62C	62 C 3,4	
62D	0		62D		
62E	2			62 E	
62F	0			62 F 1,2	
63A	3		63A		
63B	2				
63C	4				
63D	0				
63E	1		63E		
63F	3			63 F 3-7	
64A	2				
64B	3			64 B 14-17	
64C	**9**	64C4-5	64C		64C
64D	2		64D		
64E	4		64E		
64F	4		64F		
65A	4		65A		
65B	**6**	65B1-2	65B		65B
65C	1		65C		
65D	3	65D1-3	65D	65 D 4-6	
65E	**6**	65E1-4	65E		
65F	3		65F		
66A	**9**		66A		
66B	**14**		66B		
66C	**8**				
66D	**6**			66 D 13-15	
66E	4				
66F	4			66 F 5	
67A	**5**	67A1-4	67A		67A
67B	**6**			67 B	
67C	**11**			67 C 6-11	
67D	3	67D9-10	67D	67 D 7	67D
67E	**8**			67 E 5-7	
67F	2		67F		
68A	**5**		68A		
68B	**5**				
68C	**10**			68 C 1,2	
68D	4				
68E	4		68E		
68F	4				
69A	**7**		69A		
69B	3		69B		
69C	2				
69D	4		69D	69 D 3-4	
69E	3				
69F	3		69F	69 F 3-7	
70A	3		70A		70AB
70B	3				
70C	3	70C1-2	70C		70C
70D	**7**		70D		
70E	4				
70F	2			70 F 1,2	
71A	**7**		71A		
71B	3				

Table 4.4 continued

All cytological intervals	Frequency of *D1* - mediated ectopic contacts	Localization of weak points	Sites of late replication	HP1 binding sites	Natural ectopic pairing sites
71C	**5**	71C1-2	71C		71C
71D	2			71 D 1,2	
71E	0				
71F	4				
72A	4		72A		
72B	0				
72C	1				
72D	2			72 D 7-9	
72E	3		72E		
72F	3				
73A	2		73A		
73B	1				
73C	1				
73D	2				
73E	4			73 E 3-6	
73F	0				73F/74A
74A	**6**	74A1-6	74A		
74B	1				
74C	2				
74D	3			74 D 4	
74E	2				
74F	2				
75A	**8**		75A		
75B	2			75 B 1,2	
75C	**11**	75C1-2	75C		75C
75D	**5**				
75E	2				
75F	2			75 F 1,2	
76A	**8**	76A1-4	76A		
76B	3		76B		
76C	**5**				
76D	2		76D	76 D 3,4	
76E	1			76 E 1,2	
76F	0				
77A	**5**				
77B	4				
77C	3				
77D	0				
77E	2		77E	77 E 5-8	
77F	0				
78A	2		78A		
78B	1			78 B 1,2	
78C	2				
78D	1				
78E	2				
78F	0				
79A	1				
79B	1				
79C	0		79C		
79D	1		79D		
79E	2		79E	79 E 3	
79F	2				
80A	**7**		80AC		80ABC
80B	3				
80C	1				
80D	0				
80E	0				
80F	0				
81A	0				
81B	0				
81C	0				
81D	0				

Table 4.4 continued

All cytological intervals	Frequency of *D1* - mediated ectopic contacts	Localization of weak points	Sites of late replication	HP1 binding sites	Natural ectopic pairing sites
81E	0				
81F	0	81F	81F		81F
82A	3				
82B	1				
82C	1				
82D	0				
82E	2				
82F	1			82 F	
83A	3				
83B	1				
83C	**5**			83 C 5-9	
83D	1	83D1-5	83DE		83D
83E	1				
83F	1			83 F 1,2	
84A	**6**		84AB		84A
84B	2	84B		84 B 3-6	
84C	2				
84D	**14**	84D	84D		84D
84E	**9**				
84F	4			84 F 14-16	
85A	**7**		85A		
85B	**8**				
85C	3				
85D	**12**				
85E	**6**				
85F	**5**			85 F 1-8	
86A	**6**		86A		
86B	**7**				86D
86C	**5**	86C	86C		
86D	**5**	86D1-5	86D		
86E	**9**		86E	86 E 12-18	
86F	2				
87A	**7**				
87B	3	87B1-5	87B	87 B	
87C	4	87C1-3	87C		
87D	2		87D	87 D	
87E	2		87E		
87F	4		87F	87 F 4-10	
88A	4		88A	88 A 6-8	
88B	4				
88C	4			88 C	
88D	1			88 D	
88E	1		88E	88 E	
88F	1			88 F 7-9	
89A	**5**		89A	89 A	
89B	4			89 B	
89C	**6**				
89D	1		89D		
89E	3	89E1-4	89E		89E
89F	**7**				
90A	**5**	90A1-2	90A		
90B	**6**			90 B	
90C	1			90C	
90D	3		90D	90 D 3-6	
90E	0				
90F	**6**				
91A	4		91A	91 A 1-3	
91B	2		91B		
91C	2				
91D	**8**			91 D 3-5	
91E	1				
91F	**7**				

Table 4.4 continued

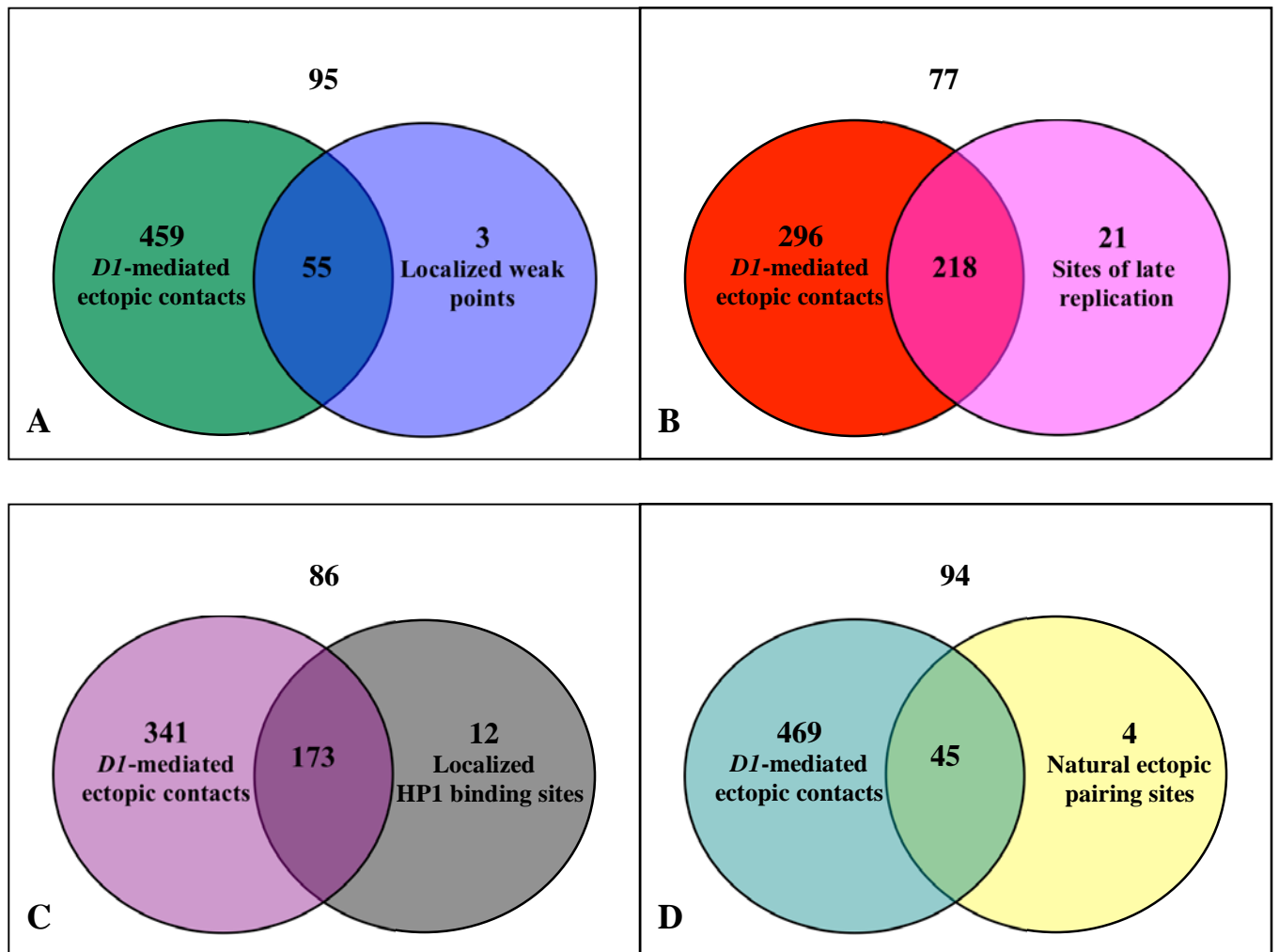| All cytological intervals	Frequency of *D1* -mediated ectopic contacts	Localization of weak points	Sites of late replication	HP1 binding sites	Natural ectopic pairing sites
92A	**8**		92A	92 A	
92B	**5**		92B	92 B 4-11	
92C	**7**		92C	92 C 3-6	
92D	**8**		92D		
92E	4	92E1-4	92E		
92F	**6**		92F		
93A	**5**	93A			
93B	2				
93C	**5**			93 C	
93D	**5**			93 D 6,7	
93E	**5**		93E		
93F	4		93F		
94A	**7**		94A	94 A 12-16	94A
94B	**8**				
94C	3			94 C 1-5	
94D	**5**	94D1-4	94D		94D
94E	2			94 E	
94F	3				
95A	3		95A		
95B	4				
95C	0				
95D	2				
95E	**5**			95 E 1,2	
95F	**6**			95 F	
96A	**9**		96A		
96B	**12**				
96C	3		96C		
96D	2		96D		
96E	**6**		96E	96 E 1,2	
96F	4		96F	96 F 12-14	
97A	2		97AB		
97B	**6**				
97C	**7**				
97D	4				
97E	4				
97F	3				
98A	**6**		98A		
98B	**8**		98B		
98C	2	98C1-2	98C		98C
98D	**5**		98D	98 D 6,7	
98E	4		98E	98 E 5,6	
98F	2		98F	98 F 1,2	
99A	1		99A		
99B	4		99B	99 B 3,6-11	
99C	2			99 C 1-6	
99D	1				
99E	2		99E		
99F	0		99F	99 F	
100A	3	100A1-2	100A		100A
100B	2		100B	100 B 6-9	
100C	3		100C		
100D	2		100D		
100E	3				
100F	**16**			100 F	

Figure 4.3: Coincidence of sites of ectopic contacts and sites exhibiting features of intercalary heterochromatin within the salivary gland polytene chromosomes. The locations of cytological intervals involved in ectopic contacts due to *D1* overexpression were compared to those of (A) weak points, (B) sites of late replication, (C) HP1 binding sites and (D) natural ectopic contact sites as described in the published literature. The *Drosophila melanogaster* polytene chromosomes are divided into a total of 612 cytological intervals. The Venn diagrams are not drawn to scale.

Table 4.5: High frequency *D1*-mediated ectopic contact sites compared to localization of weak points, sites of late replication, HP1 binding sites and the sites of natural ectopic contacts

All cytological intervals	Frequency of *D1*-mediated ectopic contacts	Localization of weak points	Sites of late replication	HP1 binding sites	Natural ectopic pairing sites
1A	21		1AB	1A 1,2	1A
1B	5			1B11	
2B	5			2B	
4B	5		4B		
6A	6		6A	6 A 3,4	
7C	9		7C		
7D	6			7 D	
8A	7		8AB		
8D	5				
9A	5		9A	9 A 4	9AB
9C	8				
10B	7	10B1–2	10B1-2		
11A	7	11A6–9	11A		11A
11B	14			11 B 17,18	
12A	6		12A	12 A 1,2	
12B	8				
13A	6		13A		
13C	5				
13E	6	13E1-2			
14A	7			14 A 1,2	
14C	5			14 C 6,7	
14D	5				
15D	6		15D		
16A	9		16A	16 A 3,4	
16D	5				16D
16F	5	16F1-4	16F		
18A	5		18A		
18B	7				
18D	5		18D		
19E	6	19E1-4	19E		19E
19F	6				
20A	7		20AF	20 A	
22B	7		22B		
23E	5		23E	23 E	
25D	5			25 D 1-5	
25E	7		25EF		25E
27A	7				
29E	9				
30B	6			30 B 3-12	
32E	5				
33A	9	33A1–2			33A
33D	5	33D1-4			
33E	5			33 E 3-10	
34A	10	34A1–4		34 A 5,6	
34B	10			34 B 6,7	
34C	8				
34D	6				
34E	7		34EF		
34F	6				
35B	12		35B	35 B	
35D	7	35D1-4	35D		
35F	6		35F		35F
36D	6	36D	36D		36D
36E	15		36E		
37A	8		37A		
37B	13				
37C	7				
37E	6				
37F	5				
38B	16		38B	38 B 3-6	
38C	7	38C1–2	38C	38 C 1,2	
39B	5				
39E	10				39E
44A	5				
45B	5			45 B 1,2	
48A	5		48AB		

Table 4.5 continued

48B	5			48 B 1-5	
49D	5				
52B	8				
55C	5		55C		
55F	5				
56C	5				
56F	7		56F		56F
57B	5		57B	57 B 3	
57E	10				
57F	5			57 F 3-11	
58D	5				
58E	5			58 E	
60F	21		60F	60 F	60F
61A	10		61A	61 A 1–3	61A
61B	6				
64C	9	64C4-5	64C		64C
65B	6	65B1-2	65B		65B
65E	6	65E1-4	65E		
66A	9		66A		
66B	14		66B		
66C	8				
66D	6			66 D 13-15	
67A	5	67A1-4	67A		67A
67B	6			67 B	
67C	11			67 C 6-11	
67E	8			67 E 5-7	
68A	5		68A		
68B	5				
68C	10			68 C 1,2	
69A	7		69A		
70D	7		70D		
71A	7		71A		
71C	5	71C1-2	71C		71C
74A	6	74A1-6	74A		
75A	8		75A		
75C	11	75C1-2	75C		75C
75D	5				
76A	8	76A1-4	76A		
76C	5				
77A	5				
80A	7		80AC		80ABC
83C	5			83 C 5-9	
84A	6		84AB		84A
84D	14	84D	84D		84D
84E	9				
85A	7		85A		
85B	8				
85D	12				
85E	6				
85F	5			85 F 1-8	
86A	6		86A		
86B	7				86D
86C	5	86C	86C		
86D	5	86D1-5	86D		
86E	9		86E	86 E 12-18	
87A	7				
89A	5		89A	89 A	
89C	6				
89F	7				
90A	5	90A1-2	90A		
90B	6			90 B	
90F	6				
91D	8			91 D 3-5	
91F	7				
92A	8		92A	92 A	
92B	5		92B	92 B 4-11	
92C	7		92C	92 C 3-6	
92D	8		92D		
92F	6		92F		
93A	5	93A			
93C	5			93 C	
93D	5			93 D 6,7	
93E	5		93E		

Table 4.5 continued

94A	7		94A	94 A 12-16	94A
94B	8				
94D	5	94D1-4	94D		94D
95E	5			95 E 1,2	
95F	6			95 F	
96A	9		96A		
96B	12				
96E	6		96E	96 E 1,2	
97B	6				
97C	7				
98A	6		98A		
98B	8		98B		
98D	5		98D	98 D 6,7	
100F	16			100 F	
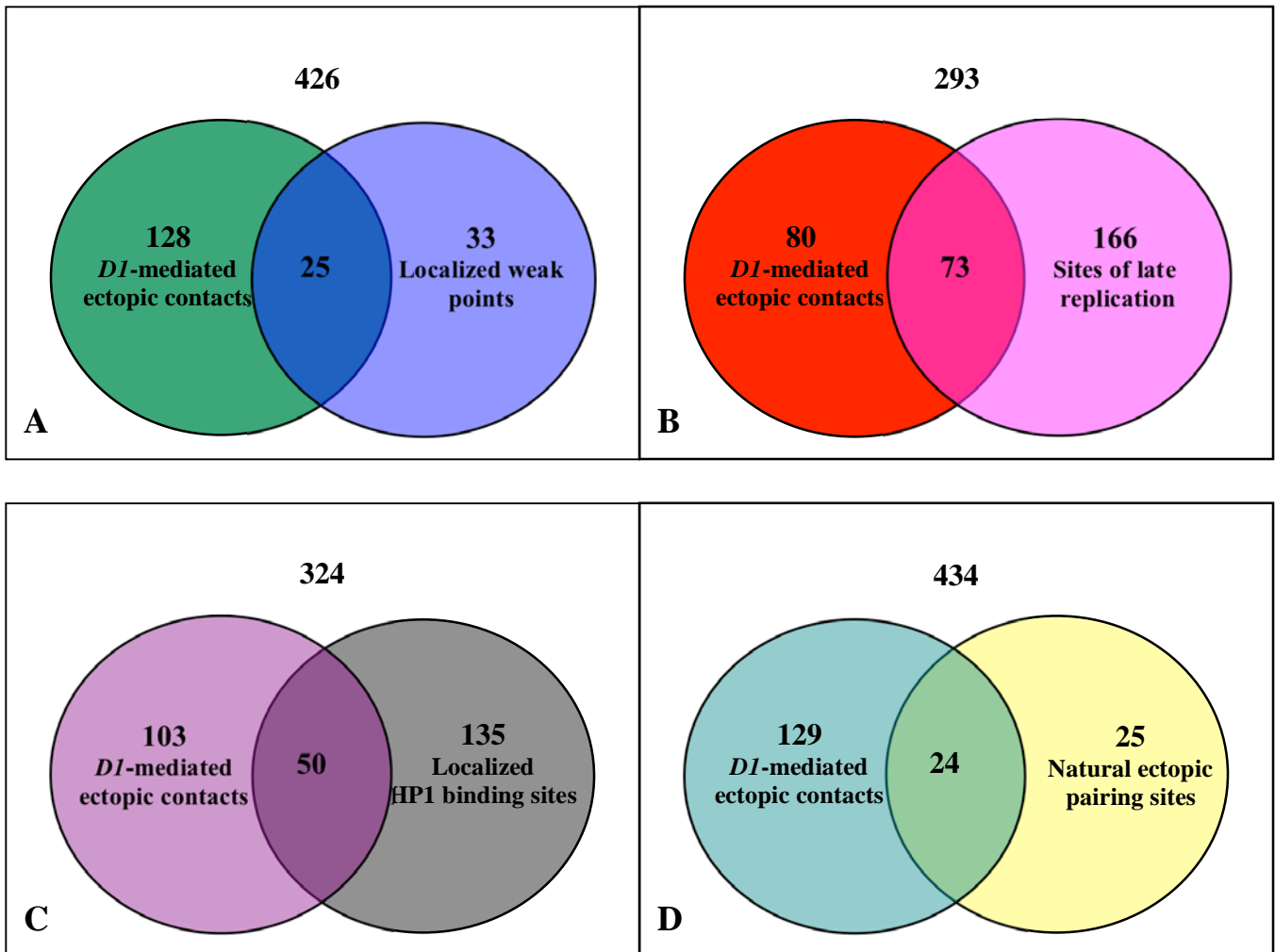
Figure 4.4: Coincidence of sites of high frequency ectopic contacts and sites exhibiting features of intercalary heterochromatin within the salivary gland polytene chromosomes. The locations of cytological intervals involved in high frequency ectopic contacts (n ≥ 5) due to *D1* overexpression were compared to those of (A) weak points, (B) sites of late replication, (C) HP1 binding sites and (D) natural ectopic contact sites as described in the published literature. The *Drosophila melanogaster* polytene chromosomes are divided into a total of 612 cytological intervals. The Venn diagrams are not drawn to scale.
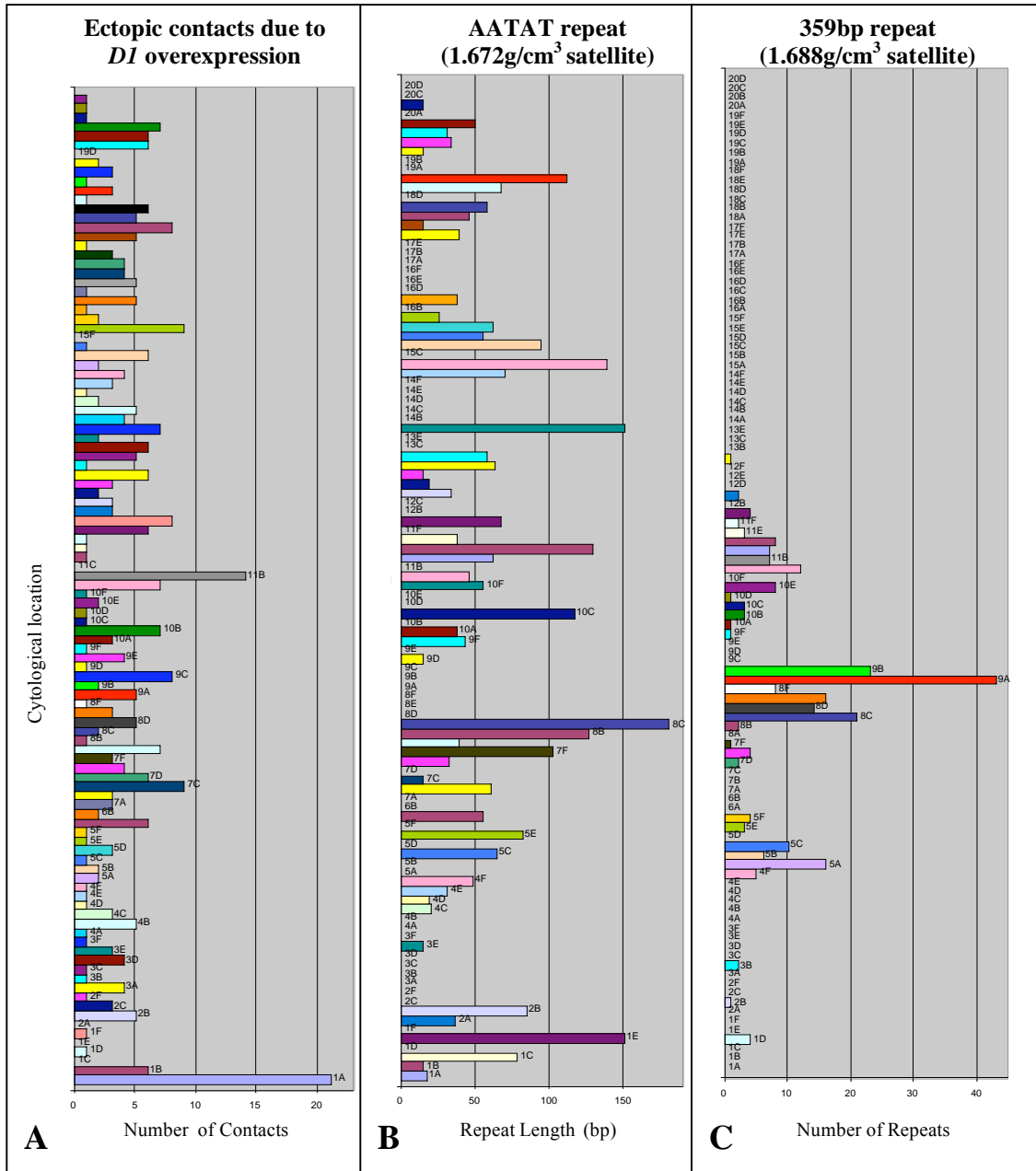
Figure 4.5: The frequency of ectopic contacts mediated by *D1* expression overlap with euchromatic regions of the X chromosome with homology to the 1.688g/cm³ satellite repeat and the 1.672g/cm³ satellite repeat. (A) The frequency of cytological intervals involved in ectopic contacts mediated by *D1* were compared to cytological regions of euchromatin of the X chromosome with homology to (B) the 1.672g/cm³ satellite repeat where repeat length is represented on the X axis and (C) the 1.688g/cm³ satellite repeat where the X axis represents the number of repeats present. Only lettered subdivisions from the X chromosome exhibiting one or more of the three characteristics above are included.
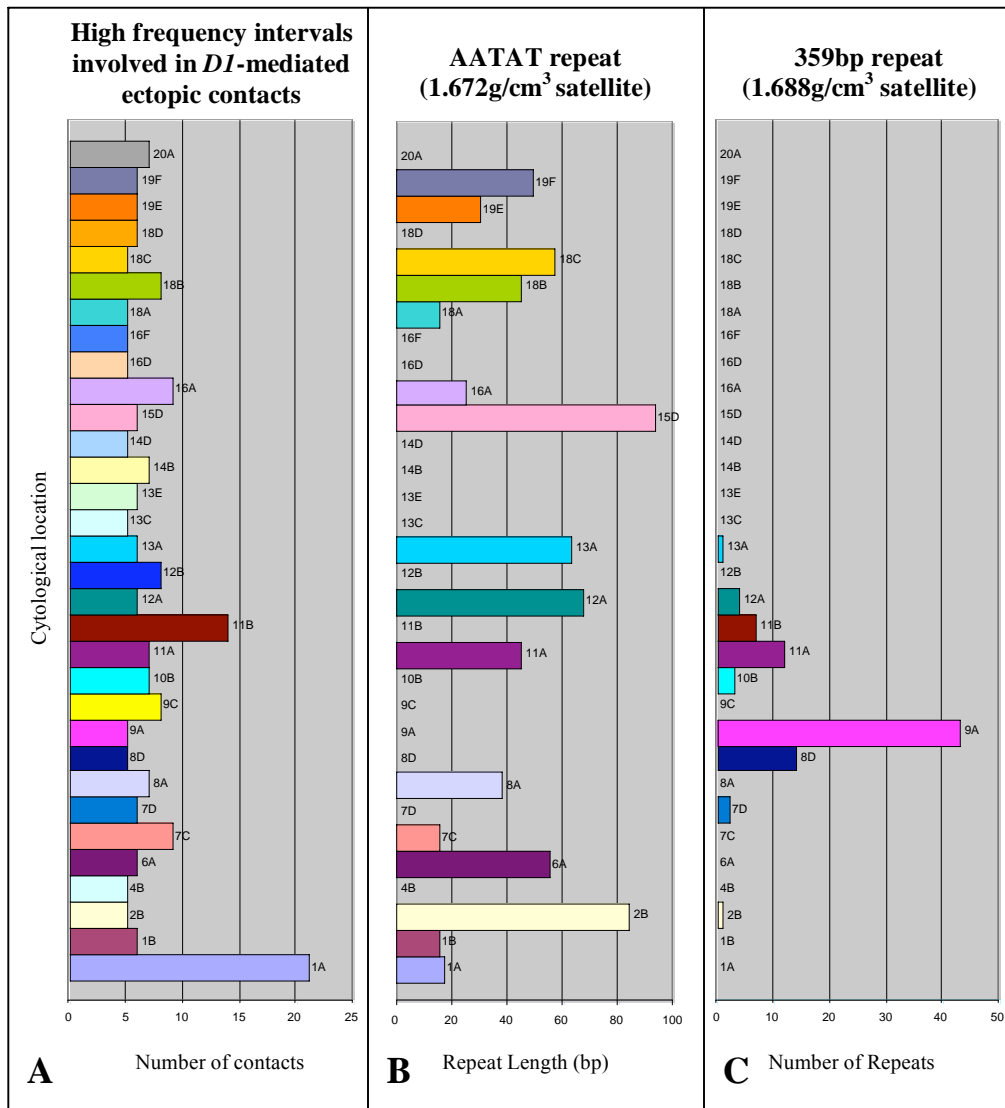
Figure 4.6: Coincidence of X chromosome cytological intervals with homology to the AATAT satellite repeat or the 359 bp[3] satellite repeat with high frequency ectopic contact sites. Only the cytological intervals involved in high frequency ($n \geq 5$) ectopic contacts mediated by *D1* overexpression are shown. (B) The distribution pattern of regions of euchromatin of the X chromosome with homology to the AATAT (*a.k.a.* 1.672 g/cm^3) satellite repeat, where repeat length is represented on the X axis. (C) The distribution pattern of regions of euchromatin of the X chromosome with homology to the 359 bp (*a.k.a.* 1.688 g/cm^3) satellite repeat, where the X axis represents the number of repeats present.
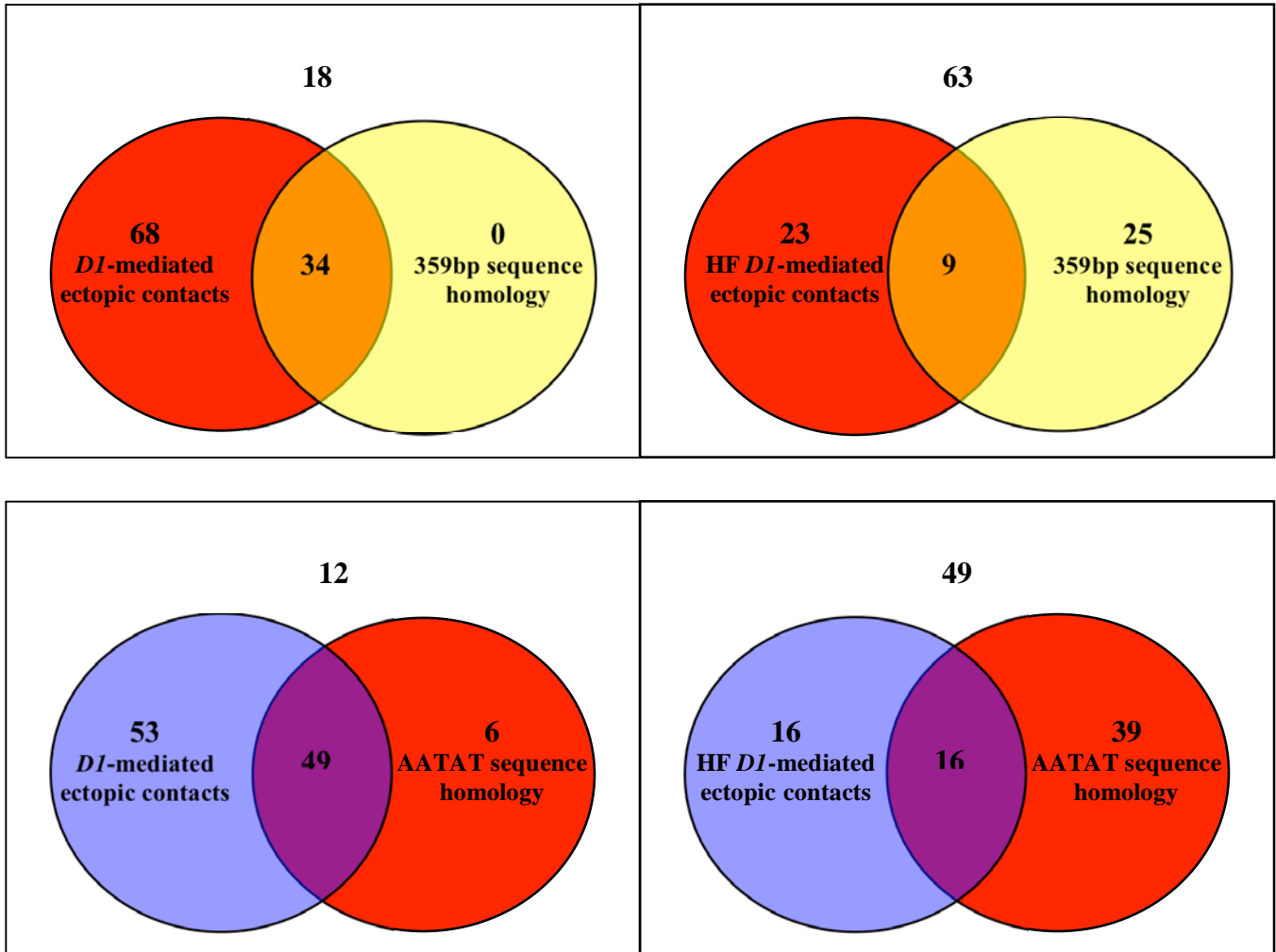
Figure 4.7: Coincidence of sites of ectopic contacts and sites with homology to the AATAT satellite repeat and the 359 bp satellite repeat along the salivary gland polytene X chromosome. The cytological intervals involved in *D1*-induced ectopic contacts were compared to cytological regions of euchromatin of the X chromosome with homology to the (A) AATAT (*a.k.a.*1.672 g/cm^3) satellite repeat and (C) the 359 bp (*a.k.a.* 1.688 g/cm^3) satellite repeat. The cytological intervals involved in high frequency ectopic contacts (n ≥ 5) mediated by *D1* were compared to regions of euchromatin of the X chromosome with homology to the (B) AATAT satellite repeat and (D) the 359 bp satellite repeat. The X chromosome is divided into 120 cytological intervals. The Venn diagrams are not drawn to scale.

Discussion

D1 overexpression and polytene chromosome morphology

Increased amounts of *D1* in the salivary glands induce changes in polytene chromosome morphology. Ectopic *D1* leads to the entanglement of chromosome arms due to numerous ectopic contacts within and between chromosomes. Ectopic associations mediated by *D1* are present on all Drosophila chromosomes. This indicates that D1 in wild-type flies may have the ability to bind to many sites throughout the euchromatin to carry out single or multiple functions.

A comparison of *D1*-induced ectopic contacts and sites of intercalary heterochromatin (IH)

A strong correlation exists between *D1*-mediated ectopic contact sites and regions of euchromatin exhibiting the heterochromatic properties of late DNA replication, underreplication of DNA, HP1 binding and natural ectopic pairing. This raises the possibility that *D1* may have a role in inducing properties of heterochromatin to euchromatin. It is not well understood why these regions of euchromatin have heterochromatic properties or the process of heterochromatinization. Perhaps the binding of D1 to the euchromatin induces structural changes resulting in heterochromatic properties or the recruitment of other transcription factors involved in heterochromatinization.

Does D1 function alone or with other transcription factors? The fact that *D1* has ten AT-hook binding motifs leads me to hypothesize that *D1* functions as a complex with other proteins. It has been hypothesized that multiple AT-hook binding domains may serve as accessory DNA binding domains for several transcription factors as a means of anchoring them to particular DNA structures [10]. In this way, AT-hook motifs seem to be auxiliary elements necessary for cooperation with other DNA-binding activities. With ten AT-hook binding domains, *D1* may induce heterochromatic properties with the aid of other transcription factors.

D1 may complex with HP1 to induce properties of heterochromatin to euchromatin. The correlation between HP1 euchromatic binding sites and *D1*-mediated ectopic sites supports this hypothesis. HP1 activity, function and binding in

99

heterochromatin have been studied at length whereas in euchromatin, a role for HP1 has not been elucidated. Perhaps HP1 is recruited by or recruits D1 to function in the heterochromatinization of certain regions of the euchromatin.

A comparison of *D1*-induced ectopic contacts and euchromatin satellite-like sequences of the X chromosome

Euchromatic satellite-like sequences may partially account for sites of *D1*-mediated ectopic contacts. Since it has been shown that D1 binds to the 1.688 g/cm^3 and the 1.672 g/cm^3 satellite repeats found in heterochromatin, I hypothesize that D1 may also bind sequences homologous to these in the euchromatin. Initial analysis of sequences homologous to the 1.688 g/cm^3 and the 1.672 g/cm^3 satellite sequences on the X chromosome compared to *D1*-mediated ectopic association sites shows a possible correlation. Due to this, it would be beneficial to perform a more sophisticated assay to better understand the *D1*-mediated ectopic sites. A possibility for BLAST analysis of the fly genome would be to input a query of X copies of the 1.672 g/cm^3 satellite sequence with strategically placed spaces allowing for several nucleotides between each AT-hook binding motif. Assaying for a possible correlation between AT-rich satellite-related sequences appropriate for multiple AT-hook binding motifs and *D1*-mediated ectopic contact sites would be a more accurate indicator of whether ectopic sites due to *D1* overexpression could be satellite-like sequences. The result may be indicative of D1 binding sites in wild-type flies.

Chapter 5: Conclusions

Elucidating the function of the chromosomal protein D1 via overexpression analysis in *Drosophila melanogaster* was the focus of this study. A number of tissues were targeted for ectopic *D1* expression in which results provided clues to the role of *D1*. A summary of the outcomes of ectopic *D1* expression is below followed by discussion and speculation of *D1* function.

Tissues in which *D1* was ectopically expressed included the Drosophila eye, mechanosensory bristles, the male and female germline, testis somatic cyst cells, mesodermal tissue, the salivary glands and ubiquitously throughout the fly. In summary of these results, ectopic *D1* expression interfered with several processes. In the eye and mechanosensory bristles, pattern formation and cellular differentiation were perturbed resulting in rough eye and loss of bristle phenotypes. *D1* overexpression driven in the male and female germline did not alter fertility but questions remain regarding the level of ectopic *D1* expression in the assay as the expression of UAS transgenes in the male and female germline is poor [66]. Ectopic *D1* expression in the somatic cyst cells of the testis driven by the *eyes absent* promoter resulted in male sterility due to a meiotic arrest during spermatogenesis while ectopic expression targeted to mesodermal tissues resulted in a reduction of male fertility due to abnormal ejaculatory duct function. In the salivary glands, *D1*-mediated polytene chromosome associations leading to chromosomes refractory to spreading were formed. Finally, ubiquitous *D1* expression, driven by the *actin* and *alphatubulin84B* promoters resulted in lethality predominately at the third larval instar stage and during the second to third larval instar molt in a *tubulin* pattern. Further analysis indicated that ectopic *D1* may be interfering in the complex gene cascade, downstream of 20-hydroxyecdysone biosynthesis.

Initial points of interest in the discussion of *D1* function are that ectopic *D1* expression resulted in the interference of a variety of processes in Drosophila as cited above. The fact that ectopic *D1* expression in differing tissue types perturbed a number of aspects of development lends to the idea that *D1*'s role is not restricted to one particular system. This idea is supported by the localization of *D1* protein in several tissues and at differing developmental stages discussed in chapter one of this thesis.

The gain-of-function phenotypes presented above are most likely the result of ectopic *D1* interference in particular wild-type gene cascades. The results of this study

indicate that *D1* may have interfered in the 20-hydroxyecdysone gene cascade as well as the cascade leading to cell fate specification in eye and bristle morphogenesis. Additionally ectopic *D1* interfered with the complex cell signaling between the somatic and germline cells of spermatogenesis and in the mesodermal development leading to fertility. Because the processes that ectopic *D1* interfered in are relatively unrelated, I am focusing on the AT hook binding of D1 to chromatin in an attempt to concentrate on a commonality of these processes.

D1 binding to chromatin may result in alterations of chromatin structure, much like described for the binding of mammalian HMGA proteins [10]. An abnormal alteration of chromatin structure due to ectopic *D1* may result in a change of gene expression patterns for that particular system. The results of this study support this hypothesis. For example, *D1* ectopic expression in an *eyes absent* pattern resulted in male sterility possibly due to the disruption of the *always early* or *cannonball* gene cascade involved in the alteration of chromatin structure to allow for increased transcription in the primary spermatocyte cells. In addition, ubiquitous, ectopic *D1* expression may have disrupted the gene cascade downstream of 20-hydroxyecdysone biosynthesis leading to lethality during the second to third larval instar molt. Also, cell fate specification was perturbed in both the photoreceptor and the bristle lineage due to excess D1 interfering in the complex gene cascade involved in wild-type pattern formation. An additional study indicated that D1 is activated by interaction with CK2 much like proteins of the HMGA family (Appendix I). Along with the many biochemical similarities of D1 with proteins of the mammalian HMGA family, this result further implicates *D1* in functioning similarly to these proteins in altering the structure of chromatin as a means of affecting gene expression.

Additionally, the possibility exists that *D1* overexpression interfered in gene expression in a generalized manner instead of specific to certain gene cascades or pathways. This hypothesis is equally attractive as investigation into a widespread expression interruption was not done as a means of differentiation.

D1 binds to the 1.688 g/cm^3 and the 1.672 g/cm^3 satellite repeats of heterochromatin [56]. In the euchromatin, D1 has been localized to only four loci. If the D1 protein is primarily present in heterochromatin, which has a low gene number in

comparison to euchromatin, there is a chance that *D1*'s role in gene regulation is exclusively heterochromatic. The result of *D1* overexpression in the salivary glands sheds some light onto this topic. The occurrence of *D1*-mediated ectopic associations of the polytene chromosomes indicates that D1 can mediate associations between polytene chromosomes, which are underrepresented in heterochromatin. Thereby, ectopic *D1* is active in the euchromatic chromosome arms supporting the idea that *D1* may have a role in euchromatin as well as in heterochromatin, even though heterochromatic binding may be preferential.

Mapping of *D1*-mediated ectopic associations led me to hypothesize that D1 is binding to AT-rich, satellite-related regions of the euchromatin. In addition, a correlation was evident in comparisons of *D1* ectopic contact sites to the localization of features of intercalary heterochromatin. The D1 protein thus may be binding to AT-rich and/or satellite-related chromatin and playing a role in the induction of heterochromatic properties to regions of the euchromatin.

Additional studies must be done in order to fully elucidate the function of *D1* through overexpression analysis. Genetic assays to determine particular transcription factors that D1 is interfering with that resulted in the perturbation of cell fate specification, the 20-hydroxyecdysone cascade, the meiotic arrest of spermatogenesis and the abnormal mesoderm development in this study could provide additional clues as to *D1*'s role. If in fact, a function of *D1* is to impart heterochromatic properties on regions of the euchromatin, it would be interesting to analyze the chromatin content of regions of *D1*-mediated ectopic associations in the polytene chromosomes to assay for commonality among the regions in reference to sequence and gene function. Also, it would be interesting to assay loss of *D1* in the salivary polytene chromosomes. Given that ectopic overexpression of *D1* provokes polytene chromosome entangling, I expect a somewhat opposite phenotype in the absence of *D1*. If *D1* functions in inducing heterochromatin properties to the euchromatin and thus in gene regulation, I hypothesize that polytene chromosomes lacking *D1* may lack chromatin organization resulting in altered chromosome morphology. It would also be informative to focus on regions of intercalary heterochromatin in *D1*-null mutants to assay for the presence of these heterochromatic features.

Like other DNA binding proteins [24], D1 may recruit or be recruited by HP1 as the sites of *D1*-mediated ectopic contacts and sites of HP1 euchromatic localization were highly correlated. It would be beneficial to assay for additional interactions involving D1 utilizing the strategy of examination of chromosome entangling due to *D1* overexpression in a mutant background. Gaining a better understanding of proteins that interact with D1 may provide clues as to certain processes that D1 participates in. Examination of said processes would be informative in light the conclusions of this study.

Appendix I: Assay to examine a possible interaction between CK2 and D1

Introduction

This side study focused on the possibility of an interaction between D1 and CK2 utilizing the chromosome entangling phenotype of ectopic *D1* expression in the salivary glands as a means of analysis. As discussed in chapter four of this thesis, ectopic *D1* expression specifically in the Drosophila salivary glands results in chromosomes that are refractory to spreading. The question posed is whether interaction between D1 and CK2 is required for the chromosome entanglement observed when *D1* is ectopically expressed.

Protein kinase CK2 is a highly expressed protein serine/threonine kinase conserved throughout evolution [48; 52; 62]. In a 1983 study by Glover *et al.*, [41] it was determined that D1 is a substrate of Drosophila CK2. In fact, D1 has been utilized as an exogenous substrate for CK2 purification [41]. The possibility that D1 is phosphorylated by CK2 is present as D1 has been identified as a phosphoprotein [40]. Assaying the chromosome entangling of ectopic *D1* expression in a background mutant for *CK2* may provide further evidence that D1 is activated by phosphorylation.

The $CK2\alpha^{Tik}$ (*Timekeeper*), a dominant mutation of the CK2α subunit and $CK2\alpha^{TikR}$, a spontaneous revertant of $CK2\alpha^{Tik}$ were utilized as mutants for *CK2*. $CK2\alpha^{Tik}$ is a dominant mutation in the catalytic subunit of CK2 in which Met161Lys and Glu165Asp coding changes exist resulting in a loss of enzymatic CK2 function [59]. $CK2\alpha^{TikR}$ has coding changes identical to $CK2\alpha^{Tik}$ but with an additional in-frame 27 base pair deletion coupled to an in-frame, six basepair insertion, resulting in an overall deletion of seven amino acids. Another amino acid change, Arg242Glu is present in this mutant as well. The deletion and additional amino acid coding change renders the CK2α subunit unable to correctly fold rendering binding of the nonfunctional $CK2\alpha^{TikR}$ subunit impossible resulting in a misfolded, catalytically dead CK2α subunit [59].

In addition, this assay is a test of potential strategy to identify protein interactors of D1. Examining the chromosome entangling due to *D1* overexpression in a mutant background may be an effective means to determine genetic interaction.

Materials and Methods

Stocks and culture conditions: Fly stocks and crosses were maintained in cotton-stoppered vials on a cornmeal and agar medium which was supplemented with yeast. Flies were maintained at 25°C unless otherwise noted. $CK2\alpha^{Tik}/TM3$, Sb and $CK2\alpha^{TikR}$ /TM3, Sb stocks were generous gifts from Dr. Ashok Bidwai [59]. Table A1 lists the genotypes of strains used in this study. Strains obtained from the Bloomington Stock Center are denoted by B followed by the stock identification number.

Synthesis of strains to induce ectopic *D1* expression: Two genotypes were isolated in preparation for the assay of ectopic *D1* expression in a *CK2* mutant background, $P\{w^+;$ *sgs3-GAL4}/+; P{EP}D1^{EP473}/TM6B, Tb^1* and $P\{w^+; sgs3$-GAL4}/+; P{EP}D1^{EP473}/ *T(2;3)TSTL, CyO, TM6B, Tb^1*. Cy$^-$, Sb$^-$, Sp$^+$ males of the genotype *w; +/CyO; P{EP}D1^{EP473}/TM3, Sb* were selected from a cross of *w; P{EP}D1^{EP473}/TM3, Sb* females and *Sp, lt^{x13p89}, P{w$^+$}/CyO cn, bw; TM3, Sb* males. Simultaneously, females of *w^{1118}; Sp lt^{x13}, P{w$^+$}/SM1, Cy, lt^H; TM6B, Tb* were crossed to males of *sn; P{w$^+$}; sgs3-GAL4}* chromosome 2 insertion line #37. Cy$^-$, Tb$^-$, Sp$^+$ virgin females of the genotype *w; P{w$^+$; sgs3-GAL4}/SM1, Cy; +/TM6B, Tb* were subsequently selected. *w; P{w$^+$; sgs3-GAL4}/CyO; P{EP}D1^{EP473}/TM6B, Tb* males and females were selected from the cross of *w; P{w$^+$; sgs3-GAL4}/SM1, Cy; +/TM6B, Tb* virgin females to *w; +/CyO; P{EP}D1^{EP473}/TM3, Sb* males and mated to create a stock.

Cy$^-$, Tb$^-$, w$^+$ females and males of *w; P{w$^+$; sgs3-GAL4}; P{EP}D1^{EP473}/ T(2;3) TSTL, CyO, TM6B, Tb* were selected from the cross of *w; l(3)/T(2;3) TSTL, CyO, TM6B, Tb* virgin females and *w; P{w$^+$; sgs3-GAL4}/CyO; P{EP}D1^{EP473}/TM6B, Tb* males. The *w; P{w$^+$; sgs3-GAL4}; P{EP}D1^{EP473}/ T(2;3) TSTL, CyO, TM6B, Tb* strain was subsequently stocked.

Salivary Polytene chromosome squashes: $CK2\alpha^{Tik}$ /TM6, Tb^1 and $CK2\alpha^{TikR}$/TM6, Tb virgin females were crossed to males of *P{w$^+$; sgs3-GAL4}/+; P{EP}D1^{EP473}/TM6B, Tb*. $CK2\alpha^{Tik}$/TM6, Tb and $CK2\alpha^{TikR}$ /TM6, Tb virgin females were also crossed with males of *P{w$^+$; sgs3-GAL4}/+; P{EP}D1^{EP473}/ T(2;3)TSTL, CyO, TM6B, Tb* in a separate assay. Alongside both assays, w^{1118} virgin females were crossed to *P{w$^+$; sgs3-GAL4}/+; P{EP}D1^{EP473}/TM6B, Tb* males and *P{w$^+$; sgs3-GAL4}/+; P{EP}D1^{EP473}/ T(2;3)TSTL, CyO, TM6B, Tb* males.

Third instar larvae raised at 25°C in non-crowded conditions, were used for all assays. Tb$^+$ larvae of the genotype *P{w$^+$; sgs3-GAL4}/+ ;P{EP}D1^{EP473}/CK2α^{TikR}* and *P{w$^+$; sgs3-GAL4}/+ ;P{EP}D1^{EP473}/CK2α^{Tik}* were selected for polytene chromosome analyses. Polytene chromosome squashes were done according to the protocol of Kennison [51]. Briefly, salivary glands were dissected in 0.7% NaCl and transferred to 10 ul of 45% acetic acid for 30 seconds. 15 ul of staining solution (2% orcein in a 50% acetic acid, 30% lactic acid solution) was deposited on a siliconized coverslip. Salivary glands were placed in staining solution for two minutes and then squashed. Excess staining solution was removed and coverslip sealed with nail polish. Slides were stored at 4°C prior to scoring. A rating scale was used ranging from one to ten to score the degree of spreading of the polytene chromosomes. A rating of one represented extreme tangling and a rating of ten represented the spreading typical of wild-type polytene chromosome squashes. Scoring was done using brightfield microscopy at 400X magnification.

Table A1: Strains used in these experiments
y w; CK2α^{Tik}/TM3, Sb
w$^+$; CK2α^{TikR}/TM3, Sb
y w sn^3;P{w$^+$; sgs3-GAL4} (B6870)
Sp, lt^{x13p89}, P{w$^+$}/CyO cn^2, bw; TM3, Sb, st^{AP1} (B2475)
w^{1118}; Sp lt^{x13}, P{w$^+$}/SM1, Cy, lt^H; TM6B, Tb^1 (B1553)
P{w$^+$; sgs3-GAL4}; P{EP}D1^{EP473}/TM6B, Tb^1
P{w$^+$; sgs3-GAL4}; P{EP}D1^{EP473}/T(2;3)TSTL, CyO, TM6B, Tb^1

Results

Interaction of D1 and CK2 is indicated by suppression of the chromosome entangling phenotype of *D1* ectopic expression in a *CK2* mutant background.

Two genetic crossing schemes were utilized in order to overexpress *D1* in a *CK2* mutant background. Both strains, when crossed with *CK2α* mutants, resulted in identical genotypes of *P{w⁺; sgs3-GAL4}/+ ; P{EP}D1^{EP473}/CK2α^{Tik}* and *P{w⁺; sgs3-GAL4}/+ ;P{EP}D1^{EP473}/CK2α^{TikR}* of Tb⁺ larvae. These third instar larvae that overexpress *D1* in a background mutant for protein kinase *CK2*, underwent salivary gland dissections and polytene chromosome squashing in order to examine their salivary gland polytene chromosomes. Polytene chromosomes of *P{w⁺; sgs3-GAL4}/+ ; P{EP}D1^{EP473}/CK2α^{Tik}* individuals exhibited *D1*-mediated chromosome entangling to a moderate extent. Chromosome arms of these polytene chromosome squashes could be relatively identified yet the severity of chromosome entanglement was not reduced enough to permit cytological mapping of chromosome arm ectopic contacts. Polytene chromosomes of *P{w⁺; sgs3-GAL4}/+ ; P{EP}D1^{EP473}/ CK2α^{TikR}* individuals exhibited *D1*-mediated polytene chromosome entanglement in which chromosome arms could not be distinguished due to the extremity of entanglement. Table A2 displays the number of polytene chromosome squashes assayed as well as the chromosome spread rating for each genotype examined along with the control.

Polytene chromosomes from the genotype *w^{1118}; P{w⁺; sgs3-GAL4}/+; P{EP}D1^{EP473}/+* were the positive control for the experiment. Polytene chromosomes from these individuals exhibited severe entanglement for all nuclei assayed due to *D1* overexpression in a wild-type background. In comparison, the chromosomes of *P{w⁺; sgs3-GAL4}/+ ; P{EP}D1^{EP473}/CK2α^{Tik}* individuals demonstrated a strong reduction in chromosome entanglement while the polytene chromosomes of *P{w⁺; sgs3-GAL4}/+ ;P{EP}D1^{EP473}/ CK2α^{TikR}* individuals were only slightly reduced in the extent of chromosome entangling. Figure A1 illustrates representative polytene chromosome squashes from the salivary glands of the three genotypes discussed above.
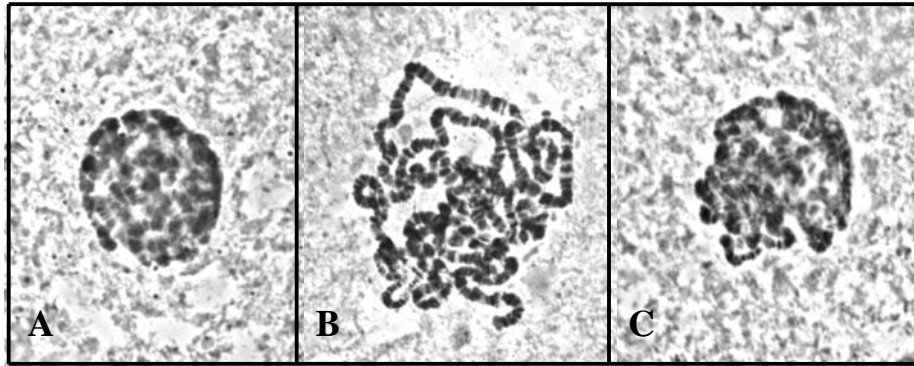
Figure A1: **A potential strategy to identify D1 protein interactors utilizing the *D1*-mediated chromosome entangling phenotype provides evidence that D1 and CK2 interact.** Orcein stained polytene chromosomes from flies overexpressing *D1* in a wild-type background (A), a *CK2α^{Tik}* background (B) and a *CK2α^{TikR}* background (C).

Table A2: The effect of *D1* overexpression in a *CK2* mutant background

Genotype	# of nuclei assayed	Chromosome spread rating[a]
w^{1118}; P{sgs3-GAL4}/+; P{EP}D1^{EP473}/+	23	1
P{sgs3-GAL4}/+; P{EP}D1^{EP473}/CK2α^{Tik}/+	32	3-4
P{sgs3-GAL4}/+; P{EP}D1^{EP473}/CK2α^{TikR}/+	33	1.5

[a]A rating scale was used ranging from one to 10 to score the degree of spreading of the polytene chromosomes. One represented extreme tangling and 10 represented the spreading typical of wild-type polytene chromosome squashes.

Discussion

This study focused on the question of whether D1 and CK2 interaction is necessary for D1 activity. The *D1*-mediated chromosome entangling phenotype was utilized as a means of addressing this by ectopically expressing *D1* in a mutant *CK2* background. Mutants of *CK2* employed in this study were $CK2\alpha^{Tik}$ and $CK2\alpha^{TikR}$. $CK2\alpha^{Tik}$ encodes a dead catalytic subunit that behaves as a dominant-negative while $CK2\alpha^{TikR}$ encodes a misfolded, dead catalytic subunit unable to bind and form the CK2 holoenzyme. The setup of this study encompassed a *salivary gland specific3-GAL4* driver targeting *D1* ectopic expression to the Drosophila salivary glands in $CK2\alpha^{Tik}$ and $CK2\alpha^{TikR}$ backgrounds respectively. *D1* was ectopically expressed in the salivary glands in a wild-type background as the positive control.

Several outcomes of this assay were possible. The phenotype of *D1*-mediated chromosome entanglement could have been suppressed in a $CK2\alpha^{Tik}$ background resulting in less severe chromosome entanglement. This would presumably be due to a reduction in ectopic contacts formed as a result of a severe decrease of CK2 activity leading to less D1 protein activity. In this situation, the phenotype of chromosome entangling due to *D1* overexpression in a $CK2\alpha^{TikR}$ background would be expected to be only slightly suppressed. Both of these results would indicate that an interaction between D1 and CK2 is necessary in order for D1 to be active and mediate ectopic contacts when overexpressed in the salivary gland chromosomes.

Another possible outcome of ectopic *D1* expression in a *CK2* mutant background is that *D1*-mediated chromosome entanglement in a $CK2\alpha^{Tik}$ background as well as in a $CK2\alpha^{TikR}$ background would be identical to ectopic *D1* expression in a wild-type background. This result would fail to support the idea that an interaction between D1 and CK2 is necessary in order for D1 to be active.

The results of the assay mirror the former outcome. Ectopic *D1* expression in a $CK2\alpha^{Tik}$ background resulted in chromosome entanglement less severe than the chromosome entangling of ectopic *D1* expression in a wild-type background. In a $CK2\alpha^{TikR}$ background, ectopic *D1* expression resulted in a slight suppression of the chromosome entangling phenotype of *D1* expression in a wild-type background. Figure

114

A1 illustrates the representative polytene chromosome squashes of ectopic *D1* expression in a wild-type background, a $CK2\alpha^{Tik}$ background and a $CK2\alpha^{TikR}$ background. This study supports the concept that an interaction between D1 and CK2 is necessary in order for D1 to be active.

Many proteins have been identified that require CK2 phosphorylation to be active. One such protein is Heterochromatin Protein 1, HP1. HP1 phosphorylation by CK2 has been shown to be required for binding to heterochromatin *in vivo* in order to carry out functions involving heterochromatin formation and gene repression [95]. Perhaps D1 is phosphorylated by CK2 in order to be active possibly to perform a function of heterochromatinization much the same way as HP1.

Studies have shown that DNA binding affinity of HMGA proteins is attenuated upon phosphorylation [12; 65; 73; 71; 79; 80; 95]. Moreover, HMGA proteins exhibit a higher residence time in heterochromatin compared with euchromatin based on an increased phosphorylation level [2]. Perhaps D1 phosphorylated by CK2, acts in a comparable manner as HMGA proteins cycling between euchromatin and heterochromatin based on phosphorylation level.

In addition to providing evidence that an interaction between D1 and CK2 is necessary in order for D1 to be active, this assay was a test to ascertain if genetic interactions could be examined utilizing the *D1*-mediated polytene chromosome entangling phenotype. This study supports the hypothesis that protein interactors of D1 could be elucidated with this strategy.

References

[1] Adams, M.D., Celniker S.E., Holt, R.A., Evans, C.A., Gocayne, J.D., Amanatides, P.G., Scherer, S.E., Li, P.W., Hoskins, R.A., Galle, R.F., George, R.A., Lewis S.E., Richards, S., Ashburner, M., Henderson, S.N., Sutton, G.G., Wortman, J.R., Yandell, H.D., Zhang, Q., 2000. The Genome Sequence of *Drosophila melanogaster*. Science 287, 2185-2195.

[2] Aleporou-Marinou, V., and Marinou, H., 2002. A Mini Review of the High Mobility Group Proteins of Insects. Biochemical Genetics 41, 291-304.

[3] Alfageme, C.R., Zweidler, A., Nahawali, A., Cohen, L., 1974. Histones of Drosophila embryos. The Journal of Biological Chemistry 249, 3729-3736.

[4] Alfageme, C.R., Rudkin, G., Cohen, L., 1976. Locations of chromosomal proteins in polytene chromosomes. Proc. Natl. Acad. Sci. 73, 2038-2042.

[5] Alfageme, C.R., Rudkin, G., Cohen, L., 1980. Isolation, properties and cellular distribution of D1, a chromosomal protein of Drosophila. Chromosoma 78, 1-80.

[6] Ashburner, M., Chihara, C., Meltzer, P., Richards, G., 1974. On the temporal control of puffing activity in polytene chromosomes. Cold Spring Harbor Symp. Quant. Biol. 38, 655-662.

[7] Ashburner, M., 1990. Puffs, genes, and hormones revisited. Cell 61, 1-3.

[8] Ashley, C., Pendelton, C., Jennings, W., Saxena, A., Glover C., 1989. Isolation and Sequencing of cDNA Clones Encoding Drosophila Chromosomal Protein D1. The Journal of Biological Chemistry 264, 8394-8401.

[9] Aulner, N., Monod, C., Mandicourt, G., Jullien, D., Cuvier, O., Sall, A., Janssen, S., Laemmli, U., Kas, E., 2002. The AT-Hook Protein D1 is Essential for *Drosophila melanogaster* Development and Is Implicated in Position-Effect Variegation. Molecular and Cellular Biology 22, 1218-1232.

[10] Avarind, L., and Landsman, D., 1998. AT-hook motifs identified in a wide variety of DNA-binding proteins. Nucleic Acids Res. 26, 4413-4421.

[11] Ayyar, S., Jiang, J., Collu, A., White-Cooper, H., White, R.A., 2003. Drosophila TGIF is essential for developmentally regulated transcription in spermatogenesis. Development 130, 2841-2852.

[12] Banks, G.C., Li, Y., Reeves R., 2000. Differential *in vivo* modification of the HMGI(Y) nonhistone chromatin proteins modulate nucleosome and DNA interactions. Biochemistry 39: 8333-8346.

[13] Beck, Y., Dauer, C., Richards, G., 2005. Dynamic localization of KR-H during an ecdysone response in Drosophila. Gene Expression Patterns 5, 403-409.

[14] Belyaeva, E.S., Aizenzon, M.G., Semeshin, V.F., Kiss, I., Koezka, K., Baritcheva, M., Gorelova, T.D., Zhimulev, I.F., 1980. Cytogenetic analysis of the 2B3-4 to 2B11 region of the X chromosome of *Drososphila melanogaster*. I. Cytology of the region and mutant complementation groups. Chromosoma 81, 281-306.

[15] Bhat, K.M., 1999. The posterior determinant gene *nanos* is required for the maintenance of the adult germline stem cells during Drosophila oogenesis. Genetics 151, 1479-1492.

[16] Blattes, R., Monod, C., Susbielle, G., Cuvier, O., Wu, J., Hsieh, T., Laemmli, U., Kas, E., 2006. Displacement of D1, HP1 and topoisomerase II from satellite heterochromatin by a specific polyamide. The EMBO Journal 25, 2397-2408.

[17] Bonaccorsi, S., Giansanti, M.G., Cenci, G., Gatti, M., Cytological Analysis of Spermatocyte Growth and Male Meiosis in *Drosophila melanogaster*. In *Drosophila protocols*. pp 87-110. Cold Spring Harbor, New York: Cold Spring Harbor Press.

[18] Bonini, N.M., Leiserson, W.M., Benzer, S., 1993. The *eyes absent* gene: genetic control of cell survival and differentiation in the developing Drosophila eye. Cell 72, 379-395.

[19] Brand, A.H., and Perrimon, N., 1993. Targeted gene expression as a means of altering cell fates and generating dominant phenotypes. Development 118, 401-415.

[20] Bridges, C.B., 1935. Salivary chromosome maps with a key to the banding of the chromosomes of *Drosophila melanogaster*. J. Hered. 26, 60-64.

[21] Burtis, K.C., Thummel, C.S., Jones, C.W., Karim, F.D., Hogness, D.S., 1990. The Drosophila 74EF early puff contains *E74*, a complex ecdysone-inducible gene that encodes two *ets*-related proteins. Cell 61, 85-99.

[22] Carlson, M., and Brutlag, D., 1977. Cloning and characterization of a complex satellite DNA from *Drosophila melanogaster*. Cell 11, 371-381.

[23] Clark, G.A., 1990. Two tests if Y chromosomal variation in male fertility of *Drosophila melanogaster*. Genetics 125, 527-534.

[24] Cortes, A., Huertas, D., Fanti, L., Pimpinelli, S., Marsellach, F., Pina, B., Azorin, F., 1999. DDP1, a single-stranded nucleic acid-binding protein of Drosophila, associates with pericentric heterochromatin and is functionally homologous to the yeast Scp160p, which is involved in control of cell ploidy. The EMBO Journal 18, 3820-3833.

[25] Courtot, C., Frankhauser, C., Simanis, V., Lehner, C., 1992. The Drosophila *cdc25* homolog *twine* is required for meiosis. Development 116, 405-416.

[26] Csink, A., and Henikoff, S., 1998. Something from nothing: the evolution and utility of satellite repeats. Trends in Genetics 14, 200-204.

[27] Dai, J.D., and Gilbert, L.I., 1991. Metamorphosis of the corpus allatum and degeneration of the prothoracic glands during the larval-pupal–adult transformation of *Drosophila melanogaster*: a cytophysiological analysis of the ring gland. Dev. Biol. 144, 309-326.

[28] Dokucu, M., Zipursky, L., Cagan, R., 1996. Atonal, Rough and the resolution of proneural clusters in the developing Drosophila retina. Development 122, 4139-4147.

[29] Duffy, J., 2002. GAL4 System in Drosophila: A Fly Geneticist's Swiss Army Knife. Genesis 34, 1-15.

[30] Emery, I.F., Bedian, V., Guild, G.M., 1994. Differential expression of *Broad-Complex* transcription factors may forecast tissue specific developmental fates during Drosophila metamorphosis. Development 120, 3275-3287.

[31] Endow, S.A., Polan, M.L., Gall, J.G., 1975. Satellite sequences of *Drosophila melanogaster*. J. Mol. Biol. 96, 665-692.

[32] Fabrizio, J., Boyle, M., DiNardo S., 2003. A somatic role for *eyes absent* (*eya*) and *sine oculis* (*so*) in Drosophila spermatocyte development. Developmental Biology 258, 117-128.

[33] Fanti, L., Berloco, M., Piacentini, L., Pimpinelli, S., 2003. Chromosomal distribution of Heterochromatin Protein 1 (HP1) in Drosophila: a cytological map of euchromatic HP1 binding sites. Genetica 117, 135-147.

[34] Fletcher, J., and Thummel, C., 1995. The Ecdysone-Inducible *Broad-Complex* and *E74* Genes Interact to Regulate Target Gene Transcription and Drosophila Metamorphosis. Genetics 141, 1025-1035.

[35] Forbes, A., and Lehmann, R., 1998. Nanos and Pumilio have critical roles in development and function of Drosophila germline stem cells. Development 125, 679-690.

[36] Fuller, MT., 1993. Spermatogenesis. In *The Development of Drosophila*, pp. 71-147. Cold Spring Harbor, New York: Cold Spring Harbor Press.

[37] Fuller, M., 1998. Genetic control of cell proliferation and differentiation in Drosophila spermatogenesis. Cell & Developmental Biology 9, 433-444.

[38] Gigliotti, S., Rotoli, D., Graziani, F., Malva, C., 2003. Oogenesis in *Drosophila melanogaster*: a model system for studying cell differentiation and development. Ital. J. Biochem. 52, 104-111.

[39] Gilbert, L., 2004. Halloween genes encode P450 enzymes that mediate steroid hormone biosynthesis in *Drosophila melanogaster*. Molecular and Cellular Endocrinology 215, 1-10.

[40] Glover, C.V., 1982. Heat shock induces rapid dephosphorylation of a ribosomal protein in Drosophila. Proc. Natl. Acad. Sci. 79, 1781-1785.

[41] Glover, C.V., Shelton, E.R., Brutlag, D.L., 1983. Purification and characterization of a type II casein kinase from *Drosophila melanogaster*. J. Biol. Chem. 258, 3258-3265.

[42] Gvozdev, V.A., Ananiev, E.V., Kotelyanskaya, A.T., Zhimulev, I.F., 1980. Transcription of intercalary heterochromatin regions in *Drosophila melanogaster* cell culture. Chromosoma 80, 177-190.

[43] Hayashi, Y., Hayashi, M., Kobayashi, S., 2004. Nanos suppresses somatic cell fate in Drosophila germ line. Proc. Natl. Acad. Sci. 101, 10338-10342

[44] Heberlein, U., Mlodzik, M., Rubin, G., 1991. Cell-fate determination in the developing Drosophila eye: role of the *rough* gene. Development 112, 703-712.

[45] Henrich, V.C., Rybczynski, R., Gilbert, L.I., 1999. Peptide hormones, steroid hormones and puffs: mechanisms and models in insect development. Vitamins and Hormones 55, 73-125.

[46] Hiller, M.A., Lin, T.Y., Wood, C., Fuller, M.T., 2001. Developmental regulation of transcription by a tissue-specific TAF homolog. Genes Dev. 15, 1021-1030.

[47] Hoskins, R.A., Smith, C.D., Carson, J.W., Carvalho, A.B., Halpern, A., Kaminker, J.S., Kennedy, C., Mungall, C.J., Sullivan, B.A., Sutton, G.G., Yasuhara, J.C., Wakimoto, B.T., Myers, E.W., Celniker, S.E., Rubin, G.M., Karpen, G.H., 2002. Heterochromatic sequences in a Drosophila whole-genome shotgun assembly. Genome Biol. 3, 00085.

[48] Jakobi, R., Voss, H., Pyerin, W., 1989. Human phosvitin/casein kinase type II. Molecular cloning and sequencing of full-length cDNA encoding subunit beta. Eur. J. Biochem. 183, 227-233.

[49] Jiang, J., and White-Cooper, H., 2003. Transcriptional activation in Drosophila spermatogenesis involves the mutually dependent function of *aly* and a novel meiotic arrest gene *cookie monster*. Development 130, 563-575.

[50] Kaufmann, BP., 1939. Distribution of induced breaks along the X chromosome of *Drosophila melanogaster*. Proc. Natl. Acad. Sci. 25, 571-577.

[51] Kennison, J.A., 2000. Preparation and analysis of polytene chromosomes. In *Drosophila protocols*. pp 111-117. Cold Spring Harbor, New York: Cold Spring Harbor Press.

[52] Kopatz, I., Naiman, T., Eli, D., Canaani, D., 1990. The nucleotide sequence of the mouse cDNA encoding the beta subunit of casein kinase II. Nuclei Acids Res.18, 3639.

[53] Leach, T., Chotokowski, H., Wotring, M., Dilwith, R., Glaser, L., 2000. Replication of Heterochromatin and Structure of Polytene Chromosomes. Molecular and Cellular Biology 20, 6308-6316.

[54] Lefevre, G., 1976. A photographic representation and interpretation of the polytene chromosome of *Drosophila melanogaster* salivary glands. In *The Genetics and Biology of Drosophila*. pp. 31-66. London: Academic Press.

[55] Lehmann, R., and Nusslein-Volhard, C., 1991. The maternal gene *nanos* has a central role in posterior pattern formation of the Drosophila embryo. Development 112, 679-691.

[56] Levinger, L., and Varshavsky, A., 1982. Protein D1 preferentially binds A+T-rich DNA *in vitro* and is a component of *Drosophila melanogaster* nucleosomes containing A+T-rich satellite DNA. Proc. Natl. Acad. Sci. 79, 7152-7156.

[57] Levinger, L., 1985. D1 Protein of *Drosophila melanogaster*. The Journal of Biological Chemistry 260, 14311-14318.

[58] Lindsley, D.L., and Tokuyasu, K.T., 1980. Spermatogenesis In: *The Genetics and Biology of Drosophila*. pp 225-294. London: Academic Press.

[59] Lin, J., Kilman, V., Keegan, K., Paddock, B., Emery-Le, M., Rosbash, M., Allada, R., 2002. A role for casein kinase 2 in the Drosophila circadian clock. Nature 420, 816-820.

[60] Lohe, A.R., and Brutlag, D.L., 1987. Identical satellite DNA sequences in sibling species of Drosophila. J. Mol. Biol. 194, 161-170.

[61] Lohe, A., Hilliker, A., Roberts, P., 1993. Mapping Simple Repeated DNA Sequences in Heterochromatin of *Drosophila melanogaster*. Genetics 164, 1149-1174.

[62] Lozeman, F.J., Litchfield, D.W., Piening, C., Takio, K., Walsh, K.A., Krebs, E.G., 1990. Isolation and characterization of human cDNA clones encoding the alpha and the alpha' subunits of casein kinase II. Biochemistry 29, 8436-8447.

[63] Matunis, E., Tran, J., Gonczy, P., Caldwell, K., DiNardo, S., 1997. *punt* and *schnurri* regulate a somatically derived signal that restricts proliferation of committed progenitors in the germline. Development 124, 4383-4391.

[64] Nakao, K., and Campos-Ortega, J.A., 1996. Persistent expression of genes of the enhancer of split complex suppresses neural development in Drosophila. Neuron 16, 275-286.

[65] Nissen, M.S., and Reeves, R., 1995. Changes in superhelicity are introduced into closed circular DNA by binding of high mobility group protein I/Y. J. Biol. Chem. 270, 4355-4360.

[66] Noguchi, T., and Miller, K., 2003. A role for actin dynamics in individualization during spermatogenesis in *Drosophila melanogaster*. Development 130, 1805-1816.

[67] Park, Y., Flilippov, V., Gill, S., Adams, M., 2002. Deletion of the ecdysis-triggering gene leads to lethal ecdysis deficiency. Development 129, 493-503.

[68] Peacock, W.J., Brutlag, D., Goldring, E., Appels, R., Hinton, C.W., Lindsley, D.L., 1973. Cold Spring Harbor Symp. Quant. Biol. 38, 405-416.

[69] Pecasse, F., Beck, Y., Ruiz, C., Richards, G., 2000. Kruppel-homolog, a Stage-Specific Modulator of the Prepupal Ecdysone response, is Essential for Drosophila Metamorphosis. Developmental Biology 221, 53-67.

[70] Perezgasga, L., Jiang, J., Bolival, B.Jr., Hiller, M., Benson, E., Fuller, M.T., White-Cooper, H., 2004. Regulation of transcription of meiotic cell cycle and terminal differentiation genes by the testis-specific Zn-finger protein matotopetli. Development 131, 1691-1702.

[71] Piekielko, A., Drung, A., Rogalla, P., Schwanbeck, R., Heyduk, R., Gerharz, M., Bullerdiek, J., Wisniewski, J.R., 2001. Distinct organization of DNA complexes of various HMGI/Y family proteins and their modulation upon mitotic phosphorylation. J. Biol. Chem. 276, 1984-1992.

[72] Pimpinelli, S., Berloco, M., Fanti, L., Dimitri, P., Bonaccorsi, S., Marchetti, E., Caizzi, R., Caggese, C., Gatti, M., 1995. Transposable elements are stable structural components of *Drosophila melanogaster* heterochromatin. Proc. Natl. Acad. Sci. 92, 3804-3808.

[73] Reeves, R., and Nissen, M.S., 1990. The AT-DNA-binding domain of mammalian high mobility group I chromosomal proteins. A novel peptide motif for recognizing DNA structure. J. Biol. Chem. 265, 8573-8582.

[74] Renner, U., Ghidelli, S., Schafer, M.A., Wisniewski, J.R., 2000. Alterations in titer and distribution of high mobility group proteins during embryonic development of *Drosophila melanogaster*. Biochim. Biophys. Acta. 1475, 99-108.

[75] Rexhepaj, A., Liu, H., Peng, J., Choffat, Y., Kubli, E., 2003. The sex peptide DUP99B is expressed in the male ejaculatory duct and in the cardia of both sexes. European Journal of Biochemistry 270, 4306-4314.

[76] Riddiford, L.M., 1993. Hormones and Drosophila Development. In *The Development of Drosophila melanogaster*. pp. 899-939. Plainview, NY: Cold Spring Harbor Laboratory Press.

[77] Rorth, P., 1996. A modular misexpression screen in Drosophila detecting tissue-specific phenotypes. Genetics 93, 12418-12422.

[78] Rorth, P., Szabo, K., Bailey, A., Laverty, T., Rehm, J., Rubin, G.M., Weigmann, K., Milan, M., Benes, V., Ansorge, W., Cohen, S.M., 1998. Systematic gain-of-function genetics in Drosophila. Development 125, 1049-1057.

[79] Schwanbeck, R., and Wisniewski, J.R., 1997. Cdc2 and mitogen-activated protein kinases modulate DNA-binding properties of putative transcriptional regulator Chironomus high mobility group protein I. J. Biol. Chem. 272, 27476-27483.

[80] Schwanbeck, R., Manfioletti, G., Wisniewski, J.R., 2000. Architecture of high mobility group protein I-C.DNA complex and its perturbation upon phosphorylation by Cdc2 kinase. J. Biol. Chem. 275, 1793-1801.

[81] Schwanbeck, R., Gymnopoulos, M., Petry, I., Piekielko, A., Szewczuk, Z., Heyduk, T., Zechel, R., Wisniewski, J.R., 2001. Consecutive Steps of Phosphorylation Affect Conformation and DNA-binding of the Chironomus High Mobility Group A Protein. Journal of Biological Chemistry 276, 26012-26021.

[82] Thisse, B., Stoetzel, C., Gorostiza-Thisse, C., Perrin-Schmitt, F., 1987. Sequence of the *twist* gene and nuclear localization of its protein in endomesodermal cells in early Drosophila embryos. EMBO 7, 2175-2183.

[83] Thomas, H.E., Stunnenberg, H.G., Stewart, A.F., 1993. Spatial and temporal patterns of *E74* transcription during Drosophila development. Cell 61, 101-111.

[84] Thummel, C.S., Burtis, K.C., Hogness, D.S., 1990. Spatial and temporal patterns of *E74* transcription during Drosophila development. Cell 61, 101-111.

[85] Tomlinson, A., Kimmel, B.E., Rubin, G.M., 1988. *rough*, a Drosophila homeobox gene is required in photoreceptors R2 and R5 for inductive interactions in the developing eye. Cell 55, 771-784.

[86] Tomlinson, A., 1988. Cellular interactions in the Drosophila eye. Development 104, 183-193.

[87] Wang, D.Z., Ray, P., Boothby, M., 1995. Interleukin-4-inducible phosphorylation of HMG-I(Y) is inhibited by rapamycin. J. Biol. Chem. 270, 22924-22932.

[88] Wang, D.Z., Zamorano, J., Keegan, A., Boothby, M., 1997. HMG-I(Y) phosphorylation status as a nuclear target regulated through insulin receptor substrate-I and the 14R motif of the interleukin-4 receptor. J. Biol. Chem. 272, 25083-25090.

[89] White-Cooper, H., Schafer, M.A., Alphey, L.S., Fuller, M.T., 1998. Transcriptional and post-transcriptional control mechanisms coordinate the onset of spermatid differentiation with meiosis I in Drosophila. Development 125, 125-134.

[90] White-Cooper, H., Leroy, D., MacQueen, A., Fuller, M.T., 2000. Transcription of meiotic cell cycle and terminal differentiation genes depends on a conserved chromatin associated protein whose nuclear localization is regulated. Development 127, 5463-5473.

[91] White-Cooper, H., Alphey, L., Glover, D.M., 1993. The cdc25 homologue *twine* is required for only some aspects of the entry into meiosis in Drosophila. J. Cell Sci. 106, 1035-1044.

[92] Wolff, T., 2000. Histological Techniques for the Drosophila Eye. In *Drosophila protocols*. pp 201-243. Cold Spring Harbor, New York: Cold Spring Harbor Press.

[93] Xiao, D., Pak, J., Wang, X., Sato, T., Huang, F., Chen, H., Huang, K., 2000. Phosphorylation of HMG-I by protein kinase C attenuates its binding affinity to the promoter regions of protein kinase C gamma and neurogranin/RC3 genes. J. Neurochem. 74, 392-399.

[94] Yao, T.P., Segraves, W.A., Oro, A.E., McKeown, M., Evans, R.M., 1992. Drosophila ultraspiracle modulates ecdysone receptor function via heterodimer formation. Cell 71, 63-72.

[95] Zhao, T., and Eissenberg, J.C., 1999. Phosphorylation of heterochromatin protein 1 by casein kinase II is required for efficient heterochromatin binding in Drosophila. J. Biol. Chem. 21, 15095-15100.

[96] Zhimulev, I.F., Semeshin, V.F., Kulichkov, V.A., Belyaeva, E.S., 1982. Intercalary heterochromatin in Drosophila. Chromosoma 87, 197-228.

[97] Zhimulev, I.F., 1998. Polytene chromosomes, heterochromatin and position effect variegation. Advances in Genetics 37, Academic Press New York.

[98] Zhimulev, I.F., and Belyaeva, E.S., 2003. Intercalary heterochromatin and gene silencing. BioEssays 25, 1040-1051.

[99] Zhimulev, I.F., Belyaeva, I.S., Makunin, I.V., Pirrotta, V., Volkova, E.I., Alekseyenko, A.A., Andreyeva, E.N., Makarevich, G.F., Boldyreva, L.V., Nanayev, R.A., Demakova, O.V., 2003. Influence of the *SuUR* gene on intercalary heterochromatin in *Drosophila melanogaster* polytene chromosomes. Chromosoma 111, 337-398.